1-1-2005

Finite element analysis of Iowa Highway 13 composite pavement

Sun-Yoong Oh
Iowa State University

Finite element analysis of Iowa Highway 13 composite pavement

by

Sun-Yoong Oh

A thesis submitted to the graduate faculty

in partial fulfillment of the requirements for the degree of

MASTER OF SCIENCE

Major: Civil Engineering (Structural Engineering)

Program of Study Committee:
Fouad S. Fanous, Major Professor
James K. Cable
Halil Ceylan
Lester W. Schmerr

Iowa State University
Ames, Iowa
2005

Graduate College
Iowa State University

This is to certify that the master's thesis of

Sun-Yoong Oh

has met the thesis requirements of Iowa State University

Signatures have been redacted for privacy

TABLE OF CONTENTS

LIST OF FIGURES

LIST OF TABLES

1.0 INTRODUCTION

1.1 Background

Resurfacing hot mix asphalt (HMA) pavements with thin Portland Cement Concrete (PCC) overlays, or "whitetopping" as it has come to be known, is a concept that dates back to 1918. This approach has seen a large increase in use in the past 15 years due to improved whitetopping technology, and the success of several high-profile projects [2]. Whitetopping provides several advantages to the conventional resurfacing of pavements with HMA. It significantly reduces time and delays associated with pavement maintenance utilizing asphalt. PCC surfaces also have proven durability and long-term performance, which allows for longer life at lower life-cycle costs as compared to asphalt surfaces [11].

The state of Iowa is one of several states known for its large amount of PCC pavements. The original design life of the initial pavement systems was established as 20 years, and much of the system had reached or exceeded the design life by the 1970s. These pavements were then continually resurfaced and possibly widened with asphalt cement concrete (ACC) to extend the life for another 10 to 15 years, or until funding could be obtained to replace the pavements [1, 11]. Due to the shorter design life and higher maintenance costs of asphalt pavements throughout that design life, whitetopping presents an attractive, lower cost alternative to continued pavement rehabilitation of asphalt surfaces.

In 1994, the Iowa Department of Transportation (IDOT) initiated a UTW project on a 7.2 mile segment of Iowa Highway 21 in Iowa County, near Belle Plaine, Iowa. The objective of that research was to investigate the interface bonding condition between an ultra-thin PCC overlay and an ACC base over time, with consideration given to the combination of different factors such as ACC surface preparation, PCC thickness, the usage of synthetic fiber reinforcement, joint spacing and joint sealing. That research continues to be one of the most referenced in demonstrating the applicability of whitetopping as a viable rehabilitation option.

In 2002, a follow-up project was initiated by IDOT to investigate and verify the findings from the 1994 study [1]. For this purpose, a 9.6-mile long stretch of Iowa Highway 13 (IA13) that extends from Manchester, Iowa to Iowa Highway 3 in Delaware County was selected as the test site. The pavement section consisted of a bottom PCC layer constructed in 1931 that was 18ft wide with a thickened edge that was 10" at the edges and 7" at the centerline of the roadway. The concrete pavement was used as the driving surface, until subsequently overlaid with 2" of asphalt concrete in 1964, with another asphalt concrete overlay of 3" in 1984.

Whitetopping was utilized in the summer of 2002 to rehabilitate the Iowa Highway 13 roadway, which was applied considering the following variables: ACC surface preparation (milled, one-inch HMA stress relief course, and broomed only); use of fiber reinforcement in concrete (polypropylene, monofilament, proprietary structural, and no fibers); joint spacing (4.5x4.5, 6x6, 9x9-foot sections); and joint/crack preparation (bridge with concrete or #4 rebars stapled to the asphalt surface). The pavement section was also widened during the overlay operation to its current 24 ft width. The details of the construction were presented in a separate construction report presented by the Center of Portland Cement Concrete Pavement Technology Center of Iowa State University [1].

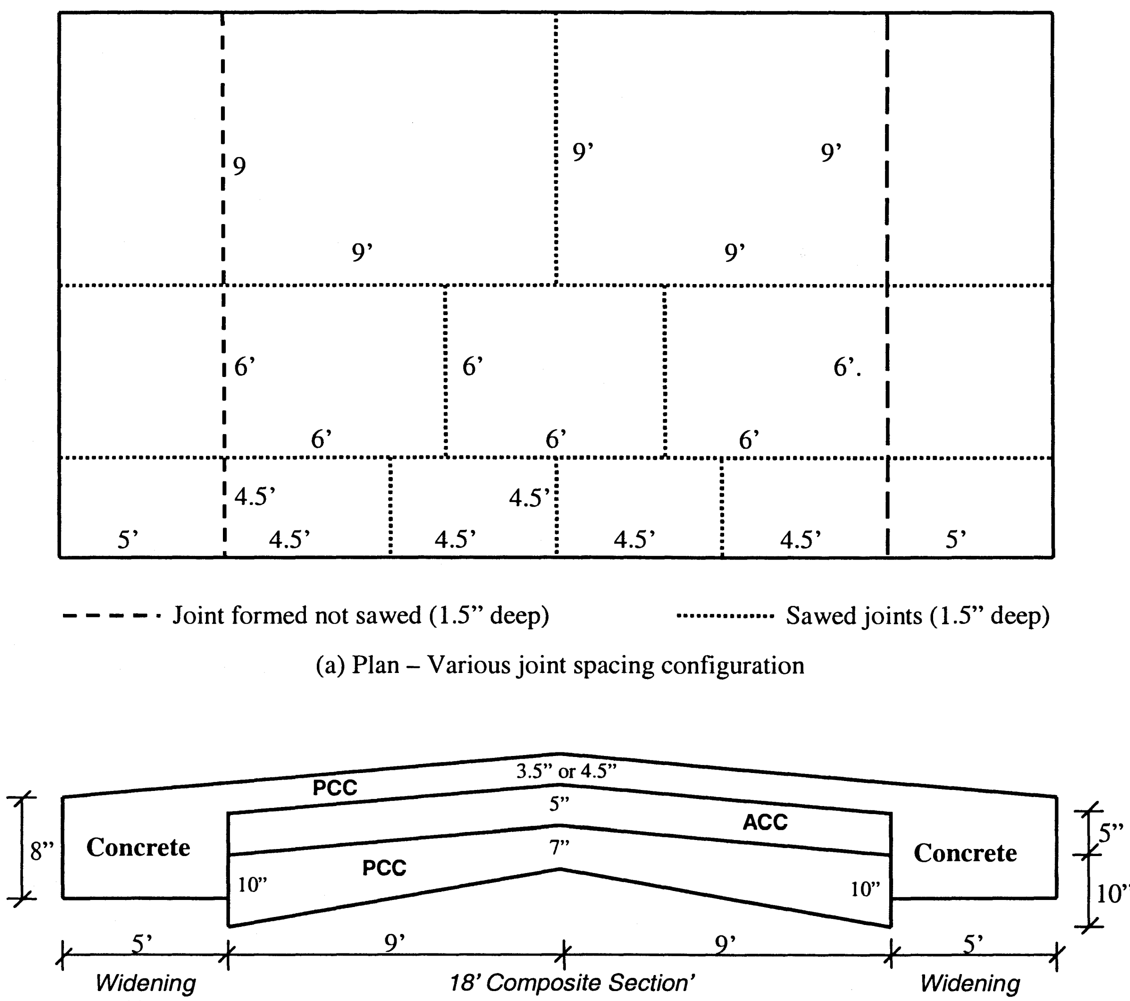

(a) Plan – Various joint spacing configuration

(b) Pavement cross-section

Figure 1-1 Schematics of the Composite Pavement (not to scale)

The construction report also included an analytical study utilizing the finite element method to predict the behavior of the composite pavement under truck loads. Several observations on the overall structural behavior of the pavement were made with regard to factors such as variation of soil subgrade reaction values, pavement cross-slope, and joint crack depth. The widening units were also found to be beneficial to pavement performance by reducing deflection and stresses. However, the state of bonding between the layers, the different joint spacings, the effect of the rebars, and the effect of temperature variation were not part of the investigation documented in Ref. [1].

The study presented herein is an extension of the initial analytical work presented in the construction report [1], and is focused on analytically investigating the factors that were not studied in the aforementioned analytical work.

1.2 Objectives

The objectives of the study presented herein were as follows:

- Develop an analytical model for a finite element analysis that can accurately predict the response of the composite pavement on Iowa Highway 13
- Investigate the behavior of the pavement as whitetopping thickness, joint spacing and depth of joint cracking was varied
- Examine the effects of bonding between the different layers on the overall structural behavior of the composite pavement
- Investigate the effects of the widening units on the deflection and stresses induced in the composite pavement when subjected to loading
- Determine the effects of bridging the pavement section and widening units with tie bars of different size and spacing
- Investigate the behavior of the pavement when subjected to different thermal conditions

1.3 Approach

To achieve the aforementioned objectives, the following tasks were completed:

- Collection of information regarding the dimensions and other considerations about the pavement on Iowa Highway 13
- Determination of the appropriate types of elements for the finite element modeling of the composite pavement. This step required:
    - Verification of the suitability of interface elements to model the interaction between pavement layers
    - Comparison of the results obtained using a general purpose finite element model with those obtained using available specialized pavement analysis software, such as ISLAB2000
    - Determination of the appropriate mesh size for the finite element model to ensure accurate results were obtained
- Calibration of the analytical results with field test data on Iowa Highway 13. This task was accomplished by:
    - Comparison of collected Falling Weight Deflectometer (FWD) test data to analysis results from pavement subjected to comparable load and ground conditions
    - Comparison of measured strain to strain results from the finite element analysis
- Analysis of the pavement model with the different design variables under consideration, which included:
    - Bonded and unbonded layers
    - Different joint spacing and crack depth
    - Different widening unit thickness and width
    - Different rebar bar size and spacing
- Investigation of the behavior of composite pavement under recorded temperature differentials

2.0 LITERATURE REVIEW

According to the *NCHRP Synthesis of Highway Practice 99*, the first recorded use of whitetopping in the United States was in 1918, where a 3- to 4-in. overlay was put in place on a project in Terre Haute, Indiana [3]. Since then, more than 500 whitetopping projects have been recorded in the United States as documented by the American Concrete Pavement Association (ACPA), more than 300 of which took place after 1991. The use of whitetopping has not been limited to the United States, however. Countries in Europe, Asia and South America have reported recent projects utilizing whitetopping [2].

Generally, three distinct categories of whitetopping are found in the literature [2,5,6]:

1. Conventional Whitetopping – a concrete overlay of 8 in. or more in thickness, designed and constructed without consideration of the bond between PCC and the underlying HMA.
2. Thin Whitetopping (TWT) – a concrete overlay of between 4 and 8 in., designed and constructed with an intentional bond to the HMA is most cases.
3. Ultra-Thin- Whitetopping (UTW) – a concrete overlay with thickness equal to or less than 4 in., requiring a bond to the HMA for good performance.

TWT overlays have been used on highway and secondary roads carrying a wide range of traffic from light to heavy loads, and have also been used for runway pavements in general use aviation airports. On the other hand, UTW overlays are best suited for more lightly loaded pavements due to the use of a thinner PCC thickness.

2.1 Fundamental Behavior of Pavement Whitetopping

Usage of UTW or TWT overlays may result in a composite structure that behaves differently from other single-layer pavement types, such as more conventional PCC or HMA structures. As illustrated in Fig. 2-1, the stress distribution in a bonded system is significantly different from an unbonded system. As UTW pavements and most TWT pavements are designed and constructed to achieve a sound bond between the top PCC and underlying HMA, the resultant composite action lowers the stresses in the PCC layer significantly as compared to the unbonded system [2]. Therefore, one can expect that the thickness for the slab would be thinner for a bonded system than for an unbonded system.

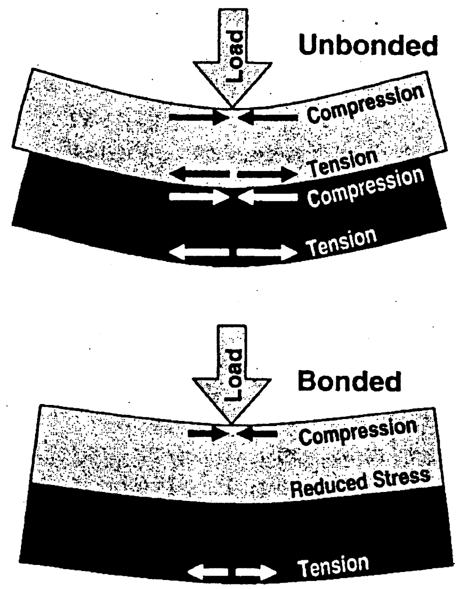

Figure 2-1 UTW and TWT Behavior Under Flexural Loading

In a three-layered system, such as the test pavement on Iowa Highway 13 where the whitetopping PCC and HMA layers are further underlain by the original PCC pavement, similar reduction in stresses due to a bonded system is also realized, with the additional benefit of reducing tensile stresses in the bottom PCC layer.

While a fully bonded UTW or TWT system would be ideal, it has been shown that only a partial bond is usually present as a result of a number of factors [4]. In such a case, the stresses would lie somewhere between the two extremes, i.e. between those induced in fully bonded and fully unbonded systems. The behavior of a pavement system with multiple layers of different material type would be increasingly complex with multiple partially bonded interfaces between the layers.

2.2 Pavement Whitetopping Studies

Many studies have been performed in recent years to determine the effectiveness of using whitetopping as a rehabilitation alternative [4], and also to determine the best combination of design parameters to ensure satisfactory pavement performance. While most of these studies have been conducted in the field, work has also been completed in combination with analytical methods, primarily utilizing finite element analysis. Many of these efforts were directed at development of a rational method for the design of UTW or TWT pavements to ensure satisfactory behavior of the pavements. As a result, first generation design and construction procedures for whitetopping have been developed and published by the Portland Cement Association (PCA) [5] and the Colorado Department of Transportation (CDOT) [4]. The following section gives a brief summary of the studies that have taken place.

2.2.1 Experimental Studies

The first modern UTW project was constructed in 1991 on an entrance road to a waste management facility near Louisville, Kentucky. That project focused on assessing the viability of UTW overlays, and successfully demonstrated that "ultra-thin whitetopping 2 to 3.5 in. thick can carry traffic loads typical of many low-volume roads, residential streets and parking lots" [7]. The project was constructed of fiber reinforced concrete panels with varying joint spacing, which were instrumented to provide data on the effect of heavy wheel loads. Among the significant findings reported was the observation that the bond between UTW and existing HMA pavement significantly reduced the stresses in the concrete section, allowing the section to perform as a composite section. Also, joint spacing had a significant effect on the rate of corner cracking, which was found to be the predominant mode of distress to the UTW overlay.

In 1993, two HMA and four whitetopping overlay test sections were constructed on TH30, a low-volume road in southern Minnesota [11]. The intent of the project was to investigate the performance of and costs associated with these test sections after several years of service, and to provide a side-by-side comparison of HMA and PCC overlays. The whitetopping sections were found to be performing very well at the midpoint of their 20-year design life, despite the low-strength concrete that was used for the whitetopping overlay. While the HMA sections were also performing well, the whitetopping sections were the more economical option for rehabilitation of low-volume roads, as the whitetopping sections in the study did not incur periodic maintenance costs. Reference [11] also noted that most of the distress that occurred to the whitetopping sections was related to "poor construction and materials rather than inherent design features".

The Minnesota Department of Transportation commissioned two other UTW projects in 1997, the first of which was located at three consecutive intersections on US-169 at Elk River, Minnesota. The objective of that project was to gain further experience with both design and performance of UTW [10]. The second was located on I-94 at the Minnesota Road Research Facility, which allowed for comparison of pavements with similar UTW design on HMA layers with different structural capacities. These pavements were heavily instrumented, and the study concluded that the measured strains emphasized the importance of the underlying HMA layer in providing support to the UTW. Attempts to back-calculate the resilient modulus of each layer led to the conclusion that the responses of the various layers were nonlinear, contrary to the original assumption that each layer was a linear elastic homogeneous layer. The study also observed that sections of the pavement where water had ready access to the pavement caused the HMA to ravel at a faster rate, particularly at the lane-shoulder joints, resulting in non-uniform bond conditions. Another important observation was that lower deflections resulted in extended pavement life.

Recently, the Accelerated Loading Facility (ALF) at the FHWA Turner–Fairbank Highway Research Center in Virginia was utilized to test the performance of UTW overlays [2]. This was accomplished by overlaying eight lanes of HMA pavement with varying UTW thickness, joint spacing and concrete mix design. A large amount of data pertaining to the design, construction and performance of the UTW overlays, such as concrete temperatures, slump, unit weight and air content were collected. Testing for concrete compressive strength, elastic modulus and flexural strength was also performed. Bond strength information between UTW and ACC layers was collected using the procedure developed by the Iowa DOT [12]. In addition, the pavement layer stiffnesses were estimated by utilizing falling weight deflectometer (FWD) testing. From the subsequent analysis of data related to the distress and the modes of failure of the pavement system, it was found that the more viscous the HMA layer, the more quickly and severely the UTW would deteriorate.

2.2.2 Analytical Studies

Several analytical methods that range in degree of difficulty from using simple closed form solutions to complex finite element models may be utilized to investigate the performance of composite pavement structures. A three-dimensional (3-D) finite element model for the stress analysis of pavements with UTW was developed as part of a 1997 study of UTW overlays at the Ellaville Weigh Station on I-10 in northern Florida by the Florida DOT. The analysis was an attempt to understand the reason for the poor performance of the UTW sections constructed at the Ellaville Weight Station. The analysis showed that the UTW sections were found to have relatively higher stresses under critical loading conditions, which appeared to explain the poor performance and high incidences of cracked slabs. The 3-D model developed was also used to perform a parametric analysis to determine the effects that various UTW design variables have on performance, such as asphalt thickness, concrete thickness, asphalt and concrete moduli, and subgrade stiffness. The 3-D finite element model was limited by the simplifications of the material behavior to elastic material, full bonding between the layers, and no load transfer between adjacent slabs (thus providing an extreme worst case scenario). Despite these limitations, the project was a valuable demonstration of the applicability of using the finite element method to aid in the study performance of whitetopping.

In 1998, the Portland Cement Association (PCA) published a report detailing the development of a first generation design procedure for UTW. The report was based on a comprehensive study involving extensive field load testing, as well as the theoretical evaluation of UTW pavement behavior utilizing 3-D finite element analysis with the NISA II software package [5]. Field test data was collected from three different sites: from a parking ramp rehabilitation project in the Spirit of St. Louis Airport, constructed in early 1995; and from two whitetopping test sections in Colorado that were instrumented and tested in 1996. Variables such as the slab thickness, joint spacing, joint condition and asphalt surface preparation were considered in the study. In addition to the development of a rational design procedure for UTW, data collected from these projects has resulted in improved design and construction specifications. Among the recommendations of the study were the installation of tie bars along the longitudinal construction joint, and that whitetopping overlay should not be placed on top of a newly laid HMA. Subsequent work has supported these findings, but emphasized that the properties of the HMA, whether existing or new, be taken into account in the overlay design [2].

Analytical work in the PCA study mentioned above also attempted to account for the load transfer between adjacent slabs as well as the soil support using a system of unidirectional springs. Attempts at modeling the interface bond condition between layers utilizing point-to-point shear-friction gap elements were unsuccessful, and the investigative team subsequently utilized a system of springs to model the interface condition. A finite element program utilizing only shell elements to model pavements – commonly referred to as a 2-D model – was used to perform a parametric analysis, rather than the 3-D model that was developed, in the interests of reducing computational time. Results of the 2-D model were then converted into equivalent 3-D model results by using predictive equations developed from linear regression analysis of results from a control case. Results from the test sections in Colorado were also used in the development of design guidelines for whitetopping by CDOT [4].

Based upon the premise that the structural design of UTW overlays requires precise predictions of loading stresses in the pavement system, a team of investigators from Tokyo, Japan developed a 3-D finite element model that takes into account the viscoelastic behavior of asphalt and the interaction between the concrete overlay and asphalt subbase [9]. Analysis was performed on the program Pave3D, which was developed by one of the investigators for the analysis of pavement structures. Loading tests for both stationary and moving loads were conducted on an instrumented test pavement which was constructed in 1999 with two different joint spacings. The measured strains were compared with the computed strains from the finite element model for both stationary and moving loads. The comparison showed that the viscosity of the asphalt subbase and the interface conditions significantly affects the stress behavior of the pavement, affirming qualitative observations in the studies mentioned earlier from an analytical perspective. The study also demonstrated the applicability and advantage of more complex formulations of the finite element method in analyzing the unique behavior of whitetopped composite pavements. However, the report pointed out that precise prediction of stresses at high temperature conditions was still difficult using the 3-D model, even by incorporating viscoelasticity of the asphalt layer.

While attempts at modeling aspects of the more complex behavior of whitetopped pavements have been successful, much effort is still needed to develop a complete model that successfully predicts pavement behavior under a variety of design variables and conditions. However, in the author's opinion, the seemingly inexhaustible combinations of design variables and project specific considerations, not to mention limited resource availability, may well render this ultimate objective unreachable.

2.3 Finite Element Modeling Techniques for Composite Pavements

Two-dimensional finite element programs such as ISLAB2000 (proprietary revision of ILSL2), J-SLAB, KenPAVE and FEACONS have been used in the analysis of pavement systems. These programs are based upon classical theories of analyzing thin plates (also known as medium-thick plates in pavement literature) on Winkler foundations. They have been effectively used to analyze pavements with various slab sizes, different joint conditions, multiple layers, and with linear temperature differentials. However, these software packages do not allow users to model pavements with varying thickness or cross-slopes. Also, representing the configuration of pavements with widened sections would be difficult if not impossible when using 2-D finite element models to analyze such a structure; therefore, analysis of a composite pavement such as the one found on Iowa Highway 13 requires the development of a 3-D model utilizing a general finite element program such as ABAQUS, ADINA or ANSYS. The analysis package ANSYS was selected for use in the work presented herein, and is presented in detail in Chapter 3 of this report.

2.3.1 Modeling of Concrete and Asphalt Layers

Eight-node solid elements, also known as brick elements, can be used to model the concrete and asphalt layers of the composite pavement. Higher order solid elements, i.e. elements with a higher number of nodes, could also be utilized; however, employing higher order elements results in higher requirements for computational resources. To minimize the burden on computational resources, and to maintain the accuracy of the finite element results, 8-node brick elements can be utilized by including what are known as "extra displacement functions" [23]. These extra displacement functions are used to correct for the parasitic shear that results from the assumed displacement functions associated with the formulation of the 8-node solid element, and allow the element to accurately represent the effects of bending in structures.

Kumara et al.[8] utilized 20-node solid elements to model the UTW pavement layers in their Florida study, whereas Wu et al.[5] and Nishizawa et al.[9] utilized the computationally economical 8-node solid element. In the work presented herein, 8-node solid elements with extra displacement functions were utilized in modeling the composite pavement on Iowa Highway 13.

2.3.2 Interface Modeling Techniques

The effect of interface condition is of particular interest in investigating the behavior of the composite pavement, as previous studies have shown that it has a significant effect on the behavior of the whitetopping pavement system. In the analytical work leading to the development of the PCA design procedure for UTW [5], Wu et al. attempted to model the interface interaction with the use of non-linear shear-friction gap elements, which were 2-node or point-to-point interface elements that were available with the finite element analysis package NISA II. The element is capable of contact determination between the two layers: 'open' or 'closed' status. If the interface is 'open', no transfer of loads between the two surfaces occurs. If 'closed', the element resists normal and tangential forces through the use of three orthogonal springs with frictional capabilities in the horizontal direction. The element was capable of allowing sliding at locations where the shear forces exceeded the shear resistance, thereby simulating partial bonding of the pavement layers. Unfortunately, convergence problems in the resulting non-linear solution process forced the investigative team to abandon this approach, and instead to adopt a model that incorporated horizontal spring elements located at the interface of the concrete and asphalt layers. A bonded interface would be associated with very high values of the horizontal spring stiffnesses, and very low values used for an unbonded interface. Partially bonded conditions would then be modeled by moderate values of the spring stiffnesses, which were determined by a trial and error process. The final model adopted by Wu et al. is shown schematically in Figure 2-2.

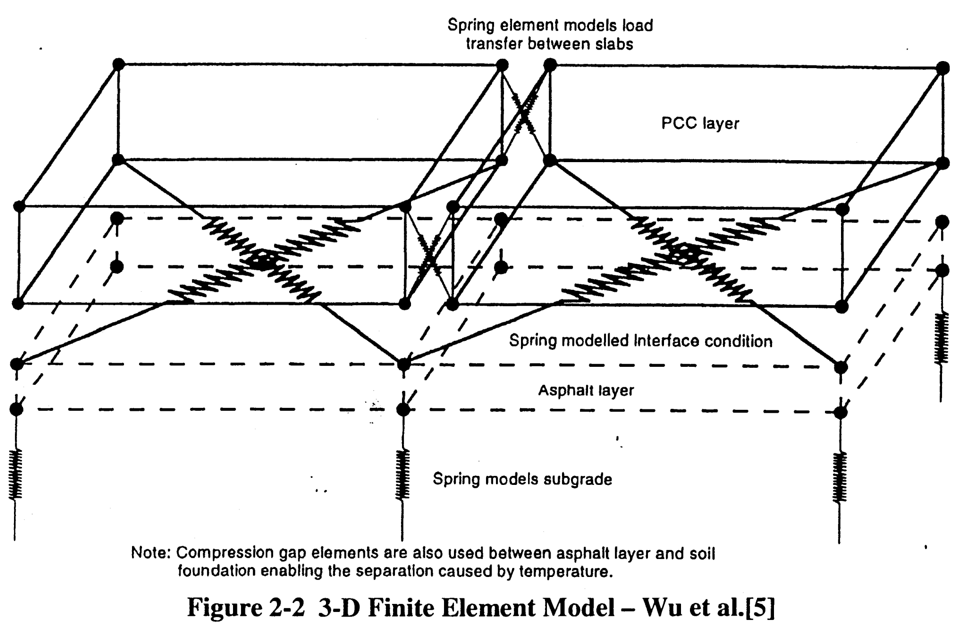

Note: Compression gap elements are also used between asphalt layer and soil foundation enabling the separation caused by temperature.

Figure 2-2 3-D Finite Element Model – Wu et al.[5]

Nishizawa et al. also utilized interface elements to model the interaction of concrete and asphalt layers, and to model the load transfer at the joints as shown in Figure 2-3 [9]. The interface element used by Nishizawa et al. in their study is similar to the shear-friction gap elements used by Wu et al.; however, instead of 2-node elements, the interface elements in this study are surface-to-surface contact elements defined by 4 nodes on each surface. The element is also represented by three orthogonal springs, denoted by the stiffnesses *k* in each of the orthogonal *t*, *n*, and *s* directions in Figure 2-3, but does not include friction capabilities. Modeling of the interface bond condition is performed by varying the tangential stiffnesses: high values for a bonded interface, and low values for an unbonded interface. Only the bonded interface was considered during the analyses performed in this study, as the field load testing indicated that a strong bond existed between the asphalt and concrete layers. Low values for the spring stiffnesses were used to model the joint interfaces due to the joint gap. Similar interface element capabilities are available in the general purpose finite element program ANSYS [24].

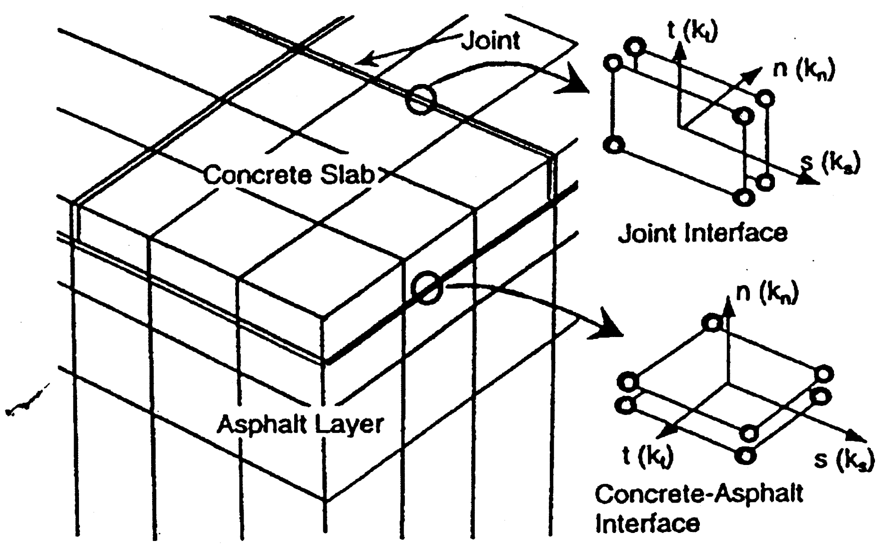

Figure 2-3 Interface Elements – Nishizawa et al.[9]

2.3.3 Foundation Modeling Techniques

In the field of pavement analysis and design, three types of foundations can be assumed: liquid, solid and layer, with liquid foundations being the most common, as the use of liquid foundations results in a matrix that requires very little time to solve [18]. A solid foundation is a more realistic representation of foundation behavior. Also known as a Boussinesq foundation, the deflection at any nodal point in a solid foundation depends not only upon the force at the node itself, but also upon the forces at all the other nodes. The stiffness of the foundation would be calculated using the Boussinesq equation [18], which depends upon the Poisson ratio and the elastic modulus of the foundation.

The layer foundation is known also known as a Burmister foundation, as Burmister's layered theory is used in the formulation of the flexibility matrix for the foundation. The layer foundation is similar to the solid foundation in that deflections at any nodal point also depend upon forces at other nodes. The formulation is much more complex, requiring multiple iterative integrations, and will not be discussed here.

Due to the wide availability of powerful processors and larger storage capacities, Huang [18] recommended the usage of the more realistic solid foundation in lieu of liquid foundations, if necessary. The studies by Nishizawa et al.[9] and Kumara et al.[8] both utilized solid foundations in their 3-D finite element models. In their development of the UTW design procedures for PCA and CDOT, Wu et al.[5] and Tarr et al.[4] utilized the more conventional liquid foundation idealization. In the absence of actual properties of the soil found at the test site, analysis of the composite pavement on Iowa Highway 13 utilized the liquid foundation idealization. Investigation of the differences resulting from the utilization of different methods of foundation idealization is beyond the scope of this study.

3.0 MODELING OF IOWA HIGHWAY 13 COMPOSITE PAVEMENT

As described in Chapter 2, the objective of this work was to investigate the structural behavior of the composite pavement located on Iowa Highway 13. Several general purpose finite element packages, such as ADINA, ABAQUS, ANSYS, etc., are available in the market and could be suitable for the purposes of this study; however, ANSYS [25-27] was chosen for the modeling and analysis of the composite pavement. ANSYS is considered to be one of the most comprehensive and versatile finite element programs today, and has been widely used for research and educational purposes. In addition, it was readily available at Iowa State University. The program offers user-friendly pre- and post-processors that have strong graphical capabilities, which can be used to display results of analyses in various forms. Colored contour plots, superimposed deformed shapes, and animations of structural deformations are among the several graphical capabilities of the ANSYS program.

3.1 Modeling of Composite Pavement for Finite Element Analysis

In order to obtain information on the effects of the different design variables for a composite pavement such as those that were detailed in Chapter 1, a fairly complex model was needed. Models similar to those utilized by Nishikawa et al. [9] and Ingram [15] can be used. In the work presented herein, solid elements were used to construct the PCC base, asphalt and whitetopping layers. Surface-to-surface interface elements were used at the interfaces between layers and between joints in the whitetopping. In addition, beam elements were used to model the tie bars in the pavement when applicable.

As presented in the previous chapter, the effect of the soil beneath the composite pavement was modeled using a Winkler foundation. With this idealization, nodal springs with the appropriate values of stiffness equivalent to the desired soil subgrade modulus are typically utilized. The ANSYS program allows users to define a Winkler foundation without having to define individual nodal springs when using plate elements; thus, a thin layer of plate elements coinciding with the bottom surface of the solid elements of the bottom PCC layer was employed to represent the effect of the Winkler foundation. This is not a new methodology, and was used extensively by Ingram [15] in her study of the performance of different tie bar shapes in PCC pavements, and also in the initial analysis of the composite pavement of Iowa Highway 30 prior to this study [1].

3.1.1 Types of Elements Used to Model the Composite Pavement

The following is a brief description of the elements that were used in modeling and analyzing the composite pavement on Iowa Highway 13.

3.1.1.1 Solid Elements

SOLID45 is an 8-node brick element used for the three-dimensional modeling of the different layers in the composite pavement. The element has 3 degrees of freedom at each node: translations in the nodal x-, y- and z-axes. Additionally, the element is capable of representing orthotropic material properties, and has plasticity, creep, swelling, stress stiffening, large deflection and large strain capabilities. The element is capable of supporting concentrated forces at the nodes, pressures on any surface, and temperature differentials across the body of the element.

As the element has only 2 nodes on each edge, the resulting interpolation functions for the element are linear. Consequently, analysis involving the basic 8-node element would yield constant strains and stresses across the element, which is inaccurate to account for bending effects. Higher order elements which involve additional nodes on each edge of the element would allow for the variation of stresses and strains across the element. Unfortunately, higher order elements would also require increased computing time during the analysis. The alternative to higher order elements would be to include extra shape functions in the element stiffness formulation [23]. ANSYS provides such an option when using SOLID45.

3.1.1.2 Plate Elements

SHELL63 is an element with both bending and membrane capabilities, with in-plane and normal loads permitted. The element is defined by 4 nodes, with six degrees of freedom at each node, incorporating translations and rotations in each of the orthogonal directions. Orthotropic material properties are permitted, and the element allows for a smoothly varying thickness across the element. An Elastic Foundation Stiffness (EFS) can be defined, which is equivalent to the soil subgrade modulus associated with a Winkler foundation. This allows for a convenient method for idealizing a liquid foundation in the pavement model that is less time consuming than defining individual nodal springs.

As solid elements do not have EFS capabilities, a very thin layer of plate elements was placed beneath the pavement structure to include the foundation effects without artificially increasing the stiffness of the pavement structure. Similar to the brick element, concentrated forces, pressures and temperature differentials may be applied to the element.

3.1.1.3 Beam Elements

A 3-D beam element, BEAM4, was selected to model the tie bars that were placed along the edge of the pavement and the widening unit. The element has tension, compression, bending and torsion capabilities. The cross-sectional area, area moments of inertia, torsional moment of inertia, and thicknesses in two directions may be specified. The element may also be defined with an initial strain if necessary. Once again, the element is capable of supporting forces, pressures and temperature differentials.

3.1.1.4 Interface Elements

ANSYS provides several elements that can be utilized to model the interface between two elements that are in contact. Contact between two surfaces can be conveniently modeled in ANSYS by utilizing the surface-to-surface contact elements TARGE170 and CONTA174. Each of these 'contact pairs' is capable of representing contact and sliding between two 3-D surfaces, with the 'target' elements (TARGE170) defining the stiffer surface, and 'contact' elements (CONTA174) defining the deformable surface. If both surfaces are of equal stiffness, either may be designated as the target or contact. The elements are superimposed on the surfaces of solid or shell elements that make up the interface, and have the same geometry and node ordering as the underlying elements. It is of utmost importance that the contact and target surface normals, as defined by the right-hand rule going around the nodes of the element, i.e. counterclockwise around nodes *i* through *l* in Figure 3-1, always point away from the element.

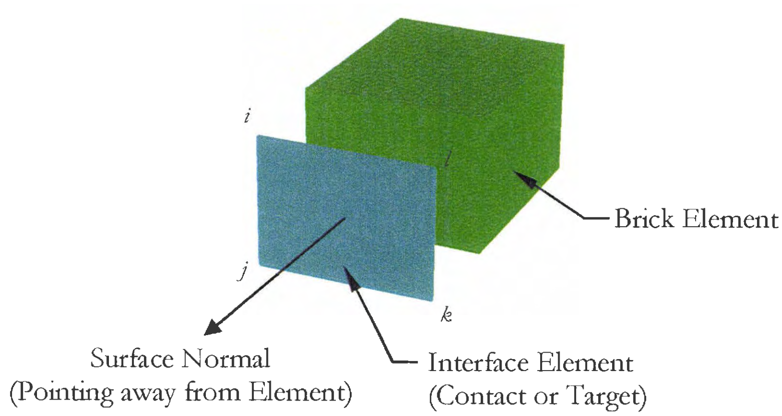

Figure 3-1 Orientation of Interface Elements

The status of contact pairs could either be 'closed', i.e. in contact; or 'open', i.e. not in contact and no load transfer between the two surfaces take place. Interface elements introduce geometric nonlinearity in the solution process, resulting in increased computing time. Consequently, iterative solutions must be repeated until the status of each interface does not change, while at the same time satisfying the force and displacement convergence criteria and ensuring that penetration between the surfaces stays within acceptable tolerances.

The mechanics of the contact pair involves normal and tangential contact stiffnesses. The normal contact stiffness governs the amount of penetration between the two surfaces. ANSYS estimates the normal contact stiffness based upon the material properties of the underlying elements; however, the stiffness can be adjusted by the user if necessary. Using a larger contact stiffness, while beneficial in reducing penetration, could result in convergence difficulties. Alternatively, a contact stiffness that is too low would allow too much penetration and render the results inaccurate.

The tangential stiffness governs the sliding of the contact surfaces with respect to one another, and is automatically defined by ANSYS to be proportional to the coefficient of friction and the contact stiffness. The friction model adopted by ANSYS is based upon Coulomb friction, where sliding occurs when the shear stress exceeds the sliding resistance, τ, which is expressed as:

$$\tau = \mu p + c\,; \qquad \text{(Eq. 3-1)}$$

where μ is the coefficient of friction, c is the cohesion sliding resistance between the two layers, and p is the normal contact pressure. A maximum contact shear stress, τ_{max}, may also be defined so that no matter what the magnitude of the contact pressure, p, sliding will occur if the maximum contact shear stress is exceeded. This is illustrated schematically in Figure 3-2. The element also supports different values of static and dynamic friction. A similar model is not provided for the normal direction, whereby cohesion in the normal direction can be specified.

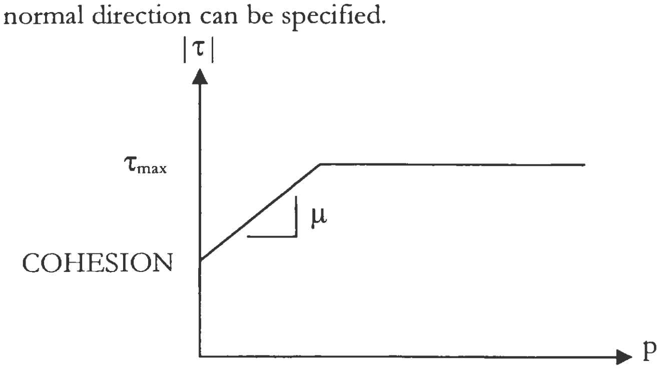

Figure 3-2 Friction Model

As bond strength information from the composite pavement on Iowa Highway 13 was available [1], this friction model could potentially allow for a more precise prediction of the pavement bond behavior by taking into account both friction between the layers and bond strength in the form of cohesion. However, this avenue of study was not pursued due to the uncertainty associated with the partial bonding mechanism, which could result from methods of construction, temperature differentials, and actual properties of the materials used in constructing the pavement structure. In addition, the model would only be able to detect instances of layer unbonding due to the loading used in the analysis, and is thus useful only when analyzing newly constructed composite pavements under controlled conditions. Bond strength information in the direction normal to the interfaces was also not available, which would render a study of the interface behavior incomplete; hence, this study was focused upon the behavior of the pavement at two extremes, i.e., fully bonded and unbonded layers.

The interface elements also provide the user with the option of pre-selecting surface interaction models for specific cases. The interface models are listed as follows:

- 'Standard' contact imposes no limits upon the behavior of the interface, and the interface elements are free to slide or separate as the situation warrants.
- 'Rough' contact models perfectly rough contact and the input value of μ is ignored, although separation is allowed.
- 'No separation' contact allows sliding of the surfaces relative to one another, but does not allow the surfaces to 'open'.
- 'Bonded' contact bonds the contact and target surfaces in all directions.

The features listed above are user-friendly for modeling different cases of surface interaction without having to manually change interface spring stiffness values as was done in previous studies [5, 9]. In this work, the 'bonded' model was used for investigating the behavior of the composite pavement when a strong bond exists in all layers. 'Standard' or 'no separation' was also used for unbonded layers, depending upon whether separation between the surfaces was expected.

3.1.2 Finite Element Modeling of Composite Pavement on Iowa Highway 13

A portion of the Iowa Highway 13 pavement was modeled for the finite element analysis utilizing the elements presented in the preceding section. The model length was 72 ft, and the cross-section was as shown in Figure 1-1. The length of the model was selected to ensure that at least one truck load could be placed on the pavement. The length of 72 ft also allowed the modeling of the joint configurations under consideration, i.e. 4.5 ft x 4.5 ft, 6 ft x 6 ft, and 9 ft x 9 ft, such that the panel edges coincided with the model boundaries.

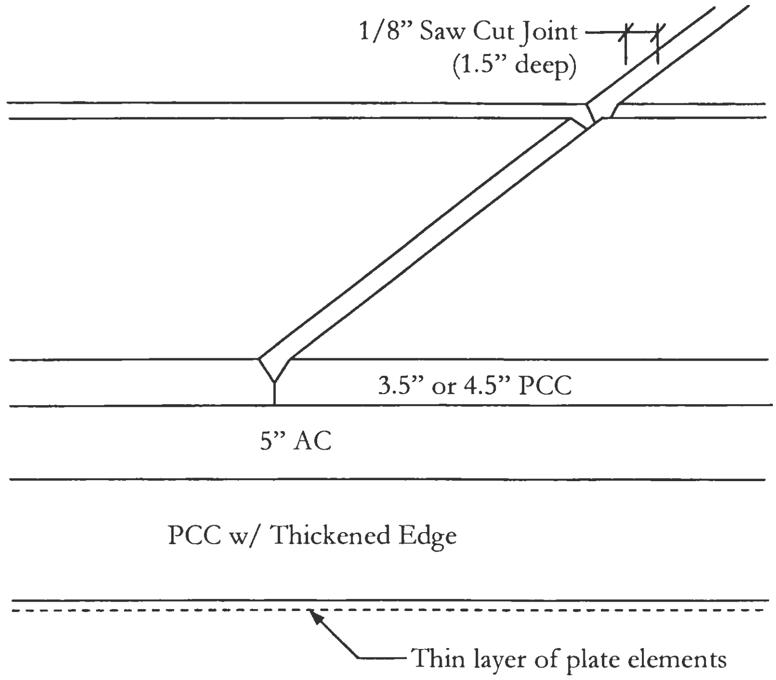

Figure 3-3 Finite Element Model Details (not to scale)

As described previously, the top PCC (whitetopping), AC and bottom PCC layers were meshed with solid brick elements. To model the soil beneath the pavement, a very thin layer of plate elements was placed underlying the bottom PCC layer, as well as beneath the widening units on both sides of the pavement. The whitetopping and AC layers were modeled with two layers of solid elements through the thickness, while the bottom PCC layer was modeled with three layers of solid elements. Interface elements were placed in between the layers, i.e. at the PCC-ACC interface, and at the ACC-whitetopping interface, so that the effects of interface bonding and unbonding could be studied. A similar approach was utilized to model the interface between PCC widening units and the original pavement structure, i.e. the two edges along lines 1-1 and 2-2 (Figure 3-5)

Saw-cut joints were modeled as V-cuts that were 1/8 in. wide at the whitetopping surface, with a depth of 1.5 in as shown in Figure 3-3, per the construction report [1]. The joint cracks in the model were analyzed with 1.5-in. depth, and with the cracks extending through the thickness of the whitetopping. Apart from the saw-cut joints, the ACC and PCC layers were assumed to be crack-free. Interface elements were utilized between the joints according to the crack depth being studied.

Each tie bar was modeled with several beam elements that were connected together to form a single tie bar. This method allows the collection of information about bending stresses, elastic strains, shear forces and moments along the length of the tie bar.

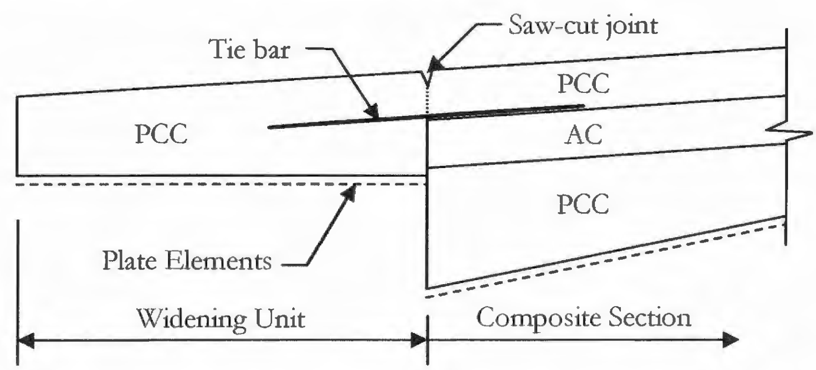

Figure 3-4 Location of Tie Bars (not to scale)

Figure 3.5 shows a model that was constructed for the analysis of the composite pavement on Iowa Highway 13, having a whitetopping thickness of 3.5 in., and joint spacing of 4.5ft x 4.5ft. A total of six models were developed to cover the range of different joint spacings, and the two whitetopping thicknesses. Modifications were made to these base models when necessary to study the effects of tie bar placement and widening unit configurations, which will be discussed in Chapter 5.

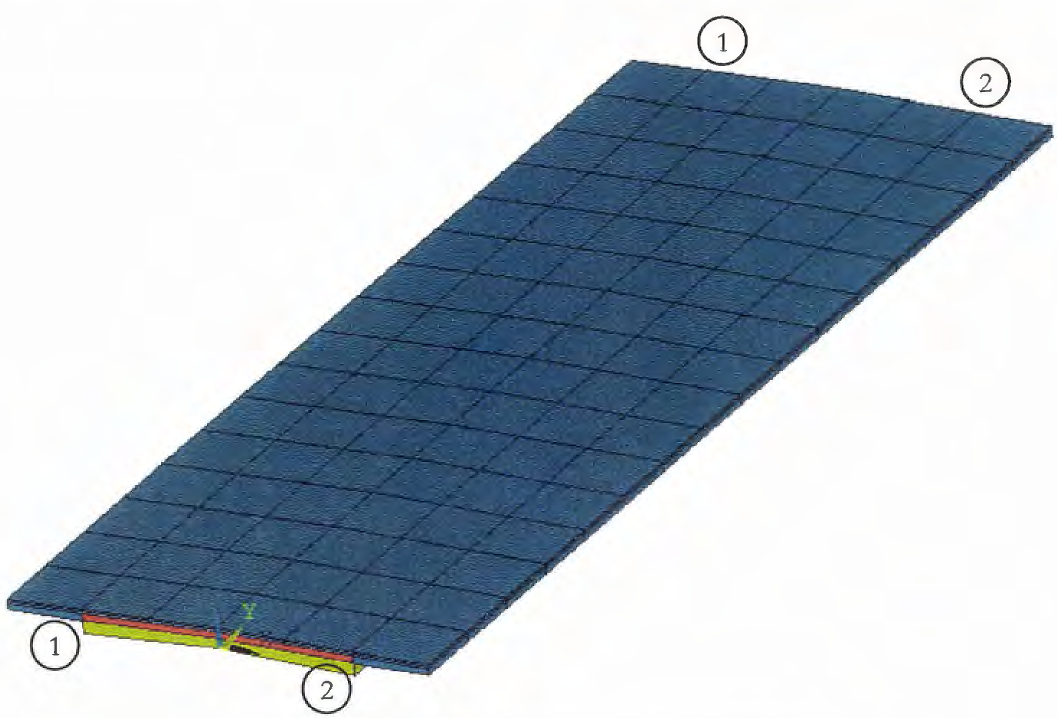

Figure 3-5 Sample Composite Pavement Model

3.2 Verification of ANSYS Model

Prior to the analysis of the composite pavement on Iowa Highway 13, steps were taken to verify the applicability of the elements and the modeling techniques chosen for the analysis of the composite pavement. A series of simple problems were devised, and the deflection and stress results from finite element analyses were compared with known solutions.

3.2.1 Analysis of a Layered Beam

In order to investigate the performance of the brick element SOLID45 in bending problems, as well as the use of the interface elements TARGE170 & CONTA174, a simple beam with a span of 20 ft under a 5-kip load at mid-span was modeled in ANSYS. The cross-sectional dimension and the material properties used in this problem are shown in Figure 3-6.

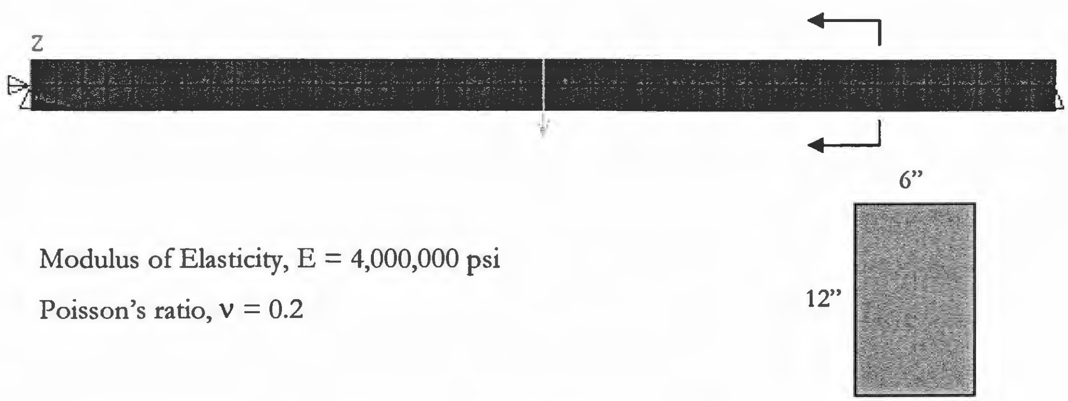

Figure 3-6 Simply Supported Beam

The beam in Figure 3-6 was modeled in ANSYS with a medium-coarse mesh, with individual elements having dimensions of 6”x6”x6”. Analysis of the simply supported problem in ANSYS yielded the following results:

$\sigma = 2038\,\text{psi}$

$\delta = 0.4189\,\text{in}$

Comparing these results with hand calculations using beam theory revealed a 2.2% and 0.1% difference in the longitudinal stress and deflection, respectively. The good agreement with theoretical results indicated that the brick elements with extra shape functions can be suitable for use in bending problems.

Further analyses were performed to determine if the interface elements performed as expected. This was accomplished by solving the following cases:

Case 1: The beam problem was analyzed assuming that the cross-section of the beam described above consisted of two 6-in. layers. A contact pair was placed at the interface between the two beam layers, with the 'bonded' interaction model selected. The results were expected to be close to those obtained above, if not exactly the same. The following values were obtained from the analysis:

$\sigma = 2046$ psi, i.e with 0.4% difference from the case analyzed above

$\delta = 0.4195$ in, i.e. with 0.02% difference from the case analyzed above

These results demonstrate that the 'bonded' interaction model is competent in representing bonded contact between two layers.

Case 2: The system was as configured in Case 1, and the 'unbonded' model interaction was investigated, with both cohesion and coefficient of friction values set to zero to simulate frictionless contact. Again, using beam theory, one expects that the stress for this case to be twice as much, and the deflection should be 4 times as much as that calculated above.

The finite element results yielded a maximum stress of 4079 psi, along with a maximum deflection of 1.667 in. These results confirm the suitability of using interface elements to represent the behavior of unbonded layers.

3.2.2 Analysis of a Plate on Elastic Foundation

A simply supported plate on an elastic foundation under uniform pressure loading, shown in Figure 3-7, was considered in examining the appropriateness of using a thin layer of SHELL63 elements to represent a Winkler foundation. The plate dimensions were 40"x40" and simply supported on all sides. The system was the same as that used by Voyiadjis & Kattan [20]. The elastic modulus of the plate material was 30×10^6 psi, with a Poisson ratio of 0.3. The uniform loading on the plate was 10,000 psi. Plate thicknesses of 2 in. and 4 in. were investigated, as were soil subgrade moduli of 200 psi, 2,000 psi and 20,000 psi. Two layers of solid elements were used to allow placement of simple supports at mid-depth of the plate.

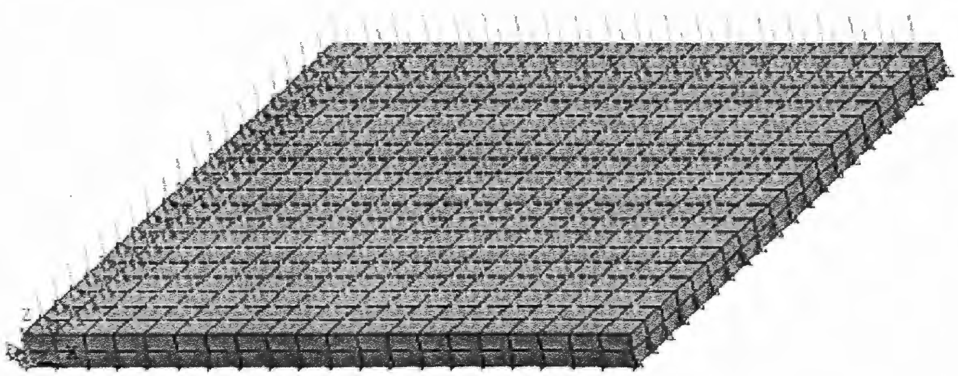

Figure 3-7 Simply Supported Plate on Elastic Foundation

Deflection results from the finite element analysis were compared with the deflections calculated by Voyiadjis & Kattan based upon their theoretical approach, and are presented in Table 3-1. *h* denotes the thickness of the plate, and *a* the horizontal dimension of the plate, which is 40" in this case.

Table 3-1 Comparison of ANSYS Results with Theoretical results

	Max Deflection (ANSYS) k (lb/in^2)			Max Deflection (Theoretical) k (lb/in^2)		
h/a	200	2000	20000	200	2000	20000
0.05	4.605	2.978	0.604	4.62572	3.06042	0.69811
0.1	0.649	0.603	0.351	0.62998	0.58941	0.35855

The close agreement of the results from the ANSYS model with the theoretical results by Voyiadjis & Kattan validates the modeling techniques used in this analysis. In particular, the use of the

EFS function with a thin layer of SHELL63 elements was demonstrated to be a viable means of representing a liquid foundation in a finite element model. Also, the results confirm once again the applicability of using SOLID45 elements to model a bending problem.

3.2.3 Comparison of ANSYS and ISLAB2000 Results

ISLAB2000 is the proprietary revision of ILSL2, which is a 2-D finite element program developed at the University of Illinois-Urbana Champaign specifically for analyzing pavements. The program has been widely used in analytical studies of pavements, including in the development of whitetopping design guidelines by the PCA and CDOT. Although the program is considered reliable by the pavement research community, ISLAB2000 is unsuitable for use in the study as it cannot adequately account for the complex geometry exhibited by the Iowa Highway 13 pavement. However, by comparing results of a pavement analyzed using ANSYS with the results obtained by ISLAB2000, the accuracy of the general finite element program can be ascertained.

For the purposes of the comparison, an 18 ft wide by 72 ft long pavement structure of 8" thick PCC was modeled. The pavement section had no joints, and was subjected to heavy truck loads. The 3-D model in ANSYS consisted of solid elements representing the PCC pavement, with a thin layer of shell elements underlying the solid elements to represent the Winkler foundation. The 2-D model in ISLAB2000 utilizes plate bending elements.

Analyses of the pavement were performed using different element sizes for both finite element programs to aid in the selection of an appropriate mesh size for the Iowa Highway 13 composite pavement model. A pseudo truck load was applied for the analyses in ANSYS and ISLAB, and the configuration is shown in Figure 3-8.

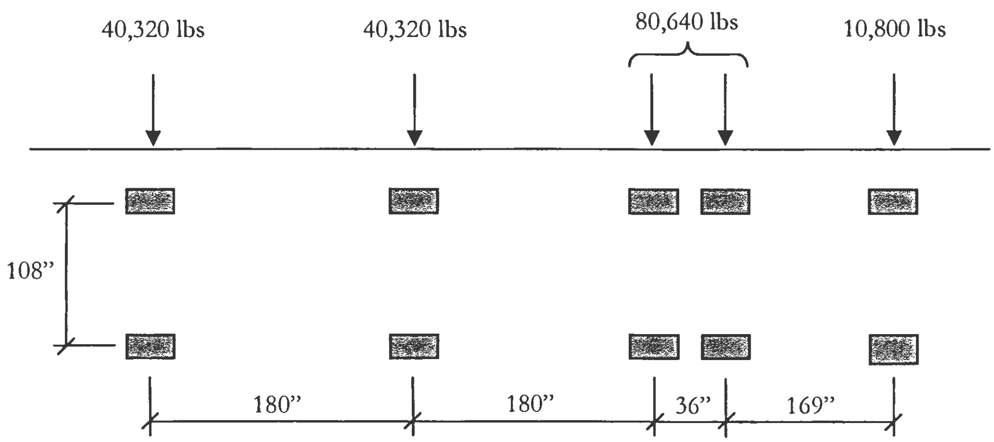

Figure 3-8 Configuration of Truck Loading for ANSYS and ISLAB2000 Comparison

The maximum deflections and stresses were obtained, and the results are summarized in Table 3-2.

Table 3-2 Comparison Between ANSYS and ISLAB2000 – Single Layer Pavement

	Elem. Size	Deflection, (in)	Transverse Stress (psi)	Longitudinal Stress (psi)
ISLAB	12”x12”	0.0207	321.0	281.7
(2-D model)	6”x6”	0.0208	312.1	345.5
	4”x4”	0.0207	310.7	328.4
	3”x3”	0.0207	308.6	333.1
ANSYS	12”x12”x8”	0.0222	249.8	231.1
(3-D model)	6”x6”x4”	0.0225	301.3	300.7
	4”x4”x4”	0.0225	311.5	323.2
	3”x3”x4”	0.0225	314.4	337.8

The results showed that for both finite element programs, variations in the stresses were converging as the element sizes were reduced. The differences in the results could be due to difference in the formulation of the stiffness of the shell element used in ISLAB2000 and the solid element in ANSYS. The size of the elements used did not seem to affect the deflection results, with ANSYS estimating slightly higher deflections for the pavement under the exact same loads than ISLAB2000.

Another analysis was performed for a pavement with 7 in. PCC overlaid with 3 in. ACC supported by a Winkler foundation. The pavement was subjected to the same truck loading shown in Figure 3-8. The pavement dimensions were changed to 60 ft long and 18 ft wide, and the interface between the layers was modeled as fully bonded. The ACC layer was modeled with 1 layer of solid elements for all cases in the solid model, although the PCC layer was again modeled with two layers of elements through the thickness when investigating finer finite element meshes.

Table 3-3 summarizes the maximum deflection and stresses predicted by both ANSYS and ISLAB2000 models. The element sizes for ANSYS listed in Table 3-3 refer to the element sizes in the PCC layer. As can be observed from the results, a finer mesh yields a good agreement between the two models, although the pattern of convergence is different. These two comparisons also show that the elements to be used in the composite pavement analysis should be limited to a size of 3"x3" or smaller to obtain accurate results.

Table 3-3 Comparison Between ANSYS and ISLAB2000 – Two Layer Pavement

	Elem. Size	Deflection (in)	Transverse Stress (psi)	Longitudinal Stress (psi)
ISLAB	12"x12"	0.0221	338.7	297.0
	6"x6"	0.0222	329.7	367.4
	3"x3"	0.0222	325.5	353.7
ANSYS	12"x12"x7"	0.0245	252.2	242.9
	6"x6"x3.5"	0.0240	317.8	326.6
	3"x3"x3.5"	0.0241	337.2	353.0

Having obtained confidence in the performance of the elements utilized, and the adequacy of the modeling techniques selected to develop the 3-D model of the composite pavement on Iowa Highway 13 for the ANSYS program, the pavement model was then analyzed and the results compared to the collected field data to further determine the applicability of the 3-D model to the composite pavement on Iowa Highway 13.

4.0 FIELD INVESTIGATION OF IOWA HIGHWAY 13 COMPOSITE PAVEMENT

In order to determine the applicability of utilizing the finite element method to analyze the composite pavement on Iowa Highway 13, field testing of the pavement was carried out. In addition, since soil data was unavailable, it was necessary to determine a representative value suitable for the soil subgrade reaction modulus, k_s. This was accomplished by comparing the measured deflection results with analytical results that were obtained using different values for the soil subgrade. Next, the pavement model was analyzed with the selected value of k_s to determine the computed strains at the gage locations, which were compared to the measured strains obtained from field testing.

4.1 Field Test

4.1.1 Collection of Deflection Data

Deflection data from the composite pavement was obtained using Falling Weight Deflectometer (FWD) testing, which has been widely used in pavement research. FWD testing was performed a total of five times from May 2002 to May 2004 at various locations along the 9.6 mile test site on Iowa Highway 13. Two of the five tests had been performed prior to overlaying and widening of the original pavement with PCC. Details of the testing procedure, testing equipment and test locations were documented in the construction report [1]. Figure 4-1 is a schematic showing the arrangement of the sensors on the FWD test equipment used on this project.

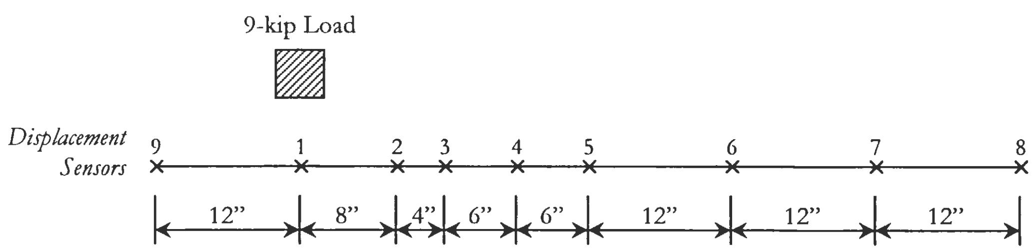

Figure 4-1 Schematic of FWD Deflection Sensors

The test locations along Iowa Highway 13 were kept constant throughout the different test dates, and were selected such that all the pavement sections constructed with different combinations of the design variables were included in the testing program. The maximum deflections (corresponding to sensor no. 1) presented in Tables 4-1 and 4-2 are the average values of several deflection readings gathered from the field test. These are tabulated according to surface preparation, joint spacing and type of fiber used in the overlay. Detailed test data was documented in the construction report [1].

Table 4-1 Breakdown of Maximum Deflection Data from FWD Test – 3.5" Whitetopping Pavement

	Max Deflection (in)								
	Scarify			HMA Stress Relief			Patch		
Fiber Type	4.5 x 4.5	6 x 6	9 x 9	4.5 x 4.5	6 x 6	9 x 9	4.5 x 4.5	6 x 6	9 x 9
No Fibers	0.00412	0.00495	n/a	0.00520	0.00369	n/a	0.00595	0.00518	n/a
Fiber Type A	n/a	n/a	n/a	0.00452	0.00526	n/a	0.00568	0.00641	n/a
Fiber Type B	0.00556	0.00442	n/a	0.00500	0.00433	n/a	0.00445	0.00531	n/a
Fiber Type C	n/a	0.00567	n/a	n/a	n/a	0.004472	n/a	0.00560	n/a

Table 4-1 Breakdown of Maximum Deflection Data from FWD Test – 4.5" Whitetopping Pavem

	Max Deflection (in)								
	Scarify			HMA Stress Relief			Patch		
Fiber Type	4.5 x 4.5	6 x 6	9 x 9	4.5 x 4.5	6 x 6	9 x 9	4.5 x 4.5	6 x 6	9 x 9
No Fibers	0.00581	0.00573	n/a	0.00497	0.00417	n/a	0.00387	0.00371	n/a
Fiber Type A	0.00539	0.00294	n/a	0.00371	0.00352	n/a	0.00530	0.00489	n/a
Fiber Type B	0.00262	0.00370	n/a	0.00424	0.00592	n/a	0.00409	0.00637	n/a
Fiber Type C	n/a	n/a	0.00510	n/a	n/a	0.00450	n/a	n/a	0.00478

4.1.2 Collection of Strain Data

The composite pavement on Iowa Highway 13 was instrumented with strain gages to obtain the strains induced in the pavement under truck loading. Five locations along Iowa Highway 13 were instrumented, each with 3 sets of gages spaced approximately two joint panels apart. The pavement configurations of the instrumented locations were as follows:

- Site 1: 3.5" whitetopping thickness, joints spaced 4.5 ft x 4.5 ft with longitudinal gage orientation
- Site 2: 3.5" whitetopping thickness, joints spaced 6 ft x 6 ft with transverse gage orientation
- Site 3: 4.5" whitetopping thickness, joints spaced 9 ft x 9 ft with longitudinal gage orientation
- Site 4: 4.5" whitetopping thickness, joints spaced 4.5 ft x 4.5 ft with transverse gage orientation
- Site 5: 4.5" whitetopping thickness, joints spaced 6 ft x 6 ft with longitudinal gage orientation

The exact stationing and layout of the gages are detailed in Appendix A.

Three cores, designated as Core 1, 2 and 3, were taken at each of the five sites listed above. At each core location, three strain gages were mounted: (1) on top of the bottom PCC; (2) on top of the ACC; and (3) on top of the whitetopping surface. Installation of the gages was performed by first coring from the top of the whitetopping to the top of the base PCC layer, after which a strain gage was placed on the PCC surface. An ACC mix was then added to fill the core up to the top of the original ACC layer, which was followed by the installation of a second strain gage on the surface of the ACC fill material. Finally, a concrete mix was used to fill the core up to the top of the whitetopping PCC, and the third strain gage was then placed on the top of the whitetopping. Unfortunately, several of the strain gages placed on the top of the whitetopping were damaged by vehicular traffic before testing was performed. Similarly, temperature gages were also installed in different cores at the five test sites listed above. These gages were used to gather data on the temperature differentials experienced by the composite pavement.

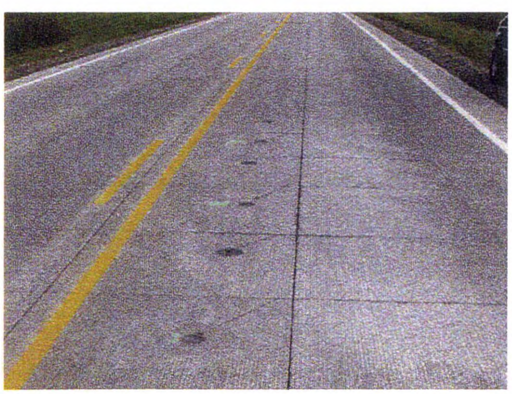

Figure 4-2 Temperature and Strain Gages Along Iowa Highway 13

Two load tests were performed on the five test sites listed above with a fully loaded truck provided by the Iowa Department of Transportation (IDOT). However, only the load test performed on September 10, 2004 was used in this study as static load tests were performed alongside moving load tests only on that testing date. The load configuration was as shown in Figure 4-3.

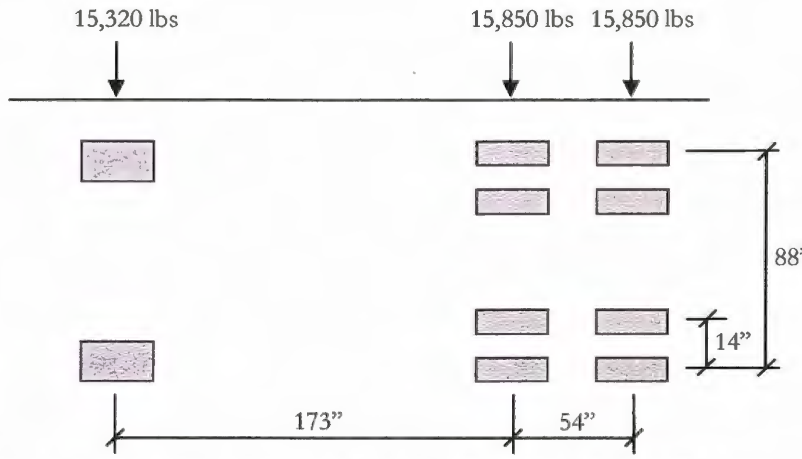

Figure 4-3 Configuration of Truck Load Used for Strain Data Collection

Figure 4-4 Test Truck Provided by IDOT for Strain Data Collection

Strain gage readings were continuously recorded as the truck was slowly driven over the three strain gage locations at each of the 5 test sites. A static load test was also performed by stopping the truck momentarily on one of the three instrumented cores at each instrumented site. Unfortunately, analysis of the data collected from the load test suggests that many of the strain gages installed did not function as intended. Only 13 of the 45 strain gages that were installed provided any discernable information.

Figure 4-5 shows a typical recording of the strain gage readings that were collected during the load test. The colored lines represent the readings from the three strain gages installed in the different layers as the truck traveled along the composite pavement. The readings at the extreme left and right of the chart correspond to the strain gage readings taken when the truck was significantly distant from the strain gages, and hence represent the 'zero' readings of the strain gages in question. The peak in the solid horizontal black line indicates the portion of the measurements that corresponds to measurements collected during the static load test, which was of particular interest to this study.

A trend-line was fitted to the readings of each strain gage on a trial and error basis to determine a best-fit line that represents the data collected adequately. Examples of these best-fit trend-lines are shown in Figure 4-5 as black, dashed lines. The strain reading for the static load test was then approximated utilizing the trend-line by taking the difference between the strains corresponding to the static test and 'zero' readings.

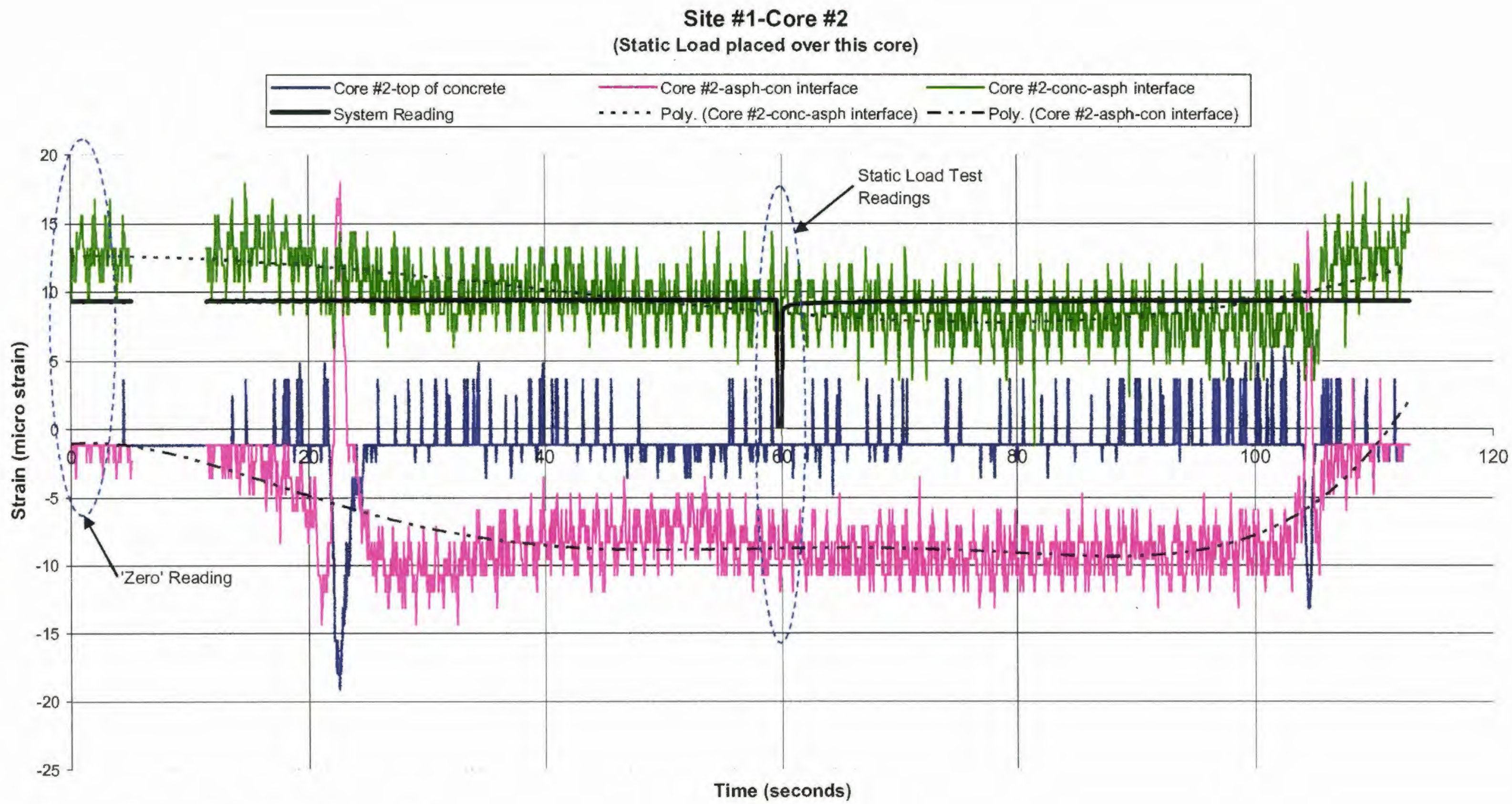

Figure 4-5 example of Strain Gage Data

4.2 Composite Pavement Analysis with Field Test Loads

The composite pavement on Iowa Highway 13 was analyzed under the different test loads described in the previous section. This required knowledge of the properties of the pavement materials and the soil subgrade reaction. Unfortunately, detailed information regarding these parameters was not available and had to be estimated from well-established norms. Information gathered from communication with IDOT provided an estimate on the compressive strength of the whitetopping layer of 4500 psi. The modulus of elasticity for the ACC layer was estimated from common values encountered in the central Iowa region [22]. Values of the ACC modulus of elasticity from the spring and fall seasons were utilized to reach an estimate of 650,000 psi for the modulus of elasticity of the ACC layer in this study. This value corresponds with the time when the different field tests were performed. Typical values of 0.35 and 0.2 were assumed for the Poisson's ratio of asphalt and concrete, respectively.

As mentioned previously, information regarding the properties of the soil beneath the pavement was not known; thus, it was necessary to determine the modulus of subgrade reaction, k_s, using a different approach. While an estimate of 75 pci was suggested [21], the value of k_s was estimated based upon the more rational method of comparing analysis results with the deflection data obtained from FWD testing.

When modeling the composite pavement using the element size of 3"x3" obtained from the sensitivity study summarized in Section 3.2.3, the resulting number of elements required to model the pavement exceeded the maximum number of elements that could be accommodated by the software. Thus, it was necessary to reduce the number of elements, and the slightly larger element size of 6"x6" was used throughout this study.

4.2.1 Comparison with FWD Deflection Data

In order to determine a suitable value of the soil subgrade modulus, the six base models developed in Section 3.1.2 were subjected to a 9-kip load placed at the edge of a transverse joint and close to the edge of the 18-ft composite section. This was similar to the magnitude and location of the load applied during FWD testing of the composite pavement on Iowa Highway 13. Different soil subgrade reaction values of 85 pci, 100 pci, and 150 pci were used to investigate the effects of the soil subgrade reaction on the deflection of the pavement. Deflection results obtained from the analysis were recorded at locations corresponding to the deflection sensors (see Figure 4-1). An example of the deformed shape of the composite pavement subjected to the 9-kip FWD loading is shown in Figure 4-6. Figure 4-7 shows the cross-section of the pavement where the maximum deflection occurred. The deflection profiles for the different pavement configurations as predicted by the finite element analysis and the corresponding measured deflection profiles are shown in Figures 4-8 to 4-13.

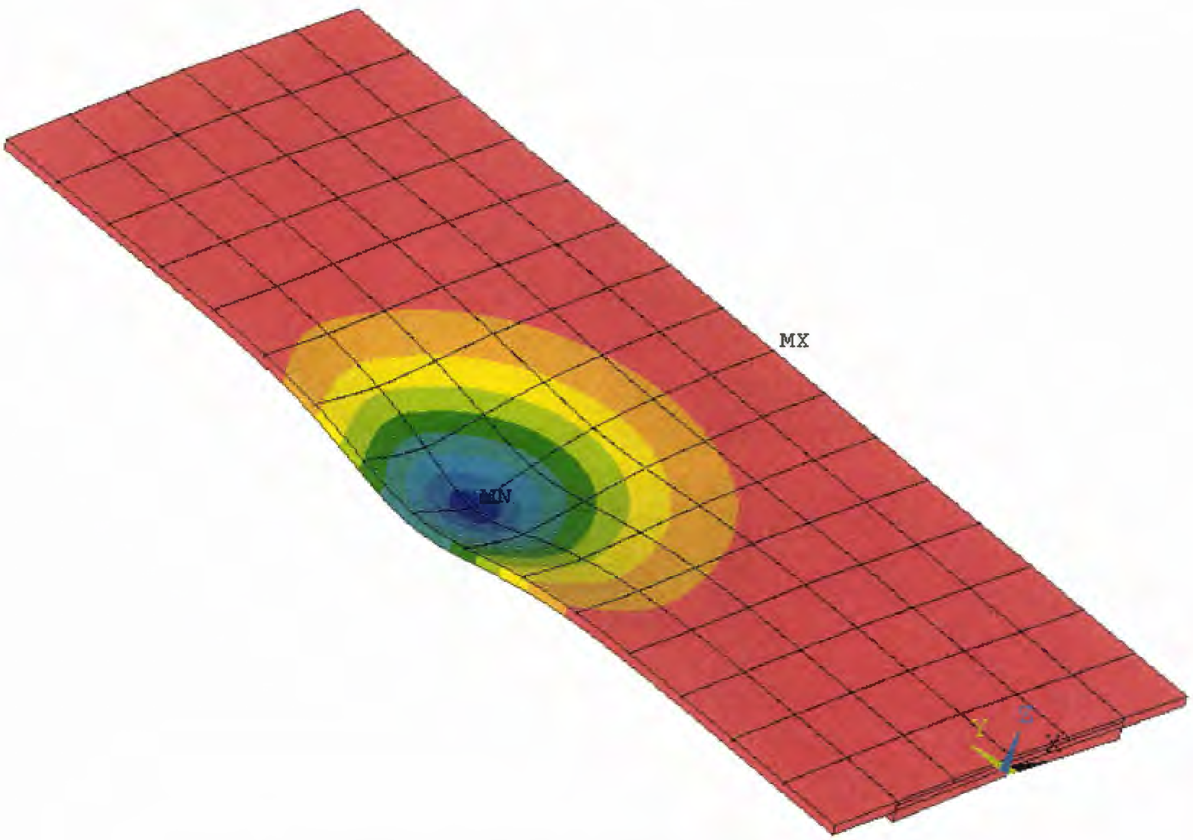

Figure 4-6 Example of Composite Pavement Deflected Shape (9-kip Load) (Plan View – Exaggerated Scale)

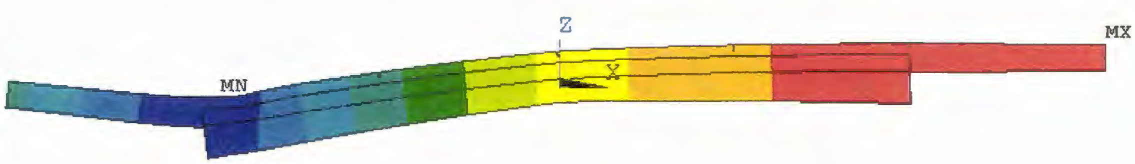

Figure 4-7 Example of Composite Pavement Deflected Shape (9-kip Load) (Cross-Section View – Exaggerated Scale)

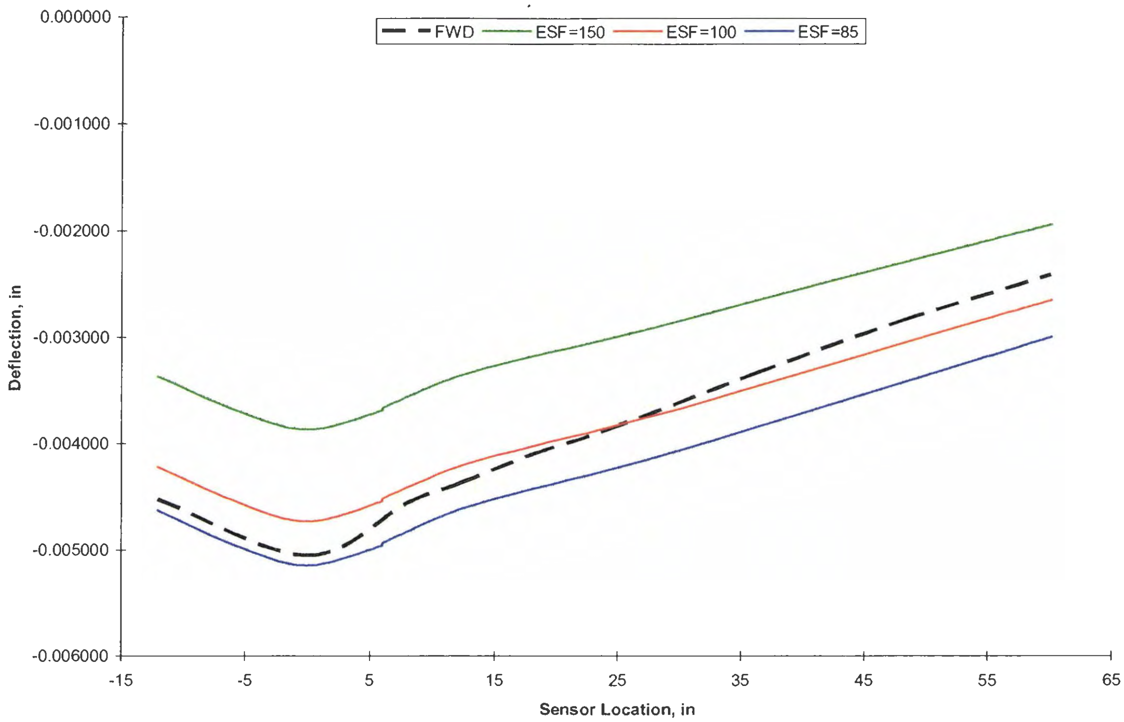

Figure 4-8 Deflection Comparison for Pavement with 3.5" Whitetopping and 4.5ft Joint Spacing

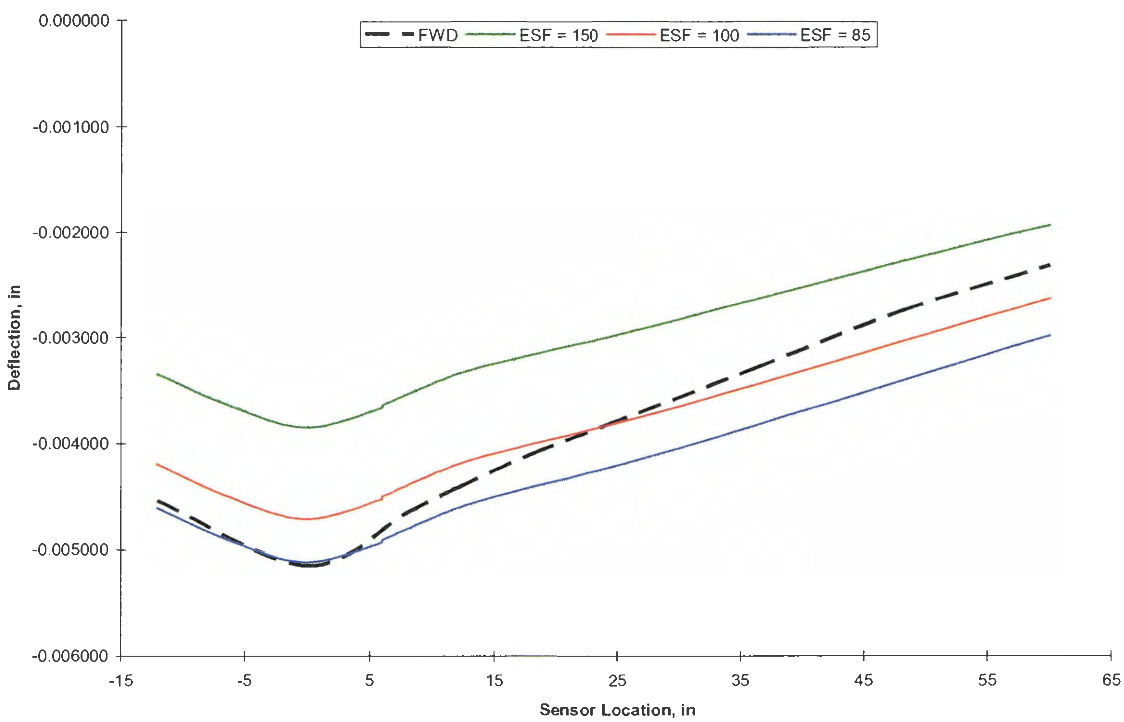

Figure 4-9 Deflection Comparison for Pavement with 3.5" Whitetopping and 6ft Joint Spacing

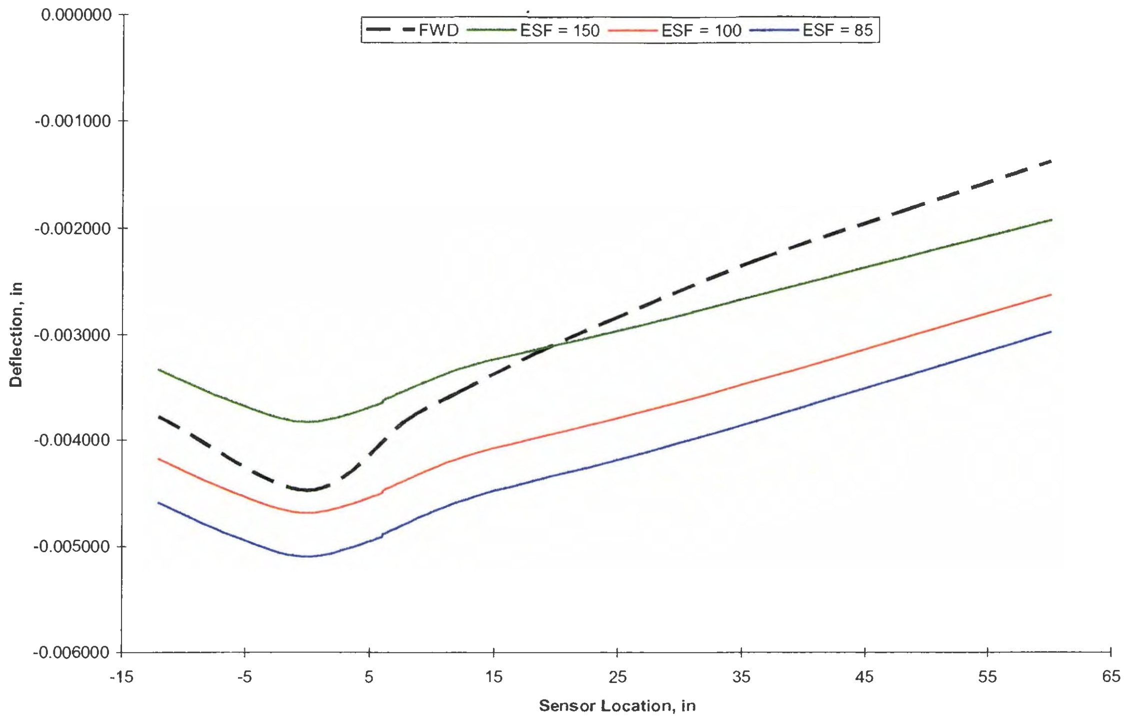

Figure 4-10 Deflection Comparison for Pavement with 3.5" Whitetopping and 9ft Joint Spacing

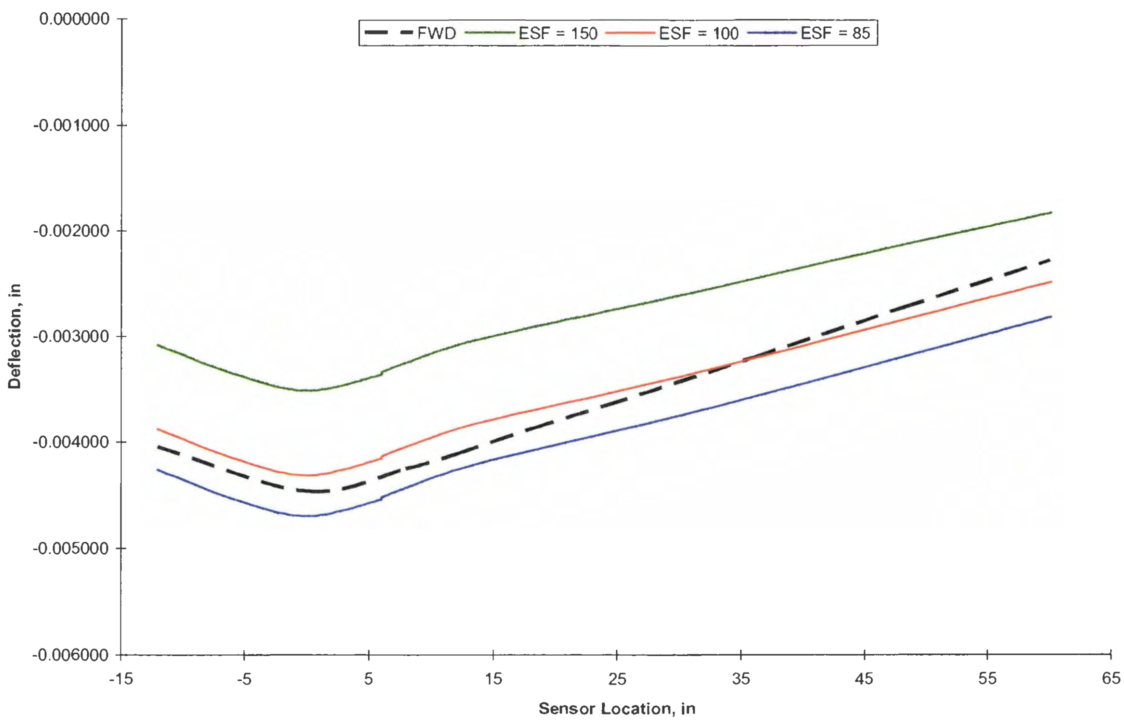

Figure 4-11 Deflection Comparison for Pavement with 4.5" Whitetopping and 4.5ft Joint Spacing

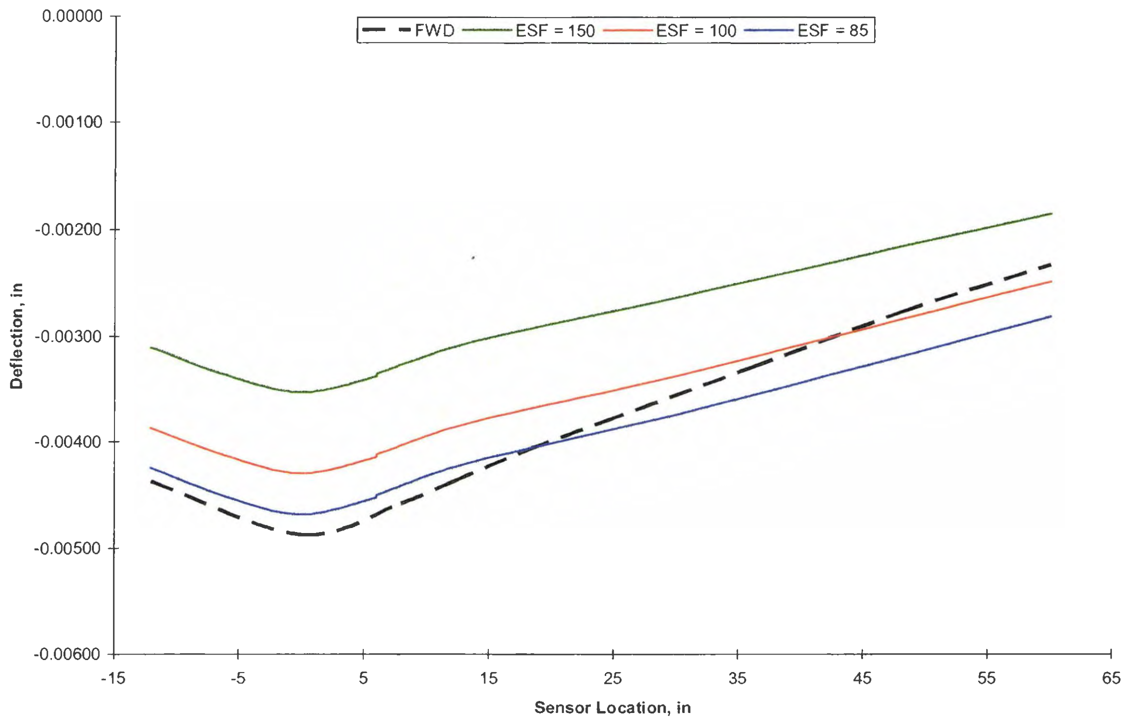

Figure 4-12 Deflection Comparison for Pavement with 4.5" Whitetopping and 6ft Joint Spacing

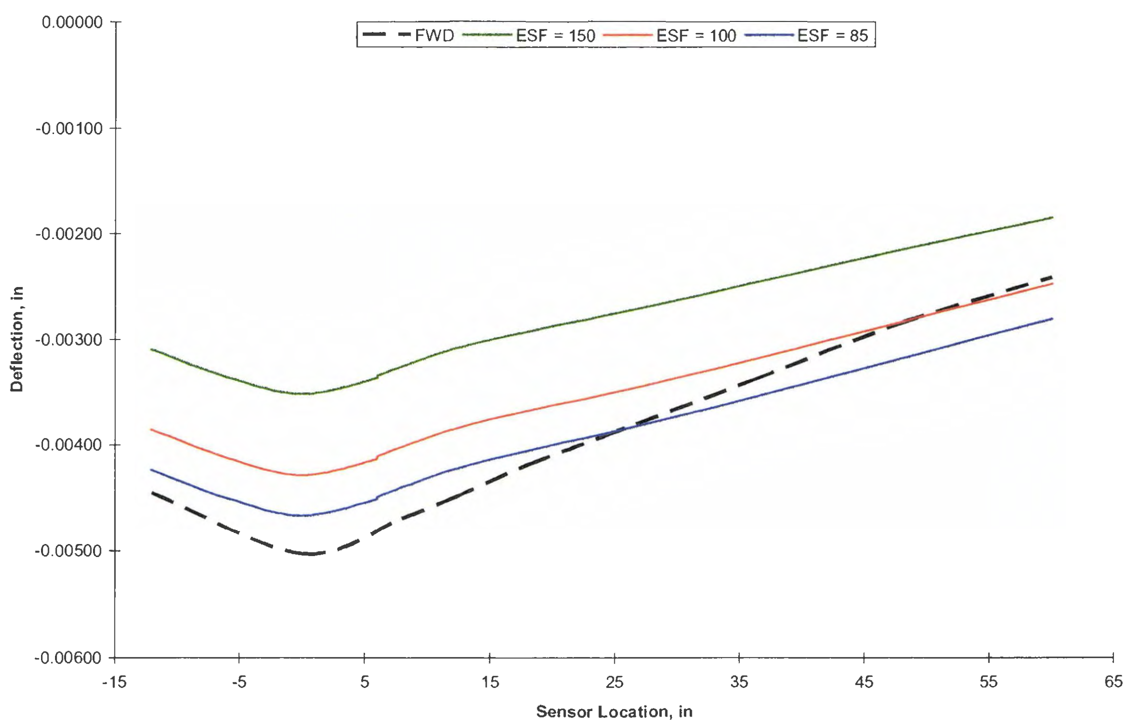

Figure 4-13 Deflection Comparison for Pavement with 4.5" Whitetopping and 9ft Joint Spacing

As can be seen from the preceding figures, the deflections obtained from FWD testing appear to be bounded by k_s values of 85~100 pci, and is closer to those obtained using k_s of 85 pci. This is slightly different from the estimate of 75 pci [21]. The lower value of 85 pci was selected as an acceptable value to represent the stiffness of the foundation beneath the composite pavement on Iowa Highway 13, and was utilized in all subsequent finite element analyses in this study.

4.2.2 Comparison with Measured Strain Data

As previously stated, the pavement models were analyzed under the truck load that was used in the field test of the composite pavement (see Figure 4-3). Fully bonded conditions were assumed in the analysis. The strains induced in the pavement were calculated at locations corresponding to the gage locations on Iowa Highway 13, and were compared to the measurements obtained from the strain gages where available. Transverse and longitudinal strains in the three different layers were considered in the comparison, which are plotted in Figure 4-14. If the strain results obtained using 3-D model and the measured results were equal, distribution of the data points along the line of equality is expected.

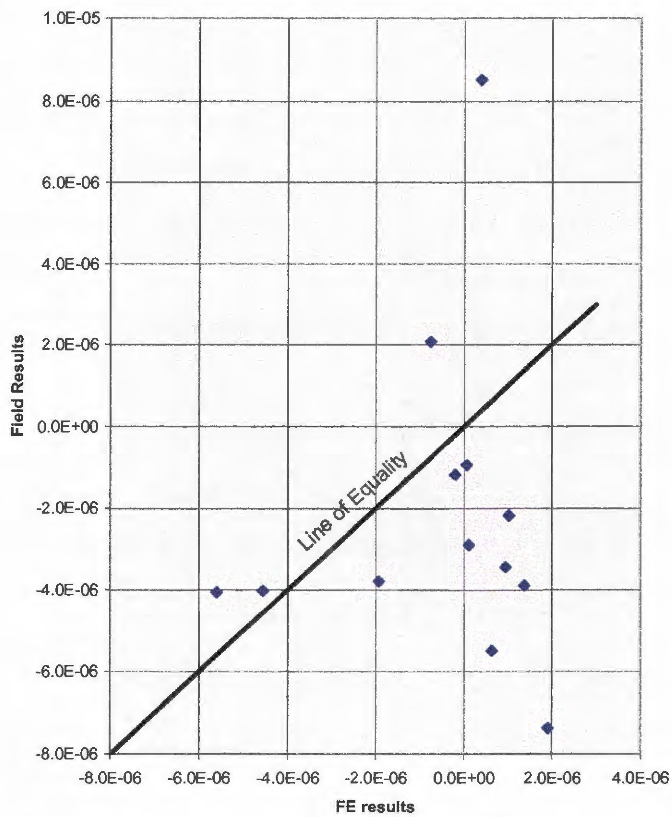

Figure 4-14 Comparison of Experimental and Analytical Strain Results

The above comparison shows some discrepancy between the results from the finite element analysis and field test results. However, the strains obtained from finite element analysis and from the field test data were both in the range of -10 to 10 microns, while the error of the strain gages used were in the range of 4~5 microns. This could be a significant part of the reason for the poor agreement between experimental and analytical results. In addition, the method of installation of the strain gages could also have contributed to the discrepancy, as removal of the original pavement material could have altered the behavior of the pavement at the strain gage locations, which can not be accurately accounted for in the 3-D model. As most of the strain gages that were installed had malfunctioned or were damaged, the accuracy of the data from the remaining strain gages that was deemed useful could also be suspect. Interference from passing traffic while the truck load testing was performed could also have easily contributed to further error in the experimental results.

Not all reasons for the discrepancy were due to experimental factors. Localized differences in the soil properties from test site to test site could exist, and would require that different values for the soil subgrade reaction be used instead of the 85 pci determined previously. Simplification of the model by assuming perfectly undamaged ACC and PCC layers underlying the whitetopping could be another source of error. Additionally, the degree of bond at the interfaces between the layers is potentially another factor contributing to the discrepancy between experimental and analytical results. Unfortunately, a lack of information regarding actual field conditions and interaction mechanism renders a highly detailed model which adequately accounts for all these factors improbable in the current analysis.

With the many factors potentially contributing to the discrepancy between field data and analytical strain values, the comparison is thus inconclusive and no determination can be made regarding the accuracy of the finite element model based upon these strain results alone. However, the favorable comparison between the deflection values and deflection profiles recorded from the field, and those obtained from analyses, generated sufficient confidence in the results from the finite element model. Hence, the finite element model was further utilized to investigate the behavior of the composite pavement on Iowa Highway 13.

5.0 ANALYSIS OF COMPOSITE PAVEMENT ON IOWA HIGHWAY 13

Following the verification of the pavement model developed for the finite element program ANSYS, the 3-D composite pavement model was subjected to different loading conditions. A parametric study was carried out to investigate the effects that whitetopping thickness, interface bonding, joint spacing, depth of joint crack, widening unit configuration and tie bar size and spacing have on overall structural behavior. The pavement was then subjected to heavy truck loads and temperature gradients recorded from the installed gages to determine the stresses that could be induced in the composite pavement in the field.

5.1 Parametric Study of Composite Pavement

Of particular interest in the study presented herein are the effects of the following factors on pavement behavior:

- Thickness of the whitetopping
- Spacing of the joints
- Depth of the cracks along the joints
- Bonding of the layers
- Width and depth of the widening units
- Size and spacing of tie bars

Therefore, the composite pavement was analyzed considering each of the variables listed above. As mentioned in Chapter 3 in the development of the 3-D finite element model, only the saw-cut joints in the whitetopping layer were modeled, and the rest of the pavement structure was assumed to be un-cracked. The soil subgrade reaction modulus, k_s, was assumed to be 85 pci. The pavement layers were considered to be fully bonded to one another, except when investigating the effects of interface bond behavior. Material properties of the different layers listed in the previous chapter were again utilized in this portion of the study. For the purposes of the parametric study, the pavement was subjected to a 9-kip load located at the edge of a transverse saw-cut joint, and at the edge of the widening unit-composite section longitudinal joint shown in Figure 3-4.

5.1.1 Whitetopping Thickness and Joint Spacing

As presented in Chapter 1, the whitetopping overlay on Iowa Highway 13 was constructed with two different thicknesses. One should expect that the thicker whitetopping would provide better pavement performance. In order to quantify this difference in the behavior of the composite pavement, a total of six pavement models, configured with combinations of the two whitetopping thicknesses (3.5 in. and 4.5 in.) and three saw-cut joint configurations (4.5 ft x 4.5 ft, 6 ft x 6 ft and 9 ft x 9 ft), were analyzed under a 9-kip load. Deflection profiles similar to those obtained by FWD testing were constructed from the results of the analyses, and are presented in Figure 5-1. The numerical values for the maximum deflection for each case are tabulated in Table 5-1. The maximum compressive and tensile stresses that were induced in the pavement by the applied load in each of the three layers are presented in Tables 5-2 and 5-3.

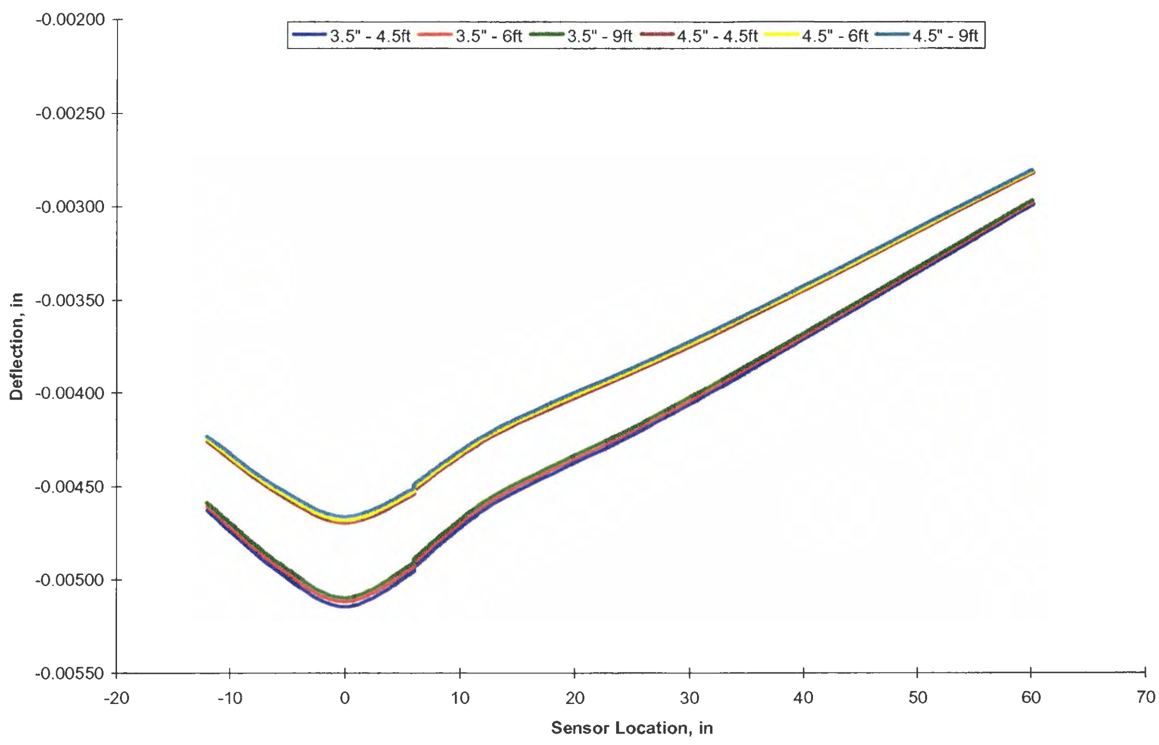

Figure 5-1 Deflection Profiles for Pavements with 3.5" and 4.5" Whitetopping Thickness

Table 5-1 Maximum Composite Pavement Deflections (9kip Load)

Joint Spacing	Max Deflection (in.)	
	3.5"	4.5"
4.5ft x 4.5ft	0.00514	0.00470
6ft x 6ft	0.00512	0.00468
9ft x 9ft	0.00509	0.00466

Table 5-2 Maximum Transverse Stresses (psi) for Different Joint Configurations (9kip Load)

	Joint Spacing	Whitetopping		ACC		PCC	
		Tension	Comp.	Tension	Comp.	Tension	Comp.
3.5"	4.5ft x 4.5ft	37.004	-108.463	14.346	-15.827	37.241	-7.667
	6ft x 6ft	37.131	-106.945	14.123	-15.976	37.733	-7.924
	9ft x 9ft	36.917	-104.428	14.123	-15.924	37.422	-8.221
4.5"	4.5ft x 4.5ft	35.643	-102.592	13.490	-12.743	34.841	-6.220
	6ft x 6ft	35.453	-101.091	13.571	-12.769	34.617	-6.455
	9ft x 9ft	34.282	-98.525	13.512	-12.721	34.287	-6.674

Table 5-3 Maximum Longitudinal Stresses (psi) for Different Joint Configurations (9kip Load)

	Joint Spacing	Whitetopping		ACC		PCC	
		Tension	Comp.	Tension	Comp.	Tension	Comp.
3.5"	4.5ft x 4.5ft	31.729	-123.174	11.544	-17.347	70.942	-16.835
	6ft x 6ft	31.079	-122.264	11.428	-17.514	70.560	-16.633
	9ft x 9ft	30.530	-121.010	11.415	-17.435	70.162	-16.572
4.5"	4.5ft x 4.5ft	31.528	-113.645	10.832	-13.994	62.897	-11.745
	6ft x 6ft	31.000	-112.791	10.899	-14.036	62.615	-11.744
	9ft x 9ft	30.466	-111.497	10.863	-13.960	62.309	-11.690

As can be seen from Figure 5-1 and Table 5-1, the deflections experienced by the pavements with thinner whitetopping overlays were about 10% larger than those with 4.5" overlays. The pavements with thicker whitetopping overlays also exhibited lower stresses, particularly in the longitudinal direction, in the range of 5.5 to 7.9% for stresses in the whitetopping layer. The thicker whitetopping layer also reduced stresses in the underlying ACC and PCC layers, with reduction of up to 11.2% in the tensile stresses at the bottom PCC layer. The combination of deflection and stress results indicate that the 4.5" overlay exhibits better performance with deflections and stresses as the design criteria.

The deflection profiles in Figure 5-1 also seem to suggest that the different joint spacings do not significantly affect pavement behavior when subjected to vertical loads. While overlays with joint spacing at 4.5 ft x 4.5 ft had the largest deflection and stresses, and overlays of 9ft x 9ft joint spacing exhibited the least amount of deflection and stresses for both thicknesses, the differences were not significant. This is in contradiction with findings from other studies [4, 8, 24] which demonstrate that pavement deflection varies with joint spacing, especially when subjected to temperature loading. The reason for the discrepancy with the findings of other studies was due to the assumption made in the current study that the underlying ACC and PCC layers were crack-free and continuous, while other studies focused on the testing or analyzing of composite pavement panels in isolation. This demonstrates that the condition of the layers underlying the overlay has a significant effect on pavement behavior.

5.1.2 Joint Crack Depth

The saw-cut joints in the whitetopping were modeled with two different depths to determine the effects of joint crack propagation through the depth of the overlay on pavement behavior. Pavement models with 3.5" whitetopping overlay and the three different joint spacings were analyzed considering the two different crack depths, and the maximum deflections obtained are tabulated in Table 5-4.

Table 5-4 Maximum Deflections Due to Varying Overlay Crack Depths (9-kip Load)

Joint Spacing	Max. Deflections (in)	
	1.5"	Full Depth
4.5ft x 4.5ft	0.00514	0.00526
6ft x 6ft	0.00512	0.00522
9ft x 9ft	0.00509	0.00516

The results in Table 5-4 revealed that modeling the joints assuming that the cracks propagated through the depth of the overlay only resulted in slightly larger deflections. The deflection profiles for the models with full overlay-depth cracks exhibited the same behavior as the corresponding model with 1.5" crack depth. The maximum stresses in the pavement layers with the joints modeled as cracked through the overlay thickness are given in Table 5-5.

Table 5-5 Maximum Stresses (psi) for Full Overlay-Depth Joint Cracks (9-kip Load)

Joint Spacing	Whitetopping		ACC		PCC	
	Tension	Comp.	Tension	Comp.	Tension	Comp.
Transverse:						
4.5ft x 4.5ft	38.747	-107.409	14.880	-16.096	39.331	-8.566
6ft x 6ft	38.226	-105.969	14.775	-16.03	38.803	-7.973
9ft x 9ft	37.795	-102.956	14.645	-16.088	38.371	-8.542
Longitudinal:						
4.5ft x 4.5ft	31.998	-113.212	11.646	-17.837	72.920	-17.535
6ft x 6ft	31.381	-114.030	11.578	-17.721	72.175	-17.342
9ft x 9ft	30.692	-110.502	11.508	-17.716	71.429	-17.211

` The results from Table 5-5 were compared to the transverse and longitudinal stresses for 3.5" whitetopping presented in Table 5-2 and Table 5-3. While the stresses induced in models with joints modeled as full overlay depth cracks were generally larger, the differences between the cases were not significant. The small differences in deflection and stresses obtained from analysis could once again be attributed to the assumption of undamaged and crack-free ACC and PCC layers underlying the whitetopping overlay.

5.1.3 Bond Condition Between Layers

The effect of the interface bond on pavement behavior was investigated by analyzing the composite behavior by assuming either full bonding between all three layers, or no bonding between all three layers, thus providing results for two extreme cases. The whitetopping overlay thickness was assumed to be 3.5 in. for this comparison, and the three different joint configurations of 4.5 ft x 4.5 ft, 6 ft x 6 ft, and 9 ft x 9 ft were also included in the investigation. Figure 5-2 compares the deflection profiles obtained from the analyses, and demonstrates that interface bonding significantly affects the deflection behavior of the pavement.

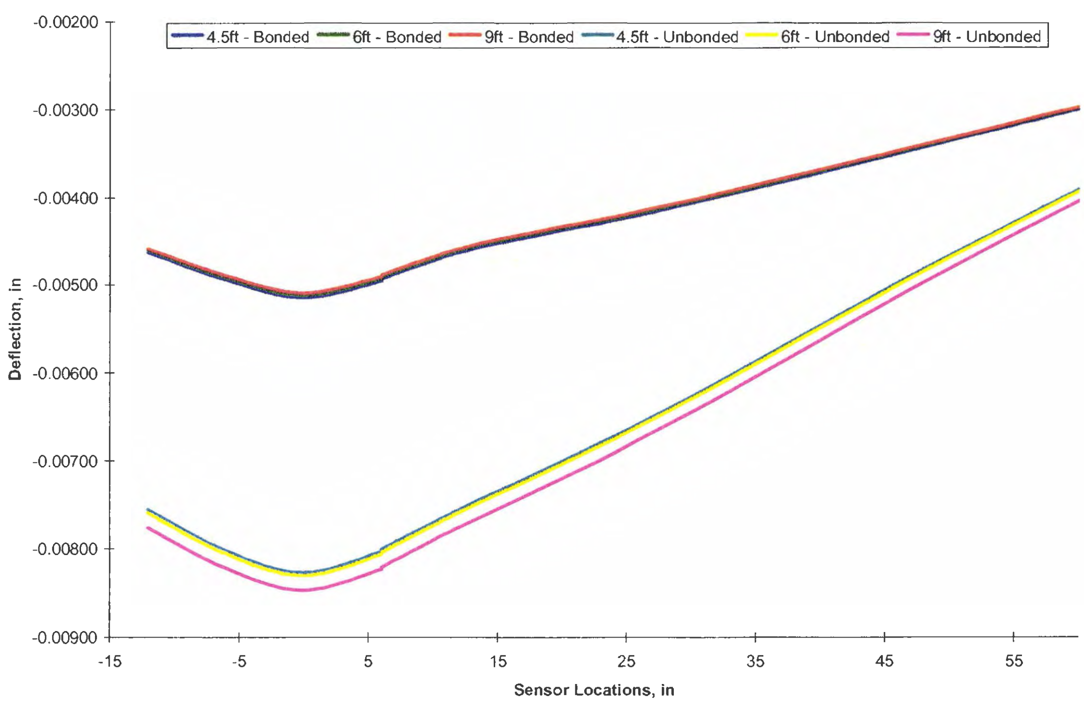

Figure 5-2 Comparison of Deflections for Bonded Layers and Unbonded Layers

Maximum deflections increased by approximately 61~66% when the layers were unbonded, as compared to the deflections obtained when the layers were fully bonded. The deflection profiles above suggest that the assumption of fully bonded contact between the layers could be reasonable, as the value of k_s needed to match the deflections of an unbonded pavement with those obtained from field testing would have been unrealistically high for the test site. To further illustrate the effects of interface bond condition on pavement behavior, maximum tensile and compressive stresses for the cases of bonded and unbonded layers are tabulated in Tables 5-6 and 5-7.

Table 5-6 Maximum Transverse Stresses (psi) for Bonded/Unbonded Composite Pavement (9-kip Load)

Joint Spacing	Whitetopping		ACC		PCC	
	Tension	Comp.	Tension	Comp.	Tension	Comp.
Bonded						
4.5ft x 4.5ft	37.004	-108.463	14.346	-15.827	37.241	-7.667
6ft x 6ft	37.131	-106.945	14.123	-15.976	37.733	-7.924
9ft x 9ft	36.917	-104.428	14.123	-15.924	37.422	-8.221
Unbonded						
4.5ft x 4.5ft	80.231	-146.043	49.855	-21.601	70.222	-73.291
6ft x 6ft	79.631	-143.794	49.482	-23.149	72.016	-74.644
9ft x 9ft	88.612	-138.081	48.314	-26.923	75.375	-77.126

Table 5-7 Maximum Longitudinal Stresses (psi) for Bonded/Unbonded Composite Pavement (9-kip Load)

Joint Spacing	Whitetopping		ACC		PCC	
	Tension	Comp.	Tension	Comp.	Tension	Comp.
Bonded						
4.5ft x 4.5ft	31.729	-123.174	11.544	-17.347	70.942	-16.835
6ft x 6ft	31.079	-122.264	11.428	-17.514	70.560	-16.633
9ft x 9ft	30.530	-121.010	11.415	-17.435	70.162	-16.572
Unbonded						
4.5ft x 4.5ft	79.917	-135.582	44.879	-22.265	105.197	-96.862
6ft x 6ft	79.377	-133.616	43.697	-23.660	105.939	-96.935
9ft x 9ft	78.986	-130.792	42.849	-26.772	107.795	-97.673

The results showed that removing the bond between the layers resulted in significant increases in the stresses that were induced in the composite pavement. For example, increases as much as 288% in the tensile stresses were seen in the asphalt layer, while tensile stresses in the whitetopping overlay increased as much as 152% when the layers were unbonded. Larger loads resulting from the heavy-truck traffic on Iowa Highway 13 could be expected, and maintaining bonded conditions between the layers is essential in keeping deflections and stresses low due to these larger loads.

Data on the bond strength of the composite pavement were documented in the construction report [1], and the average bond strength was in the range of 155 to 302 psi, depending on the surface preparation. These are higher than the shear stresses between the interfaces that were obtained from the analyses. The analyses revealed a maximum interface shear stress of no more than 40 psi with the 9-kip load that was utilized.

5.1.4 Widening Unit Dimensions

Several analyses were performed to determine the differences in deflection that would be induced in the pavement with varying widening unit dimensions, specifically different widths and depths. For this purpose, the composite pavement was analyzed considering widening unit widths of 1, 2, 3, 4, 5, 6, and 7 feet. The edge thickness was assumed to be at 8". The maximum deflections corresponding to the different widths were obtained from finite element analysis and are plotted in Figure 5-3. The maximum deflection obtained from the analysis of an un-widened pavement is also included for comparison.

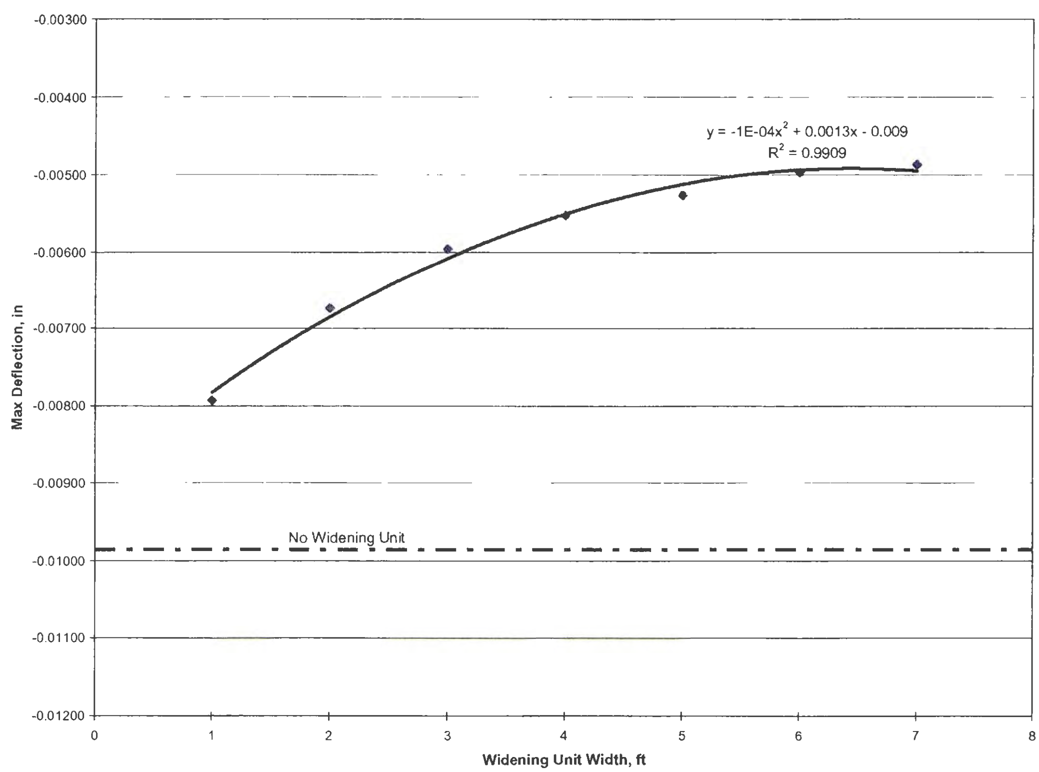

Figure 5-3 Maximum Deflections – Varying Widening Unit Widths (9-kip Load)

The effect of different depths of the widening units on deflections was also investigated by varying the edge thicknesses of the widening units. Widening units with thicknesses of 6, 8, 10, 12 and 15 inches were analyzed in conjunction with widths of 1 and 2 feet. The maximum deflections that were induced in the pavement are plotted in Figure 5-4.

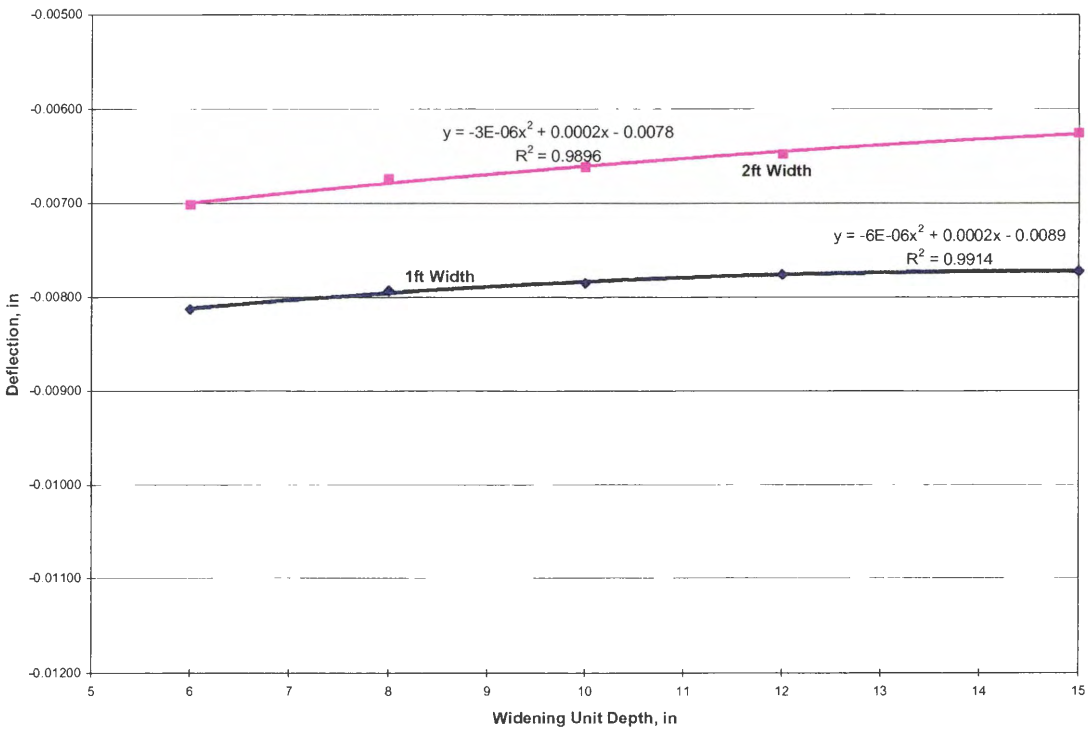

Figure 5-4 Maximum Deflections – Varying Widening Unit Depths (9-kip Load)

The figures show that as the widening width was increased, deflections induced in the composite pavement decreased. Similar to result found in the initial analytical work [1], the pavement experienced a 53% reduction in maximum deflection when the widening units were configured with 5 ft width and 8 in. thickness; however, with successively larger widening unit widths, the reduction in deflection gained diminished. Figure 5-4 suggests that any benefit in deflection reduction for widening units larger than 7 ft would be minimal. On the other hand, while increasing widening unit depth leads to decreasing pavement deflection, the reduction gained was not as dramatic as that for increasing widening unit width. The results suggest that for widened pavements structures, increasing widening unit width may be the most efficient method for achieving lower deflections.

The initial analytical work presented in the construction report speculated on the reason for the lower deflections experienced by the widened composite pavement on Iowa Highway 13. The study proposed that the arched shape of the pavement cross-section along with the widening units permitted the development of lateral confinement forces that helped reduce the magnitude of deflection. The 3-D finite element model developed in Chapter 3 was also utilized to investigate the validity of the "arch effect" proposed in the initial analytical work. Modifications were made to the finite element model by inserting interface elements between the widening units on either side of the composite pavement, as illustrated in Figure 5-5. The interface elements were defined with the 'standard' interface condition, thus allowing sliding and separation of the widening units from the 3-layer composite section, which would prevent load transfer between the widening unit and the 18 ft composite section. This procedure isolates the proposed 'arch effect' on the behavior of the pavement, i.e. development of additional lateral confinement due to the arched shape cross-section, thus allowing the deflection reduction to be quantified independently of load transfer between the widening units and the composite section.

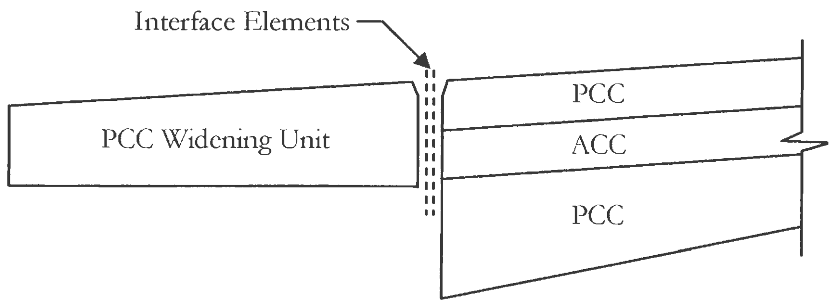

Figure 5-5 Insertion of Interface Elements Between Widening Unit and Composite Section

The pavement model with the modifications described above was analyzed under a 9-kip FWD load, and the maximum deflection was compared to a pavement model in which the widening units were completely removed. Figure 5-6 shows the plot of the deflected shape produced by finite element analysis.

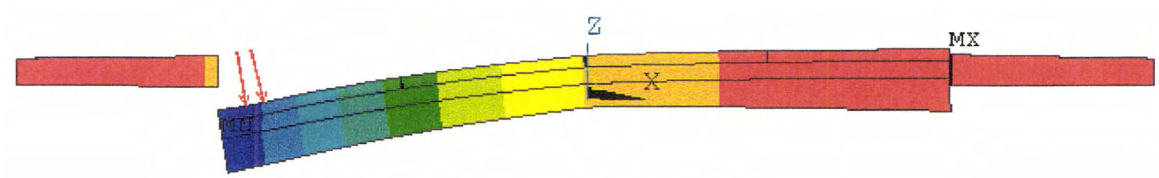

Figure 5-6 Separation at Widening Unit-Composite Section Interface (Cross-Section View – Exaggerated Scale)

As can be seen, separation occurred at the widening unit-composite section interface, implying successful removal of the load transfer effect. However, no difference was found between the deflections of the widened and un-widened pavements when the load transfer effect was removed, implying that the reduction in deflection previously seen was not due to the additional confinement effects of an arch-shaped pavement as was speculated. If the reduction in deflection is to be realized when constructing a widened pavement structure, positive load transfer will have to be ensured between the composite section and the widening units.

The behavior of the composite pavement was further investigated by setting the interface interaction of the interface elements located between the widening units and the composite section to 'no separation'. The maximum deflection obtained from analysis was 0.00541 in., which was only slightly greater than the deflection obtained from the original, unmodified model, i.e. 0.00526 in. This result suggests that as long as the widening units are not allowed to separate from the composite section, the benefits of deflection reduction will be realized.

5.1.5 Tie Bar Size and Spacing

The results in the previous section demonstrate that maintaining a means for load transfer between the widening units and the composite section is essential to reducing deflections induced in the pavement. Load transfer across the joint could be ensured by mechanisms such as aggregate interlock at the joint interface, or by the installation of tie bars across the joint; however, the contribution of aggregate-interlocking across the joint is not easily quantifiable or controllable by design. An alternative is to use tie bars to ensure sufficient load transfer between the two widening units and the composite section.

As detailed in the construction report, 36 in. long #4 rebars were placed at 30 in. on center at the longitudinal joints between the widening units and the composite section (see Figure 3-4) at selected locations along the test section on Iowa Highway 13. With the assumption of the absence of the aggregate-interlock mechanism, the 3-D pavement model was utilized to investigate if the tie bar size and spacing listed above was sufficient to ensure load transfer between the widening units and the composite. As described in Chapter 3, the tie bars were modeled for finite element analysis using beam elements. Analysis results showed that in the absence of the aggregate interlocking between the widening unit and the pavement, a maximum deflection similar to that of the composite section without widening units was obtained. This indicated that the bar size and spacing utilized in the project were not sufficient to ensure load transfer across the joint.

Consequently, additional analyses were performed to determine if the tie bar mechanism could be utilized to ensure load transfer across the longitudinal widening unit-composite section joint. The first configuration that was investigated was the utilization of #4 rebars spaced 12 in. on center; however, the analysis results showed that there was insignificant reduction in the pavement deflection. The analysis was repeated utilizing #8 rebars that were spaced at 30 in. on center. The results yielded a maximum deflection of 0.00773 in, which was less than that obtained with the two previous tie bar configurations. The deflected shape of the pavement is shown in Figure 5-7, which demonstrates that the tie bar configuration involving #8 rebars spaced at 30 in. on center is successful at preventing complete separation between the widening units and the composite section, thus preventing a complete loss of load transfer at the joint.

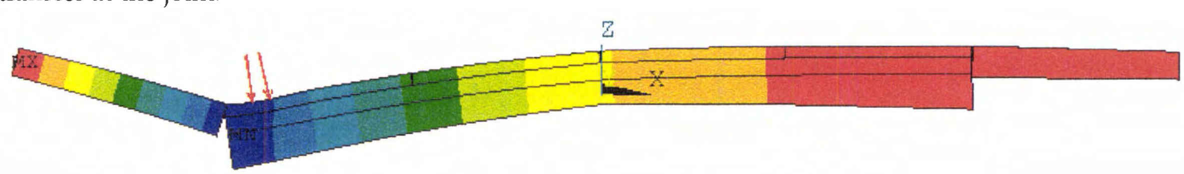

Figure 5-7 Partial Separation at Widening Unit-Composite Section Interface (Cross-Section View – Exaggerated Scale)

The results indicate that the use of tie bars can ensure a degree of load transfer between the widening units and the composite section. However, bars that were larger and more closely spaced than those used in the project would be needed to achieve perfect load transfer between the widening units and the composite section, assuming tie bar action was the only load transfer mechanism considered.

5.2 Pavement Behavior When Subjected to Truck Loading

Following the parametric study of the previous section, the 3-D composite pavement model was subjected to truck loading to investigate the behavior that the composite pavement on Iowa Highway 13 may exhibit under day-to-day service conditions. The pavement model considered had an overlay thickness of 3.5 in. and joint spacing of 4.5 ft x 4.5 ft with fully bonded layers. The truck configuration used for the collection of field strain data (Figure 4-3) was selected for this part of the investigation, as the fully loaded truck was rated as a heavy traffic load. Analysis of the composite section was performed by positioning a single truck at three different locations across the pavement section to reflect variable driving patterns on the roadway. Figure 5-8 shows the position of the outer wheel path on the pavement section.

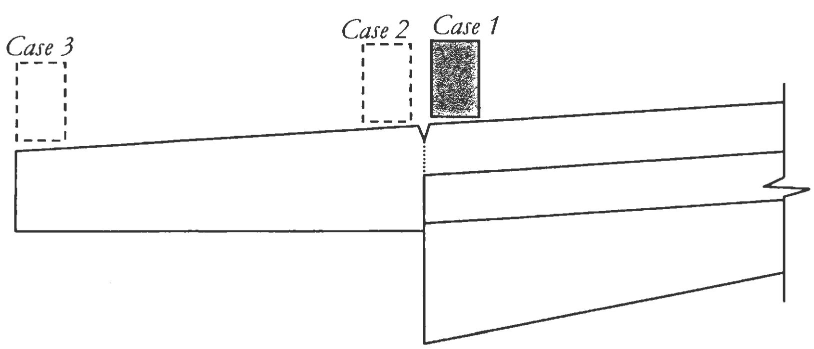

Figure 5-8 Location of Truck Outer Wheel on Composite Pavement

The maximum deflections and stresses in the different layers obtained from the analyses of the three different loading cases are presented in Table 5-8. The two cases where the outer wheel path was located on a widening unit exhibited significantly worse deflection and stresses than when the outer wheel path was confined to the composite section. In particular, stresses in the whitetopping overlay for Case 3, where the outer wheel path was located on the edge of the widening unit were markedly higher than the other two cases.

Table 5-8 Maximum Deflection and Stresses in the Composite Pavement (Single Truck Load)

Layer	Max Deflection, in	Max Trans. Stress, psi		Max. Long. Stress, psi	
		Tension	Comp.	Tension	Comp.
Case 1					
Whitetopping		52.370	-94.003	35.030	-101.823
Asphalt	-0.009863	20.884	-9.935	14.088	-10.320
Base Concrete		52.675	-12.497	64.459	-20.935
Case 2					
Whitetopping		74.257	-96.860	71.587	-104.510
Asphalt	-0.011782	10.392	-9.542	6.406	-9.121
Base Concrete		42.519	-11.600	62.225	-24.420
Case 3					
Whitetopping		92.695	-81.632	174.090	-190.696
Asphalt	-0.028069	3.430	-26.944	2.405	-15.105
Base Concrete		21.311	-59.621	62.909	-26.972

The pavement model was further analyzed by loading both lanes of the pavement model with the test truck load configuration. The outer wheel paths were confined within the composite section on both sides of the pavement in all cases. The different configurations of the truck loads that were considered are shown schematically in Figure 5-9.

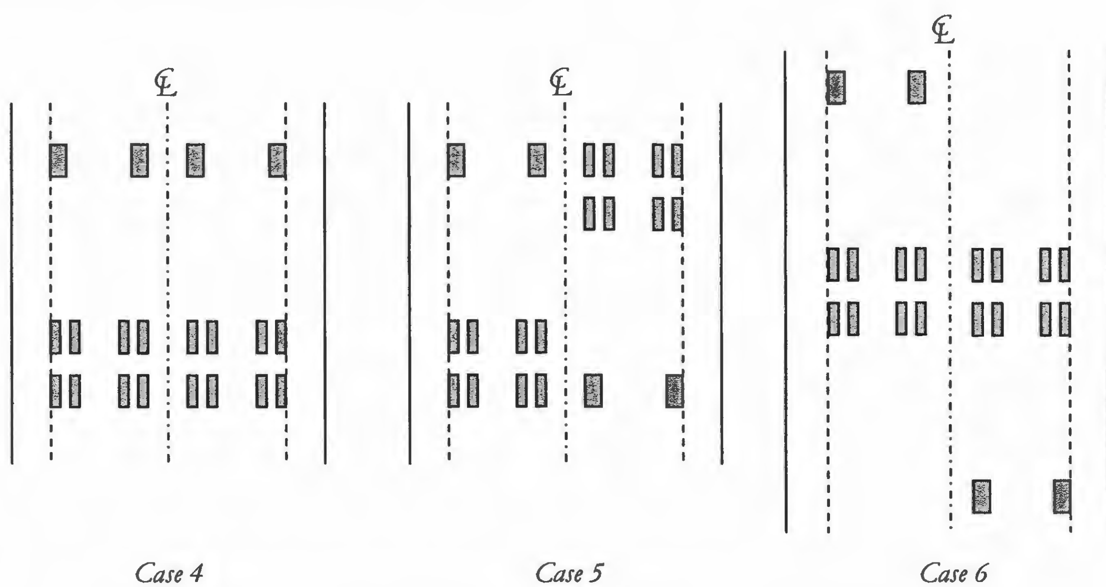

Figure 5-9 Configuration of Truck Loads with Two Lanes Loaded

The maximum deflection and stresses obtained from the analyses of the three cases listed above are shown in Table 5-9.

Table 5-9 Maximum Deflection and Stresses in the Composite Pavement (Double Truck Load)

Layer	Max. Deflection, in	Max. Trans. Stress, psi		Max. Long. Stress, psi	
		Tension	Comp.	Tension	Comp.
Case 4					
Whitetopping		67.871	-93.065	70.988	-111.15
Asphalt	-0.012728	8.082	-9.543	5.095	-9.187
Base Concrete		35.243	-11.194	68.968	-26.657
Case 5					
Whitetopping		69.089	-92.203	71.255	-111.037
Asphalt	-0.011782	8.17	-9.536	5.055	-9.297
Base Concrete		40.52	-12.194	63.49	-25.106
Case 6					
Whitetopping		67.924	-83.378	70.908	-95.052
Asphalt	-0.012517	8.323	-9.513	5.244	-9.005
Base Concrete		37.194	-11.696	68.62	-28.632

Generally, the cases where the truck loads were placed side-by-side yielded the highest stresses. While the stresses for Case 4 & 5 were not always higher than that obtained by the single truck in Case 1, longitudinal tensile stresses were approximately twice that of Case 1. In addition, the maximum contact stress in the plane of the interface elements for the cases investigated above were less than 80 psi obtained from the whitetopping-ACC interface in the edge loading case (Case 3). This was again much less than the bond strength values presented in the construction report [1].

As the loading in Case 5 induced the highest tensile stresses in the whitetopping layer, a final analysis was performed by placing the outer wheels for two trucks at the edges of the pavement, positioned side-by-side and facing opposite directions, similar to the orientation in Case 5. The results from this analysis considering this load configuration, hereafter referred to as Case 7. The results are summarized in Table 5-10.

Table 5-10 Maximum Deflection and Stresses Due to Worst Case Loading of the Composite Pavement

Layer	Max. Deflection, in	Max. Trans. Stress, psi		Max. Long. Stress, psi	
		Tension	Comp.	Tension	Comp.
Case 7					
Whitetopping		99.525	-86.779	173.324	-191.823
Asphalt	-0.027157	3.896	-29.246	2.826	-16.486
Base Concrete		14.630	-64.866	62.937	-26.608

As can be seen, the use of two truck loading placed on the edge of the pavement induced the highest transverse stresses in the composite pavement, while the longitudinal stresses were not significantly different from the case with a single truck loading on the pavement edge (Case 3). The maximum in-plane contact stress for this case was found to be a little less than 70 psi, occurring at the whitetopping-ACC interface.

5.3 Pavement Behavior When Subjected to Temperature Differential

The behavior of the composite pavement when subjected to temperature differentials was considered separately. As material non-linearities and large deflections were not considered in the course of this study, superposition of the results from static load and temperature analyses would sufficiently represent the effects of these two loading conditions on the pavement.

In order to investigate the effects of temperature differentials on the composite pavement on Iowa Highway 13, the composite pavement developed and presented in Chapter 3 was subjected to two temperature gradients that produced upward and downward curling of the pavement. The two gradients were +22.5°F at the top, and -16.2°F at the bottom, as illustrated in Figure 5-10. These gradients were the maximum gradients that were obtained from temperature gage recordings from the 5 test sites on Iowa Highway 13.

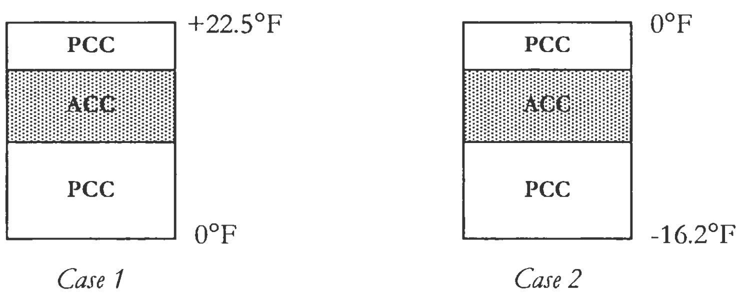

Figure 5-10 Temperature Differentials Applied to the Composite Pavement

The pavement model selected for the analysis had an overlay thickness of 3.5 in., with joints that were cracked through the thickness of the overlay. All three joint spacings, i.e. 4.5 ft x 4.5 ft, 6 ft x 6 ft, and 9 ft x 9 ft, were investigated and the pavement layers were considered to be fully bonded. Typical values of the coefficient of thermal expansion were assumed for the PCC and ACC layers, i.e. 5.5×10^{-6} in./in./°F and 5.0×10^{-6} in./in./°F, respectively.

Analysis of the composite pavement with the positive temperature gradient, i.e. Case 1, resulted in the upward deflection at the centerline of the pavement, and downward deflection of the pavement edges, creating a downward curl. The exact opposite occurred in Case 2, where the centerline of the pavement was deflected downward and the pavement edges were deflected upwards, resulting in an upward curling of the composite pavement.

The maximum deflections and maximum stresses at the interfaces of the different layers that were obtained from analyzing the different pavement configurations are summarized in Table 5-11. The maximum interface shear and normal stresses occurred at the whitetopping-ACC interface for all cases. Case 2 was found to induce larger deflections and interface stresses in the composite pavement, regardless of joint spacing.

Contrary to the findings in previous sections, the interface stresses for the two temperature loading cases were significant. Interface shear stress in the case of negative temperature differentials could possibly exceed the value of the interface bond strength of the composite pavement, which was in the range of 155 to 302 psi, depending upon surface preparation [1]. The normal tensile stresses induced at the interface in Case 2 were at least twice the in-plane shear stresses, which could be a significant factor leading to interface debonding. Clearly, consideration of the partial bonding mechanism is of great importance when accounting for the effect of temperature differentials in the pavement section.

Table 5-11 Maximum Deflections and Whitetopping-ACC Interface Stresses (Temperature Differential)

Joint Spacing	Max. Deflection (in.)	Max. Contact Stresses (psi)		
		In-Plane	Normal - Comp.	Normal - Tension
Case 1				
4.5ft x 4.5ft	0.023587	102.419	-284.883	22.879
6ft x 6ft	0.023691	104.450	-267.336	15.824
9ft x 9ft	0.023270	136.424	-280.078	50.049
Case 2				
4.5ft x 4.5ft	0.032213	166.854	-335.221	370.967
6ft x 6ft	0.033286	157.815	-329.699	397.073
9ft x 9ft	0.034255	194.646	-383.496	396.829

The maximum transverse and longitudinal stresses induced in the three layers of the composite pavement were obtained from analyses of the pavement model under the two temperature gradients considered, and are presented in Table 5-12 and Table 5-13.

Table 5-12 Maximum Transverse Stresses in the Composite Pavement (Temperature Differential)

Joint Spacing	Whitetopping		ACC		PCC	
	Tension	Comp.	Tension	Comp.	Tension	Comp.
Case 1						
4.5ft x 4.5ft	153.452	-419.785	97.207	N/A	133.186	-38.388
6ft x 6ft	145.111	-426.310	93.690	N/A	125.073	-37.648
9ft x 9ft	149.312	-431.886	95.099	N/A	129.470	-36.203
Case 2						
4.5ft x 4.5ft	215.513	-147.404	123.999	-29.069	27.603	-182.550
6ft x 6ft	195.673	-158.787	119.820	-32.929	18.085	-194.571
9ft x 9ft	246.435	-152.000	137.351	-31.668	38.235	-201.728

Table 5-13 Maximum Longitudinal Stresses in the Composite Pavement (Temperature Differential)

Joint Spacing	Whitetopping		ACC		PCC	
	Tension	Comp.	Tension	Comp.	Tension	Comp.
Case 1						
4.5ft x 4.5ft	148.489	-461.134	87.923	N/A	182.985	N/A
6ft x 6ft	148.907	-490.741	86.236	N/A	182.943	N/A
9ft x 9ft	145.869	-502.778	87.674	N/A	181.357	N/A
Case 2						
4.5ft x 4.5ft	240.687	-131.503	128.068	N/A	61.191	-218.978
6ft x 6ft	268.864	-143.246	122.084	N/A	11.913	-218.919
9ft x 9ft	282.616	-153.459	141.475	N/A	25.812	-244.599

These results demonstrate that the stresses induced in the composite pavement by temperature differentials could be several times those induced by vertical loads. While the stresses induced in Case 1 were not significantly different in the pavements with different joint spacing, differences in stresses due to the different joint spacings used were more pronounced in the case of the negative temperature gradient. The joint spacing of 9 ft x 9 ft generally resulted in larger stresses in the different layers, particularly in the whitetopping overlay, which is to be expected as shorter joint spacings have been shown to reduce curling stresses [4].

Once again, the assumption that the underlying layers are undamaged and crack-free might have contributed to the relatively small differences found between the different joint spacings, as the pavement behavior was essentially monolithic. One may expect larger differences between the stresses in pavements with different joint configurations as joint crack depth propagates through the thickness of the pavement section.

As the contact stresses indicate a high possibility of debonding of the three pavement layers, attempts were made to predict the stresses and deflections of the pavement model with the layers unbonded. The interface element behavior was set to 'standard' to allow for separation of the layers as well as sliding, as differential curling of the different layers was expected due to the distribution of the temperature gradients.

While test runs with smaller, discrete composite panels successfully modeled the differential curling of smaller, discrete composite panels, convergence difficulties were encountered when modeling the unbonded behavior of the full pavement model developed in this study. In the author's opinion, the complexity of the expected solution due to the combination irregular geometry, multiple contact pairs with 'standard' interface behavior, and the applied temperature gradients could have contributed to the non-convergence. Due to the lack of time, this portion of the study was not pursued further.

6.0 SUMMARY, CONCLUSIONS AND RECOMMENDATIONS

6.1 Summary

The state of Iowa is known for its extensive use of PCC pavements, where the potential for cost savings from whitetopping is a very attractive alternative to continued pavement rehabilitation with asphalt. To gain further experience in the use of whitetopping for pavement rehabilitation, the state of Iowa has sponsored the current research to test and monitor a 9.6-mile stretch of Iowa Highway 13.

The usage of whitetopping overlays results in unique pavement structures that are fundamentally different from other conventional pavement types, and much effort has gone into studying the effects that whitetopping overlays have on pavement performance. To date, contributions from both experimental and analytical studies from around the world have provided much needed insight into the factors that should be considered in the design and construction of whitetopping overlays. For example, first generation design and construction guidelines have been developed by PCA and CDOT. In addition, previous analytical studies have also demonstrated the feasibility of utilizing the finite element method to aid in the study of pavements with whitetopping overlay.

Owing to the irregular geometry of the composite pavement on Iowa Highway 13, three-dimensional finite element models were developed using the ANSYS finite element program to aid in the investigation of the behavior of the composite pavement. Solid and shell elements were used in modeling various configurations of the pavement structure on Iowa Highway 13. In order to study the effects of the interface bonding between the different layers, interface elements capable of modeling bonded and unbonded interactions were utilized. In addition, beam elements were used to represent tie bars where necessary. The applicability of the modeling techniques were then tested and affirmed by comparison of the results obtained from ANSYS with beam and plate theories, and by comparison with the ISLAB2000 software package.

The applicability of the 3-D model developed in ANSYS to the composite pavement on Iowa Highway 13 was then tested by comparing the results from the finite element analysis to measured deflection and strain data from the field. Deflections from the field were in good agreement with the deflections obtained from analysis. On the other hand, comparisons of analytical and measured strains were inconclusive. This could be due to various factors that could not be adequately controlled experimentally, or precisely accounted for in the analytical process. However, based upon the results of the deflection comparisons, the finite element models developed for the Iowa Highway 13 composite pavement were deemed adequate to further investigate the structural behavior of the pavement.

A parametric analysis was performed to determine the effects of whitetopping thickness, joint spacing, joint crack depth, interface bond, widening unit configuration and tie bar size and spacing. In addition, temperature data collected from the field was utilized to analyze the effect of temperature gradient on the composite pavement behavior.

6.2 Conclusions

Based on the limited modeling and analyses conducted herein, the following are some conclusions that were made regarding the structural behavior of the composite pavement on Iowa Highway 13:

- The behavior of a composite pavement with fully bonded layers, subjected to actual truck loads and temperature differentials, can be accurately predicted with the 3-D model developed with this study.
- The interface elements in the ANSYS program are suitable for modeling the fully bonded and unbonded interface conditions between the different pavement layers.
- Thicker whitetopping overlays were found to improve pavement performance by lowering deflections and maximum stresses that were induced in the composite pavement under static loading.
- Investigations into pavement behavior as a function of the different joint spacing or different crack depths demonstrate that the condition of the layers underlying the whitetopping greatly influence the behavior of the pavement. With the assumption of undamaged, crack-free base PCC and ACC layers, joint spacing and crack depth did not have a significant effect on pavement performance.
- Composite pavements with fully bonded and unbonded layers exhibited very different behavior. For example, the deflections and maximum stresses induced in pavements with unbonded layers were significantly higher than in pavements with fully bonded layers.
- The width, rather than the depth, of the widening units has a significant effect on reducing the deflection.

- Load transfer between the widening units and the composite section of the pavement section must be maintained to reduce the deflection induced in the pavement under vertical traffic loads.
- Even in the absence of the aggregate-interlock load transfer mechanism, tie bars with reasonable size and spacing were capable of providing the aforementioned load transfer between the widening units and composite section.

6.3 Future Recommendations

The following are the recommendations for further study:

- The FWD deflection data should be normalized such that the effects of variable temperatures and foundation stiffnesses may be isolated.
- The quality of the strain data obtained from the field should be improved by ensuring the integrity of the gages after installation, which can easily be attained if these gages are installed during the construction of new pavements. Also, interference from passing traffic should be eliminated during data collection.
- The non-linear material properties for both asphalt and concrete should be included to account fundamental material behavior, such as concrete cracking or asphalt viscosity that could influence the behavior of the pavement.
- Time factors such as concrete fatigue, creep and shrinkage need to be incorporated into a study of pavement performance to determine the long-term destructive effects.
- Detailed information on the condition of the layers underlying the whitetopping is needed for the precise prediction of pavement behavior. However, this approach could be unfeasible due to the unlimited variation of actual pavement conditions in the field over a relatively short length. An alternative approach could be to assume the propagation of whitetopping joints through the thickness of the pavement with appropriate load transfer efficiency values determined from trial and error and applied between the resulting pavement panels to approximate actual pavement behavior.
- Modeling of the partial bonding condition between the different pavement layers should be an essential part of future work, since this factor has a significant effect on the overall behavior of composite pavements.

- The variation in the stresses at the layer interfaces could be significant when the pavement is subjected to temperature differentials. This implies that treatment of the partial bonding mechanism is of particular importance to adequately account for the effects of temperature differentials on composite pavement behavior.
- The effects of using tie bars and aggregate interlock mechanism on the load transfer between the widening units and composite section need to be further investigated.
- The behavior of the pavement structure under moving loads, which is a better approximation of the actual traffic loads that a pavement is subjected to during normal operation, should be investigated.
- The unbonded behavior of the composite pavement subjected to temperature differential should be investigated.

APPENDIX A:

LOCATION OF INSTRUMENTED SITES

Date: 9-10-2004
Site: # 1
Station: 439+10
Slab size: 4.5' x 4.5'
Gage orientation: longitudinal

Truck speed 1- 2 mph

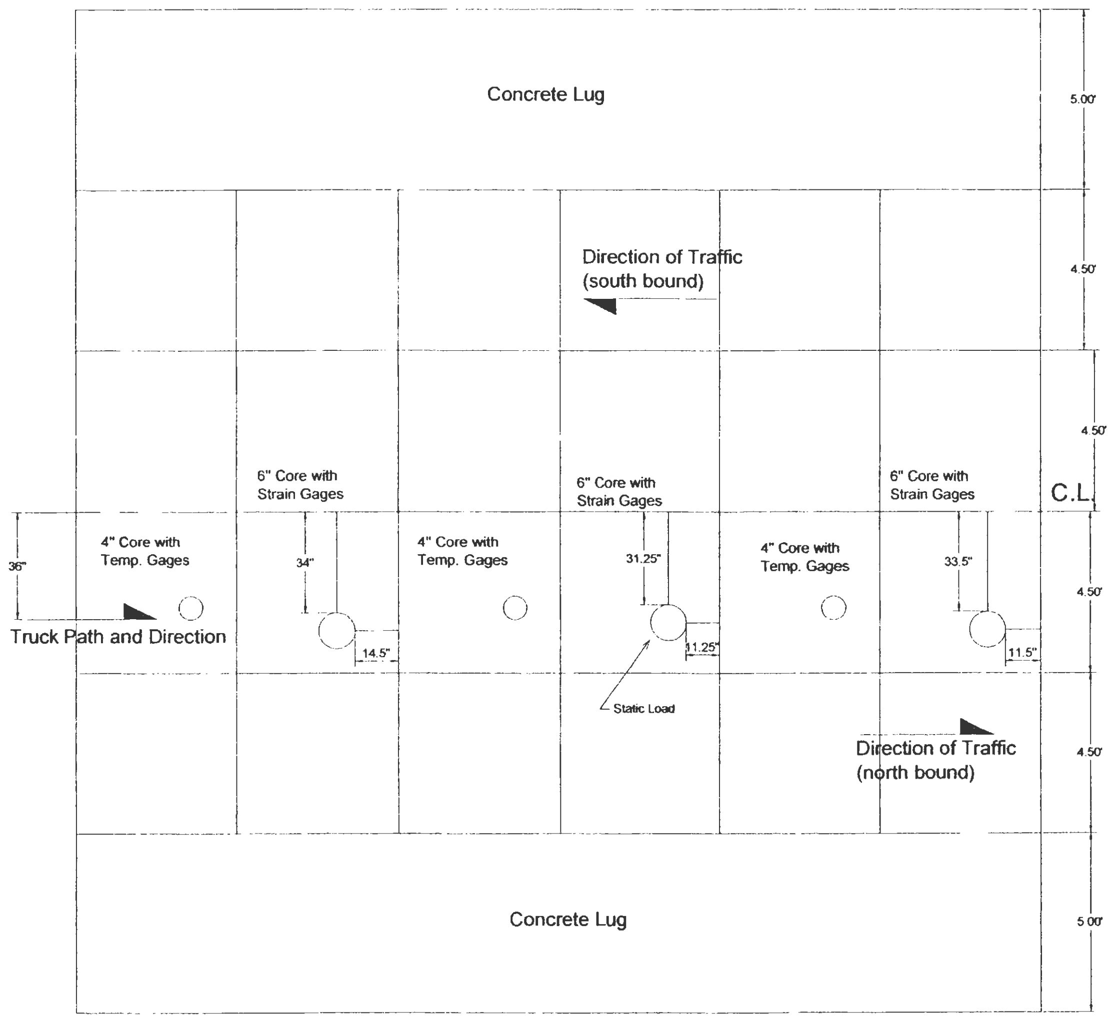

Date: 9-10-2004 Truck speed 1- 2 mph
Site: # 2
Station:
Slab size: 6' x 6'
Gage orientation: transverse

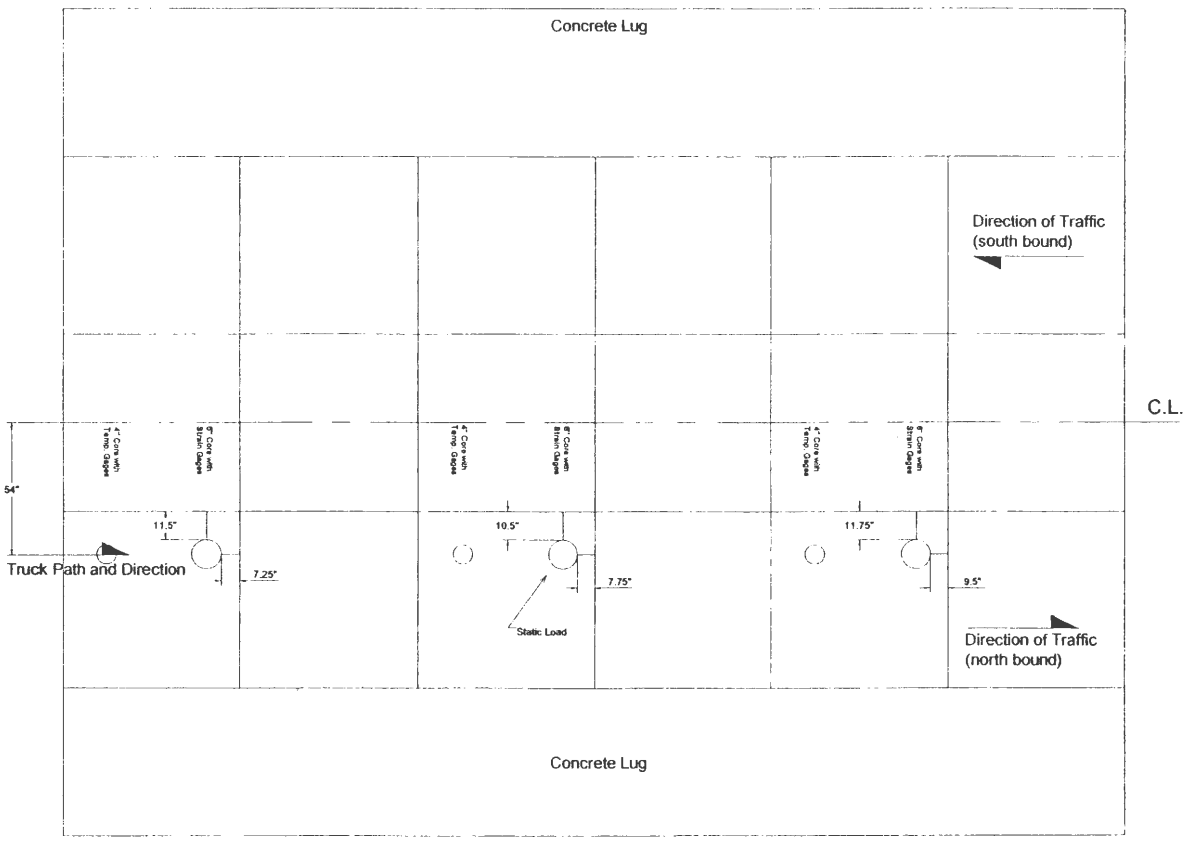

Date: 9-10-2004
Site: # 3
Station: 495+00
Slab size: 9' x 9'
Gage orientation: longitudinal

Truck speed 1- 2 mph

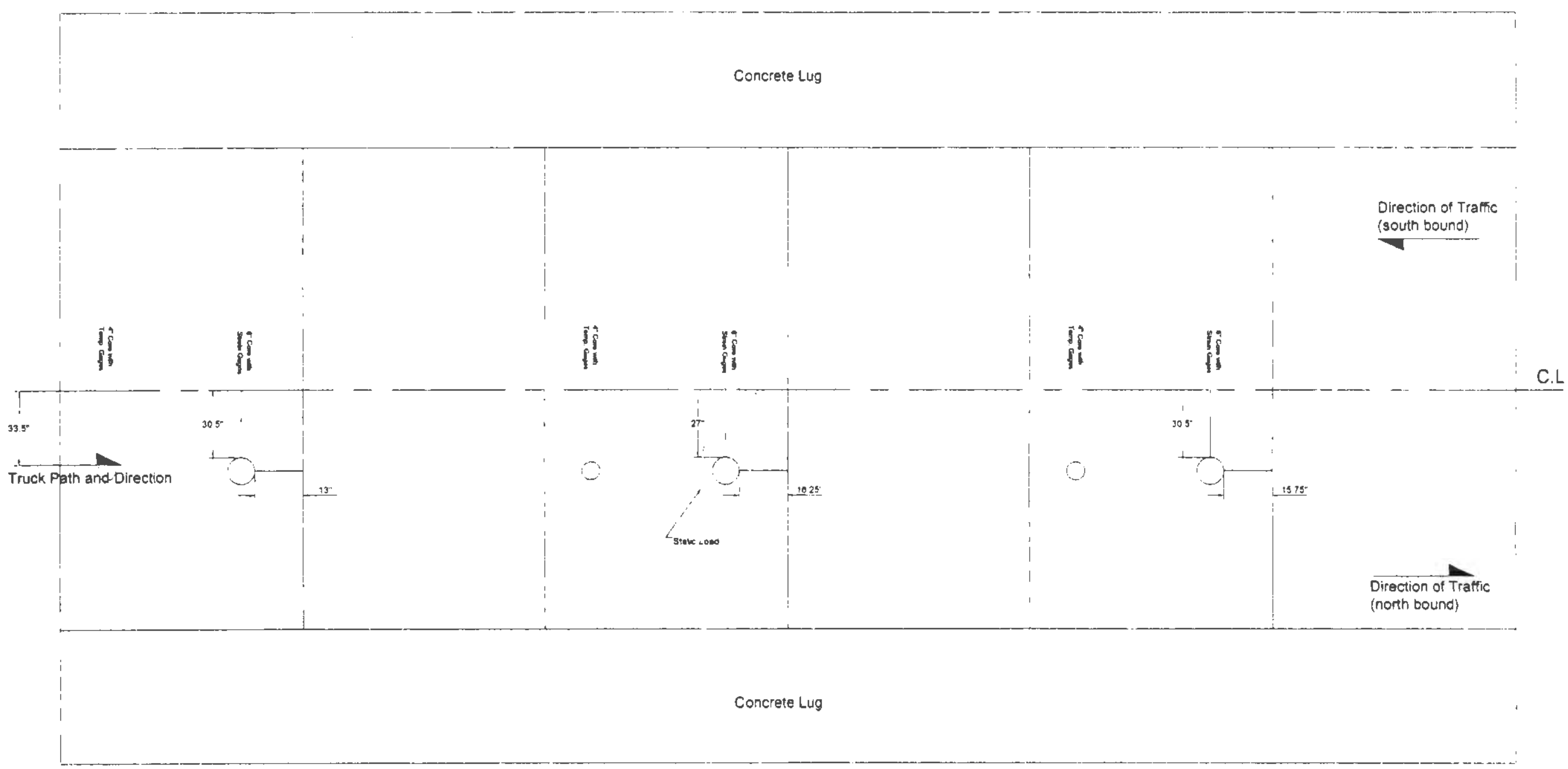

Date: 9-10-2004

Truck speed 1- 2 mph

Site: # 4

Station: 500+10

Slab size: 4.5' x 4.5'

Gage orientation: transverse

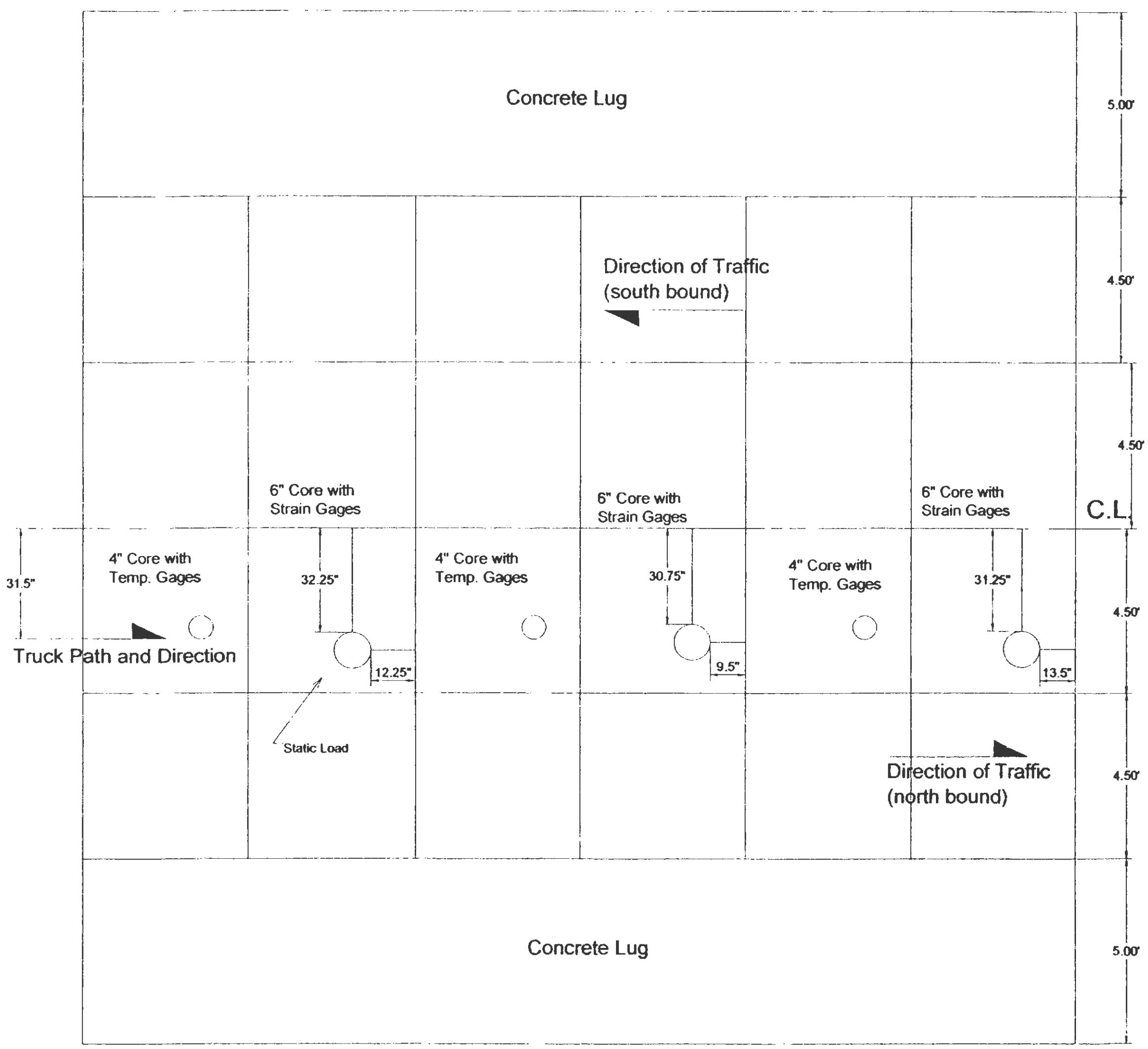

Date: 9-10-2004 Truck speed 1- 2 mph
Site: # 5
Station: 507+10
Slab size: 6' x 6'
Gage orientation: longitudinal

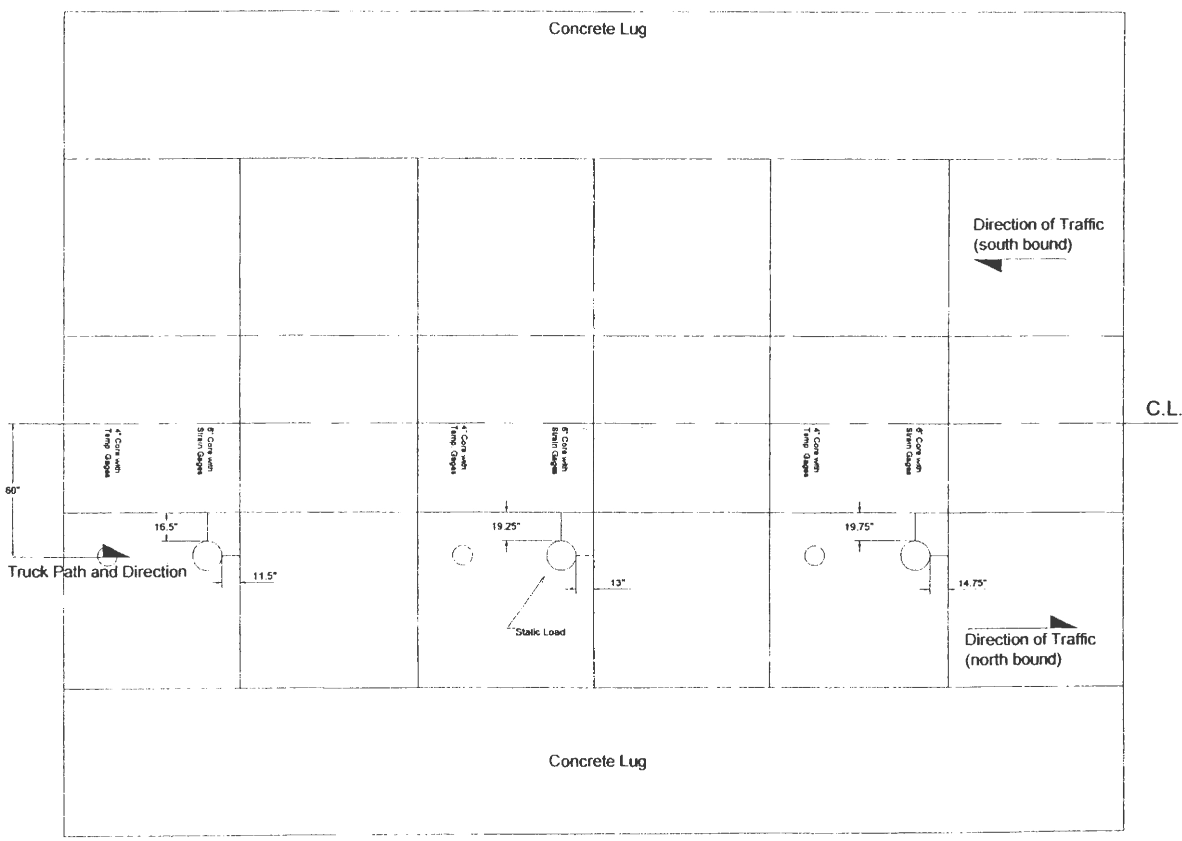

APPENDIX B:

STRAIN GAGE DATA

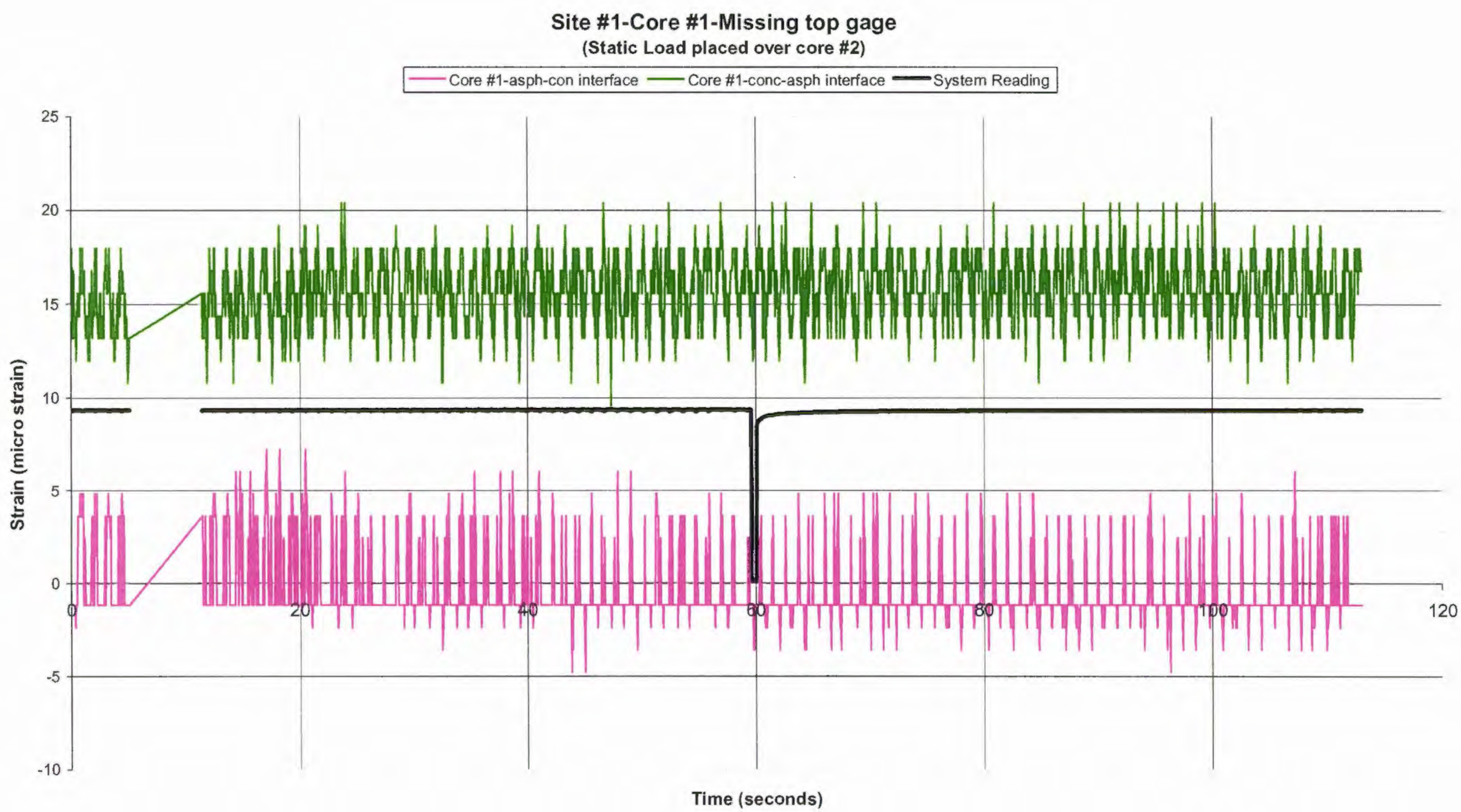
Site #1-Core #1-Missing top gage
(Static Load placed over core #2)
Core #1-asph-con interface
Core #1-conc-asph interface
System Reading
Strain (micro strain)
25
20
15
10
5
0
-5
-10
0
20
40
60
80
100
120
Time (seconds)

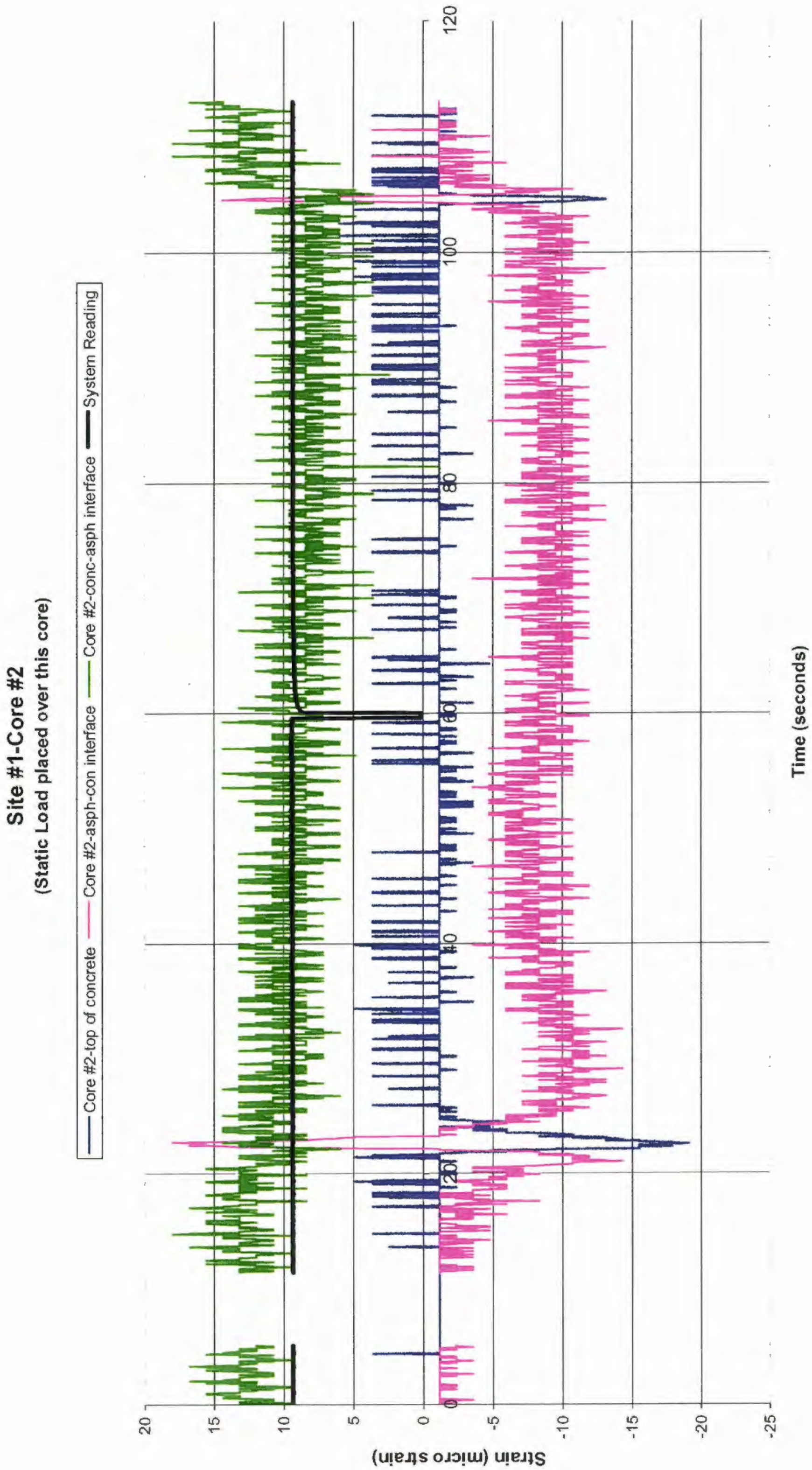
Site #1-Core #2
(Static Load placed over this core)
Core #2-top of concrete
Core #2-asph-con interface
Core #2-conc-asph interface
System Reading
Strain (micro strain)
Time (seconds)
20
15
10
5
0
-5
-10
-15
-20
-25
0
20
40
60
80
100
120

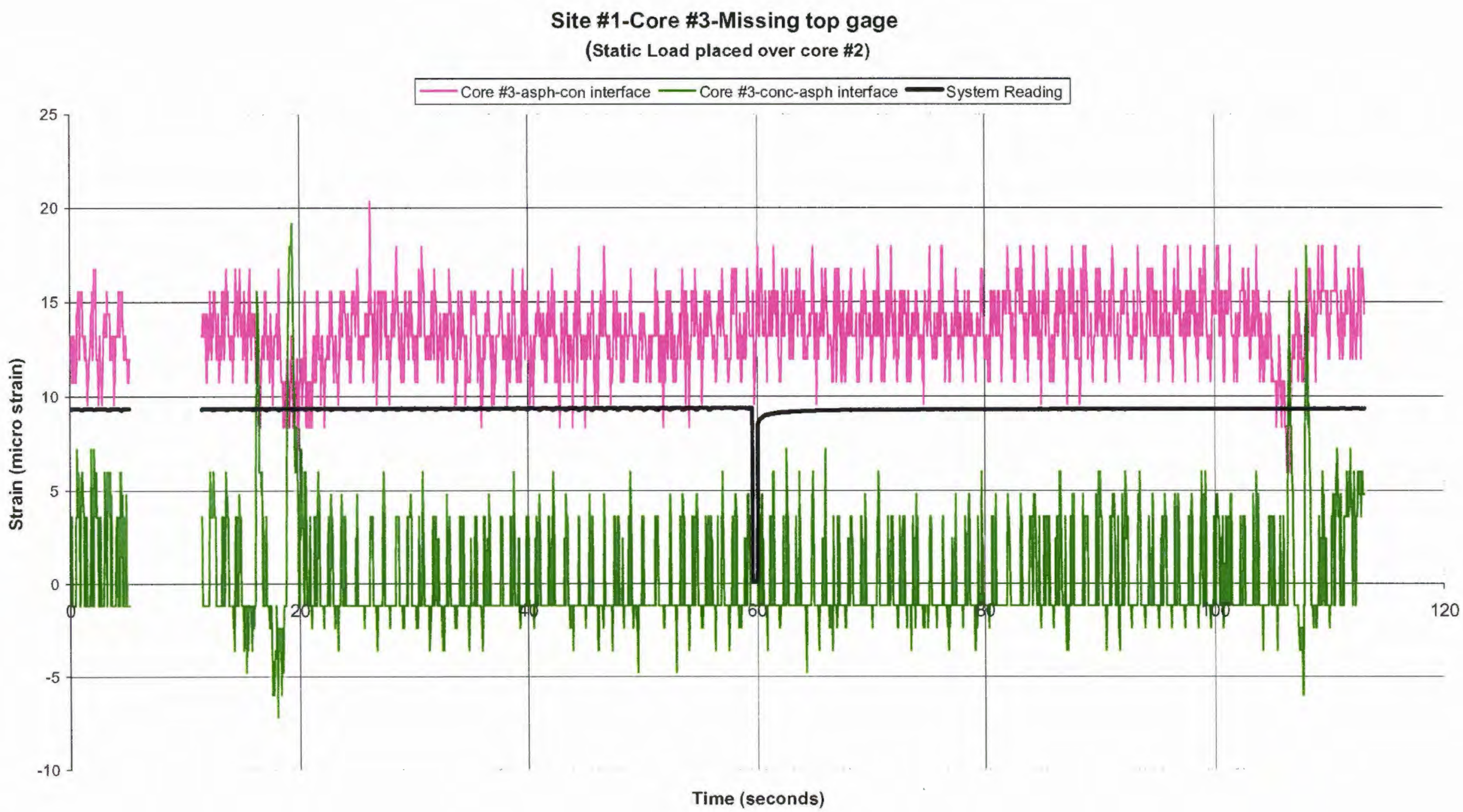
Site #1-Core #3-Missing top gage
(Static Load placed over core #2)
Core #3-asph-con interface
Core #3-conc-asph interface
System Reading
25
20
15
10
5
0
-5
-10
Strain (micro strain)
0
20
40
60
80
100
120
Time (seconds)

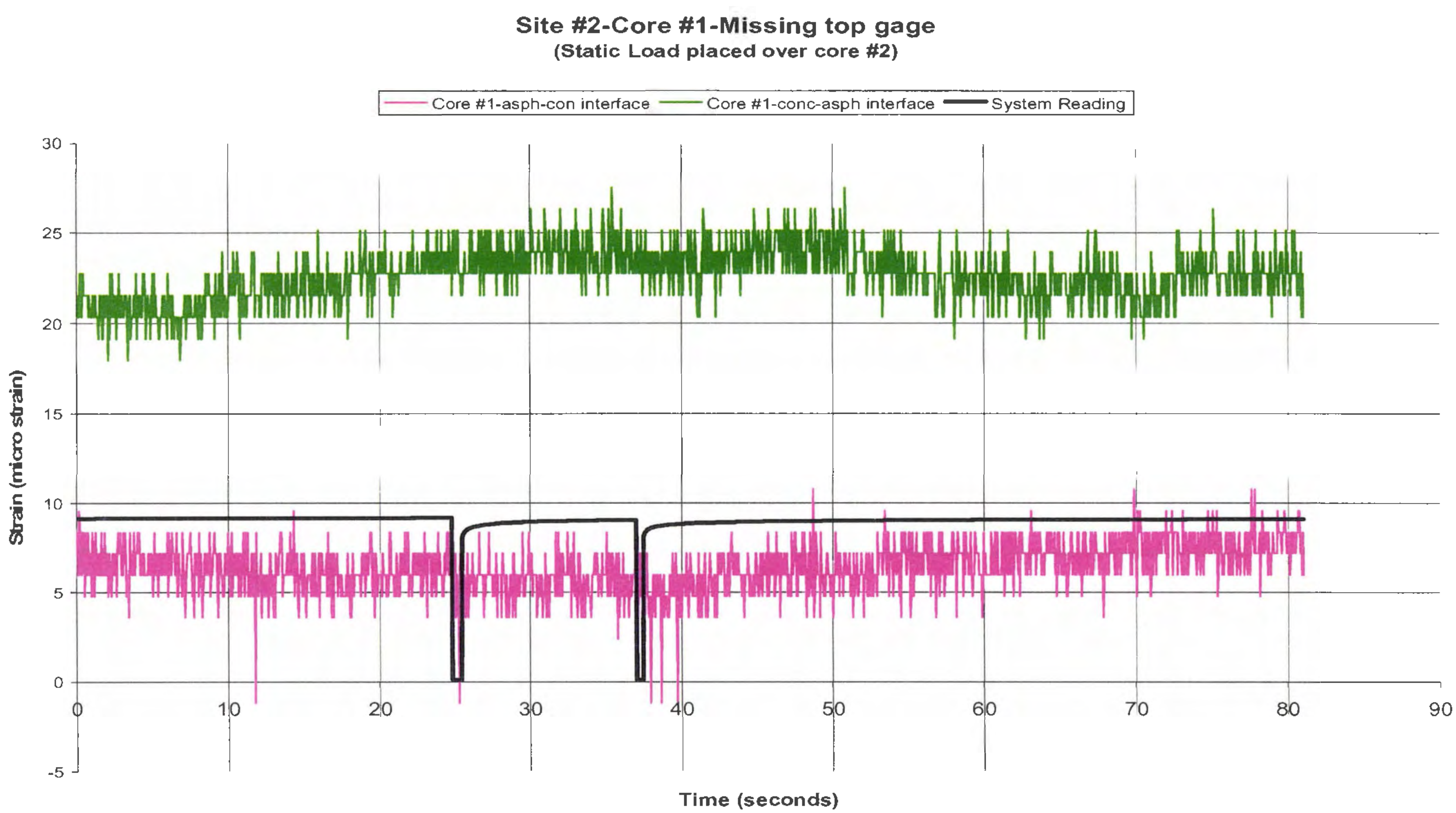
Site #2-Core #1-Missing top gage
(Static Load placed over core #2)
Core #1-asph-con interface
Core #1-conc-asph interface
System Reading
Strain (micro strain)
30
25
20
15
10
5
0
-5
0
10
20
30
40
50
60
70
80
90
Time (seconds)

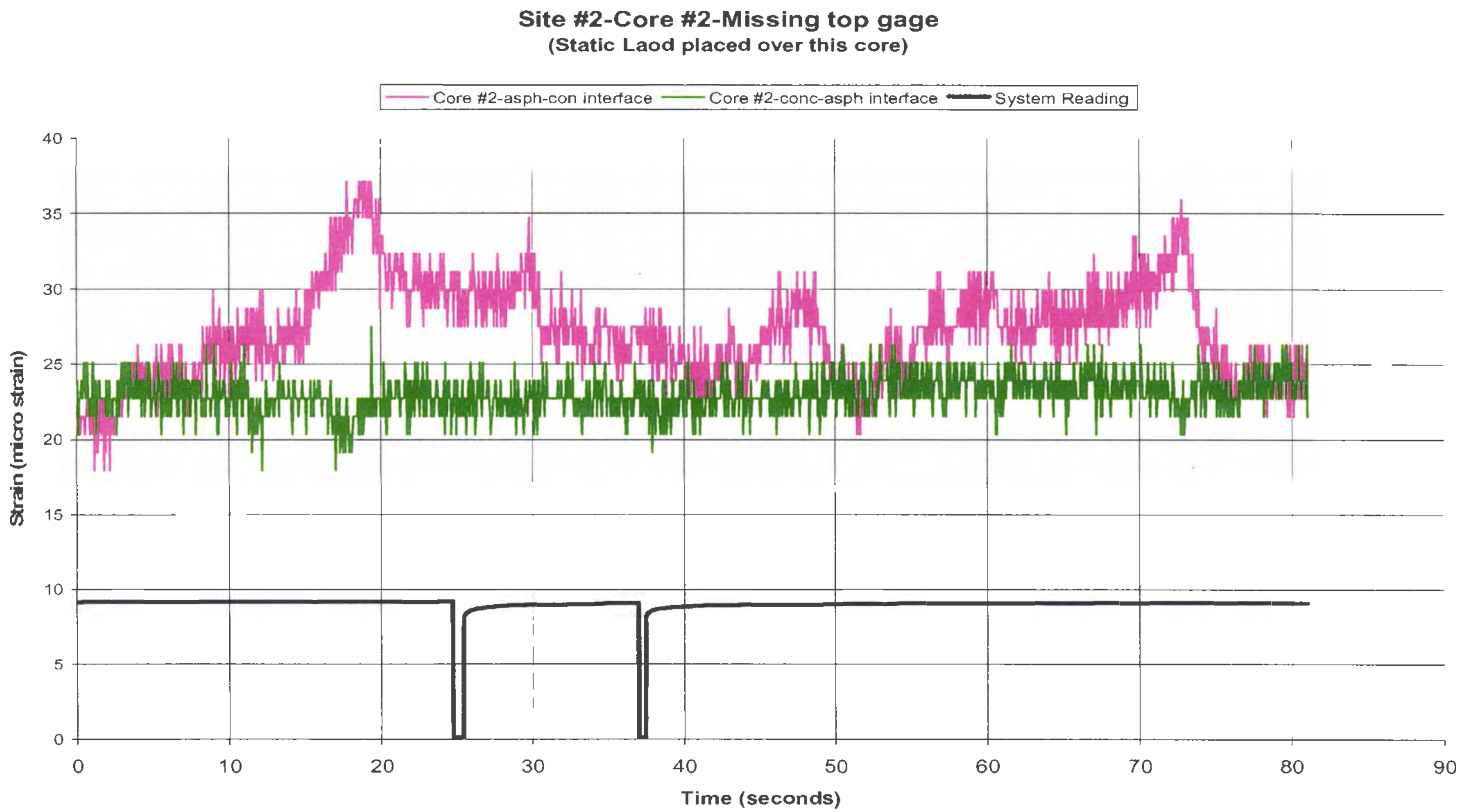
Site #2-Core #2-Missing top gage
(Static Laod placed over this core)
Core #2-asph-con interface
Core #2-conc-asph interface
System Reading
Strain (micro strain)
0
5
10
15
20
25
30
35
40
0
10
20
30
40
50
60
70
80
90
Time (seconds)

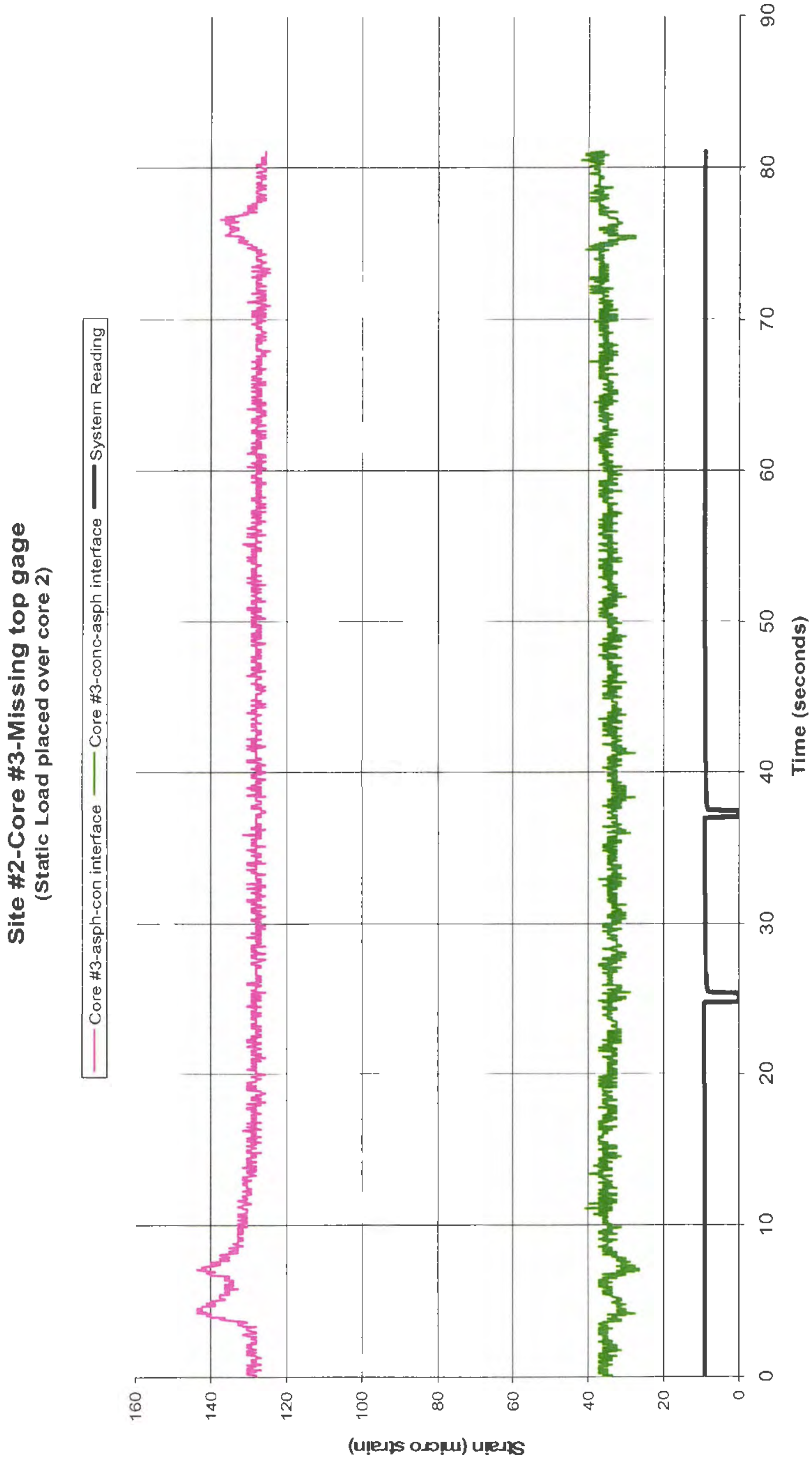
Site #2-Core #3-Missing top gage
(Static Load placed over core 2)
Core #3-asph-con interface
Core #3-conc-asph interface
System Reading
Strain (micro strain)
Time (seconds)
0
20
40
60
80
100
120
140
160
0
10
20
30
40
50
60
70
80
90

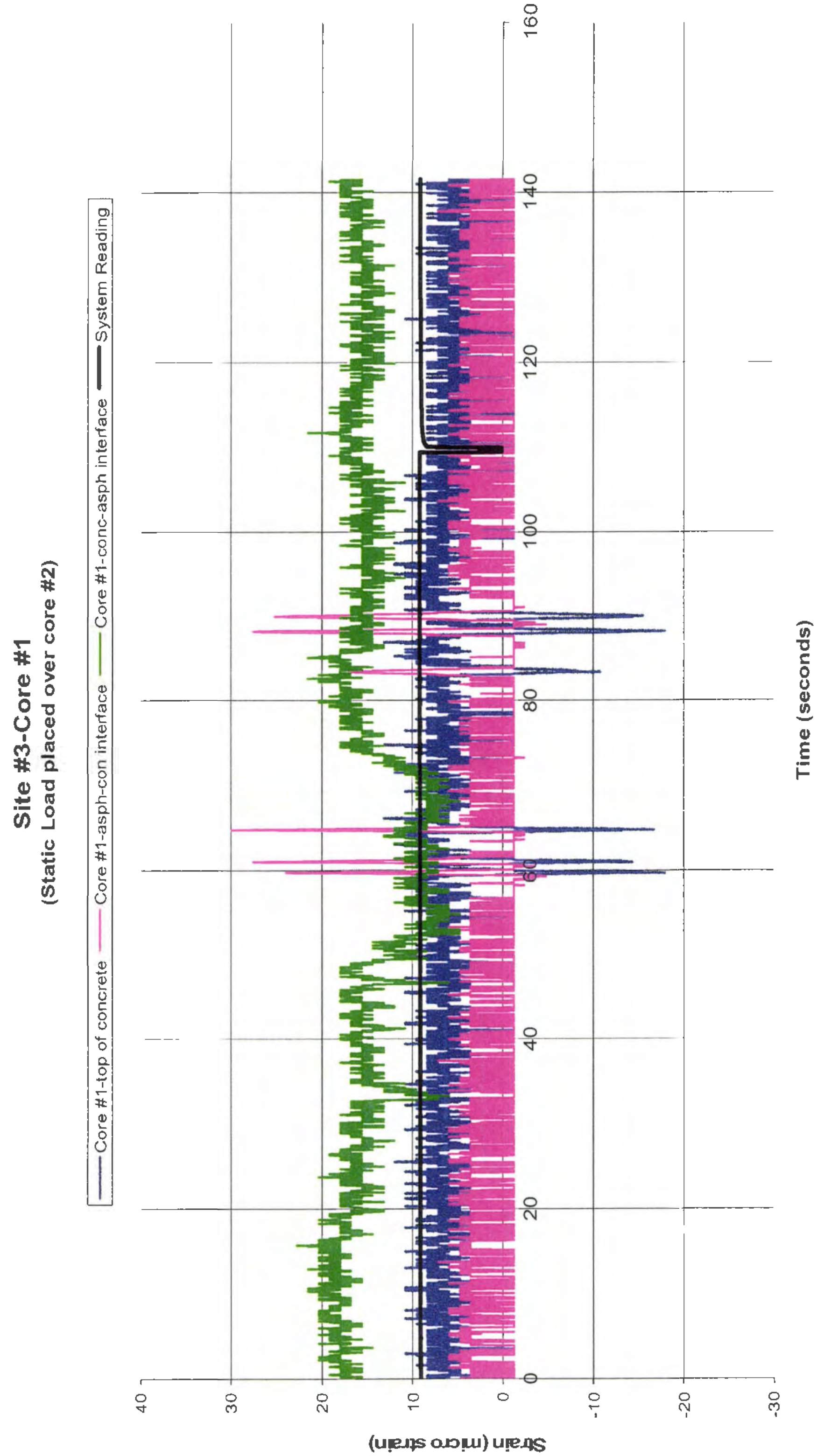
Site #3-Core #1
(Static Load placed over core #2)
Core #1-top of concrete
Core #1-asph-con interface
Core #1-conc-asph interface
System Reading
Strain (micro strain)
Time (seconds)
40
30
20
10
0
-10
-20
-30
0
20
40
60
80
100
120
140
160

Site #3-Core #2
(Static Load placed over this core)

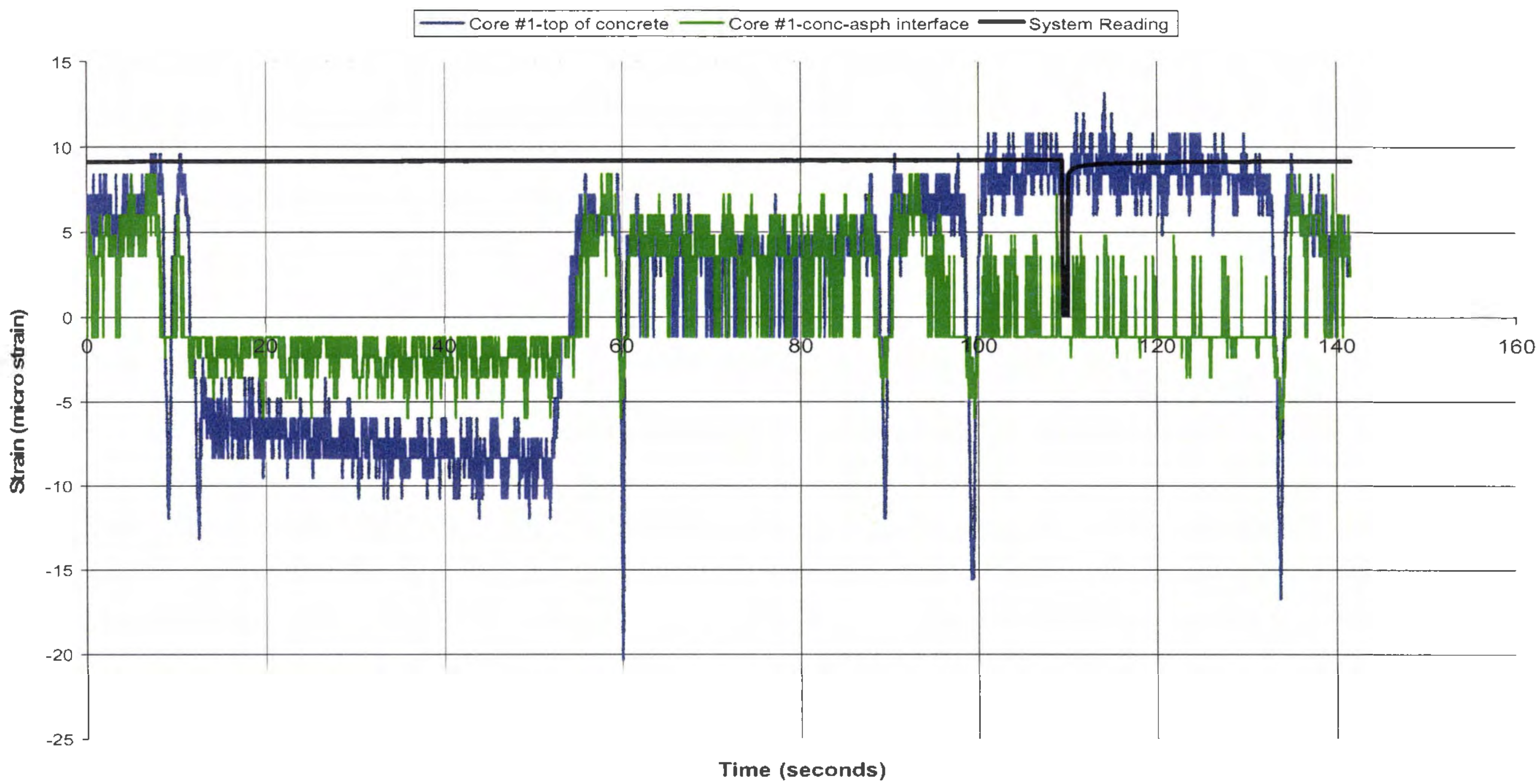

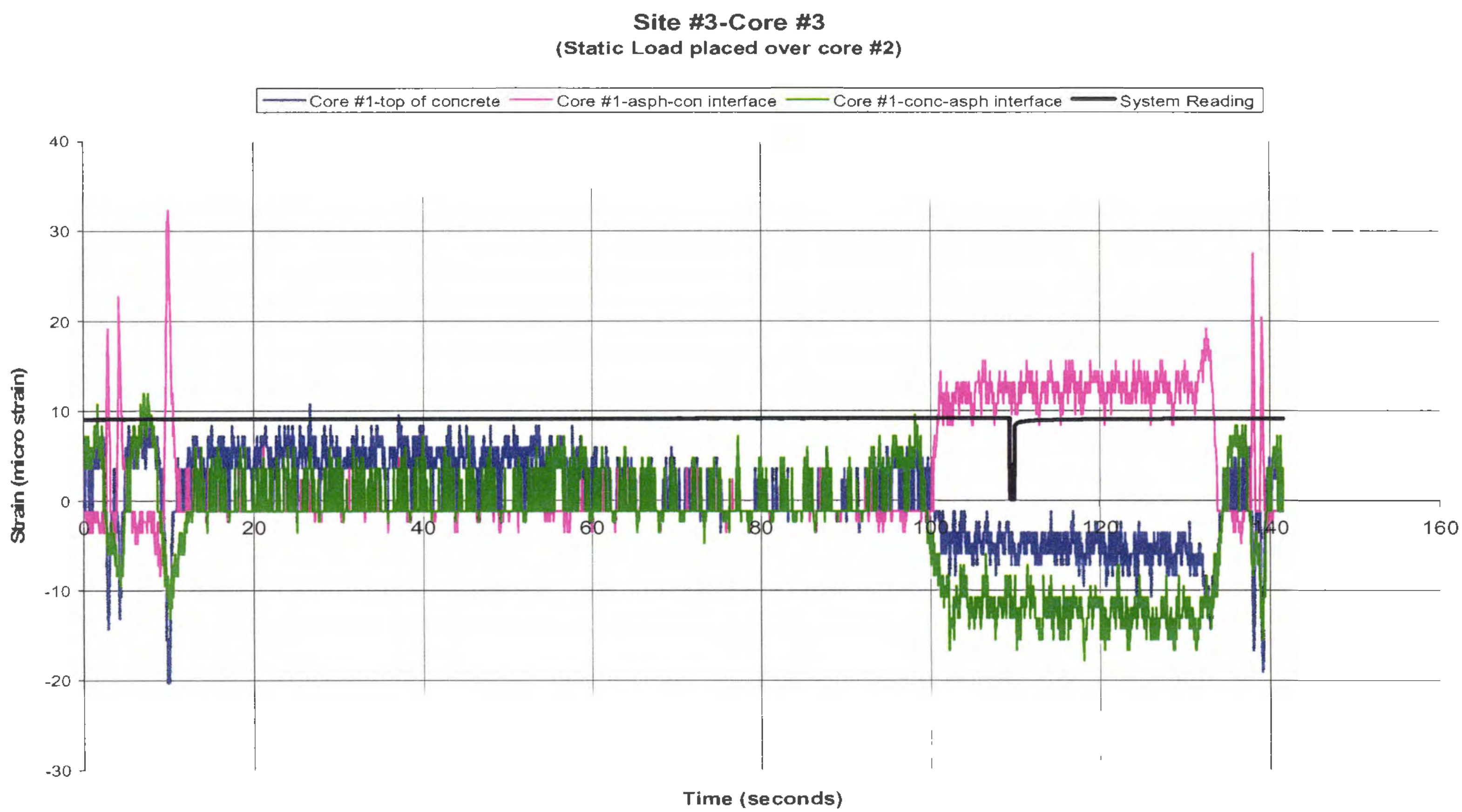

Site #3-Core #3
(Static Load placed over core #2)
Core #1-top of concrete
Core #1-asph-con interface
Core #1-conc-asph interface
System Reading
Strain (micro strain)
40
30
20
10
0
-10
-20
-30
0
20
40
60
80
100
120
140
160
Time (seconds)

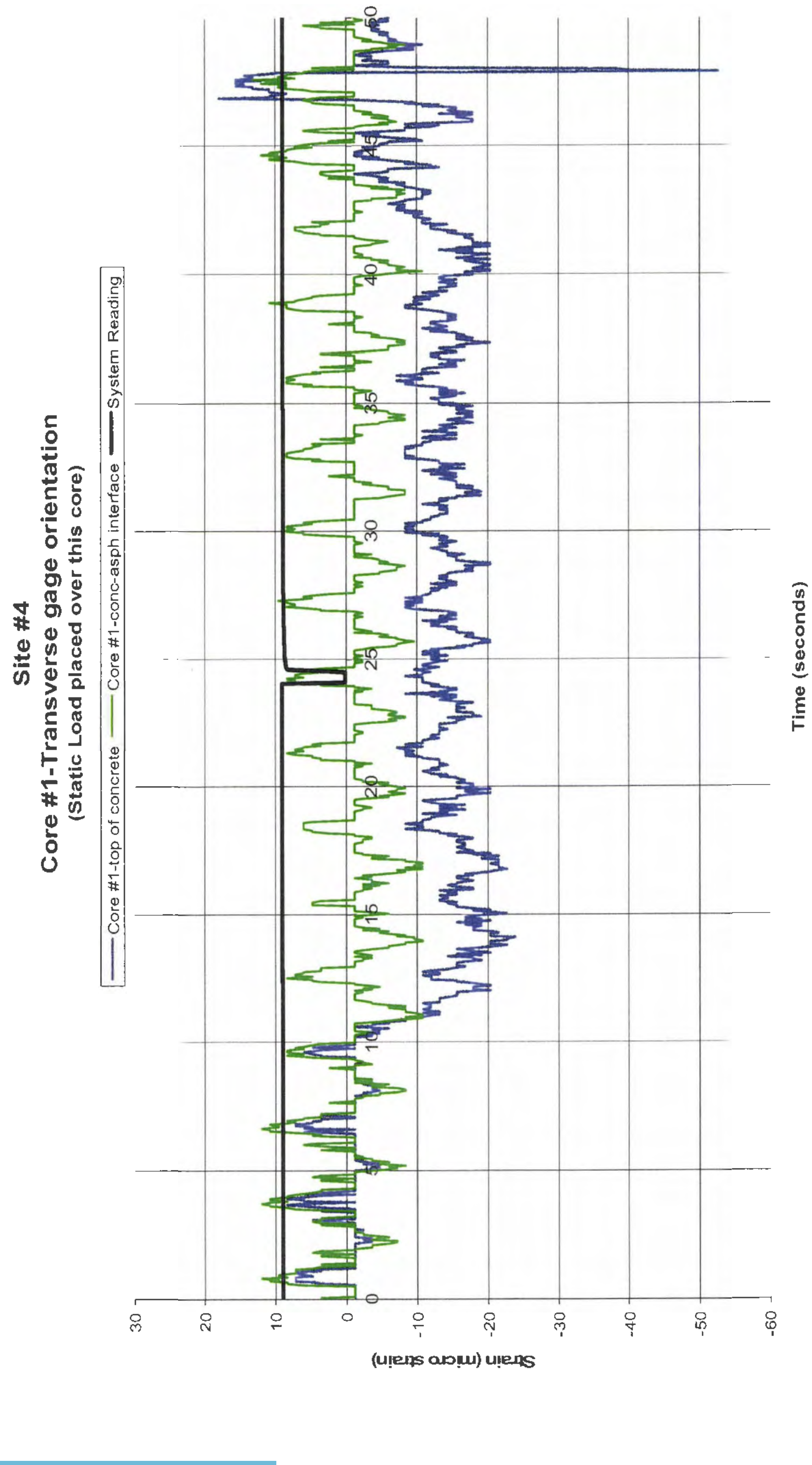
Site #4
Core #1-Transverse gage orientation
(Static Load placed over this core)
Core #1-top of concrete
Core #1-conc-asph interface
System Reading
Strain (micro strain)
Time (seconds)
30
20
10
0
-10
-20
-30
-40
-50
-60
0
5
10
15
20
25
30
35
40
45
50

Site #4
Core #2-Longitudinal gage orientation
(Static Load placed over core #1)

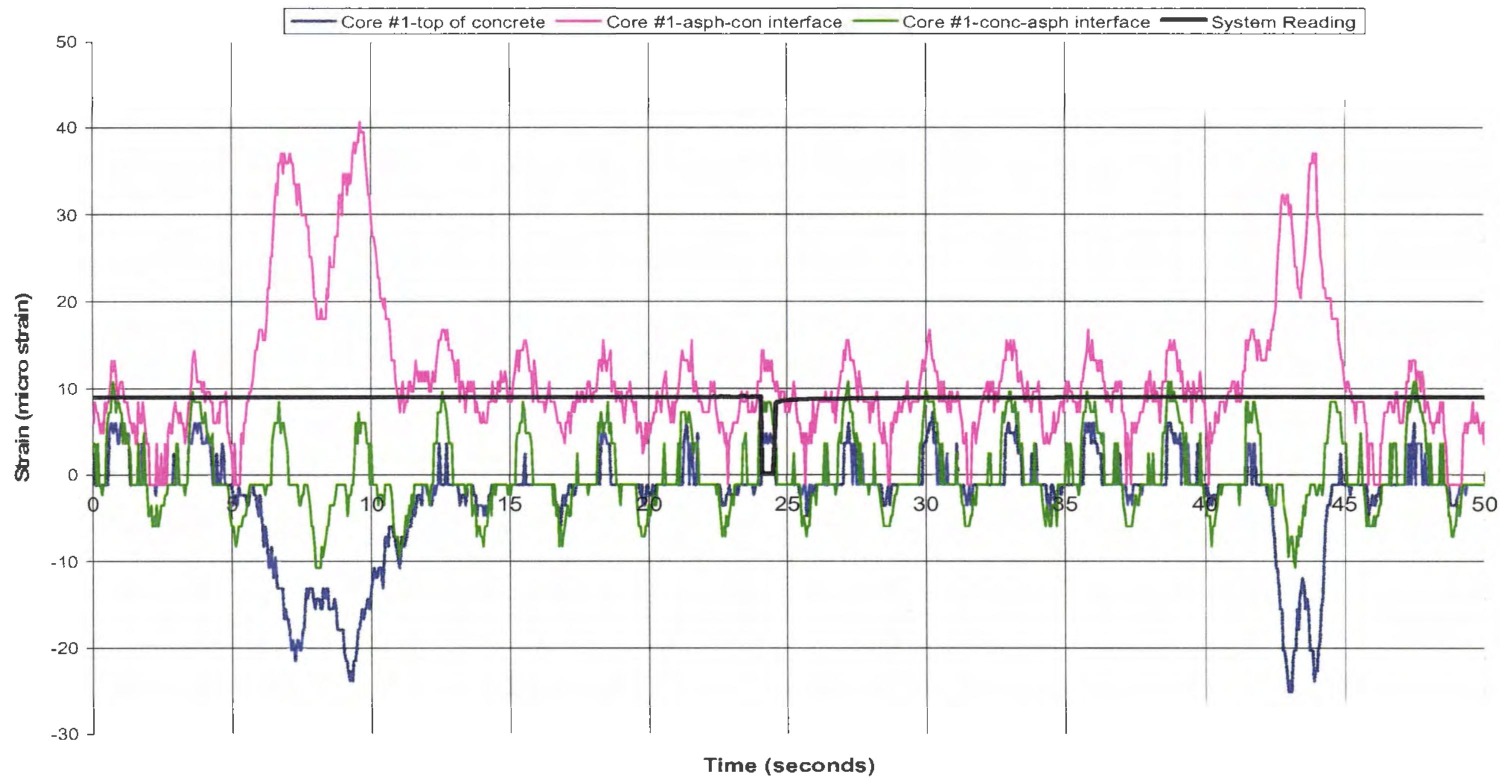

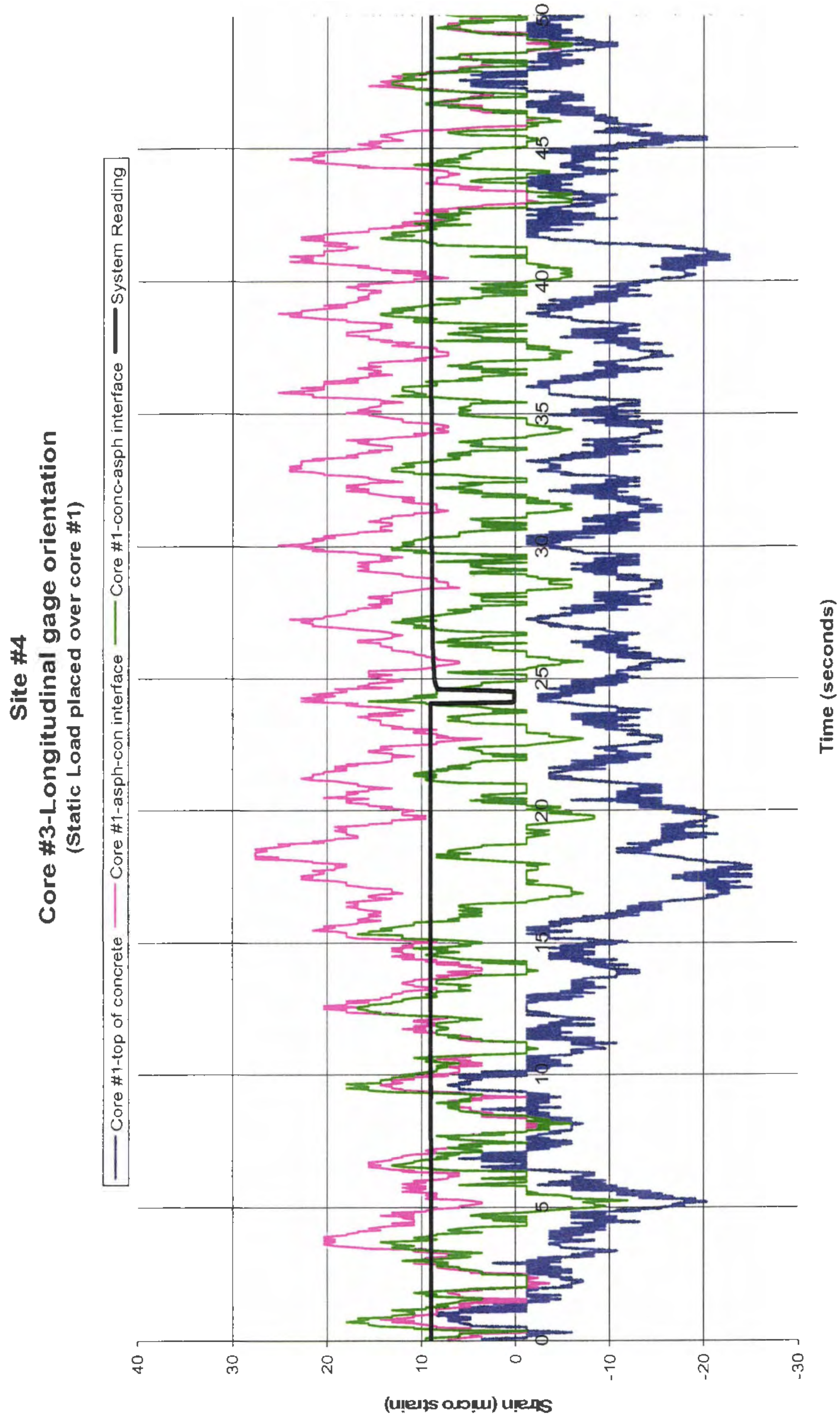
Site #4
Core #3-Longitudinal gage orientation
(Static Load placed over core #1)
Core #1-top of concrete
Core #1-asph-con interface
Core #1-conc-asph interface
System Reading
Strain (micro strain)
40
30
20
10
0
-10
-20
-30
Time (seconds)
0
5
10
15
20
25
30
35
40
45
50

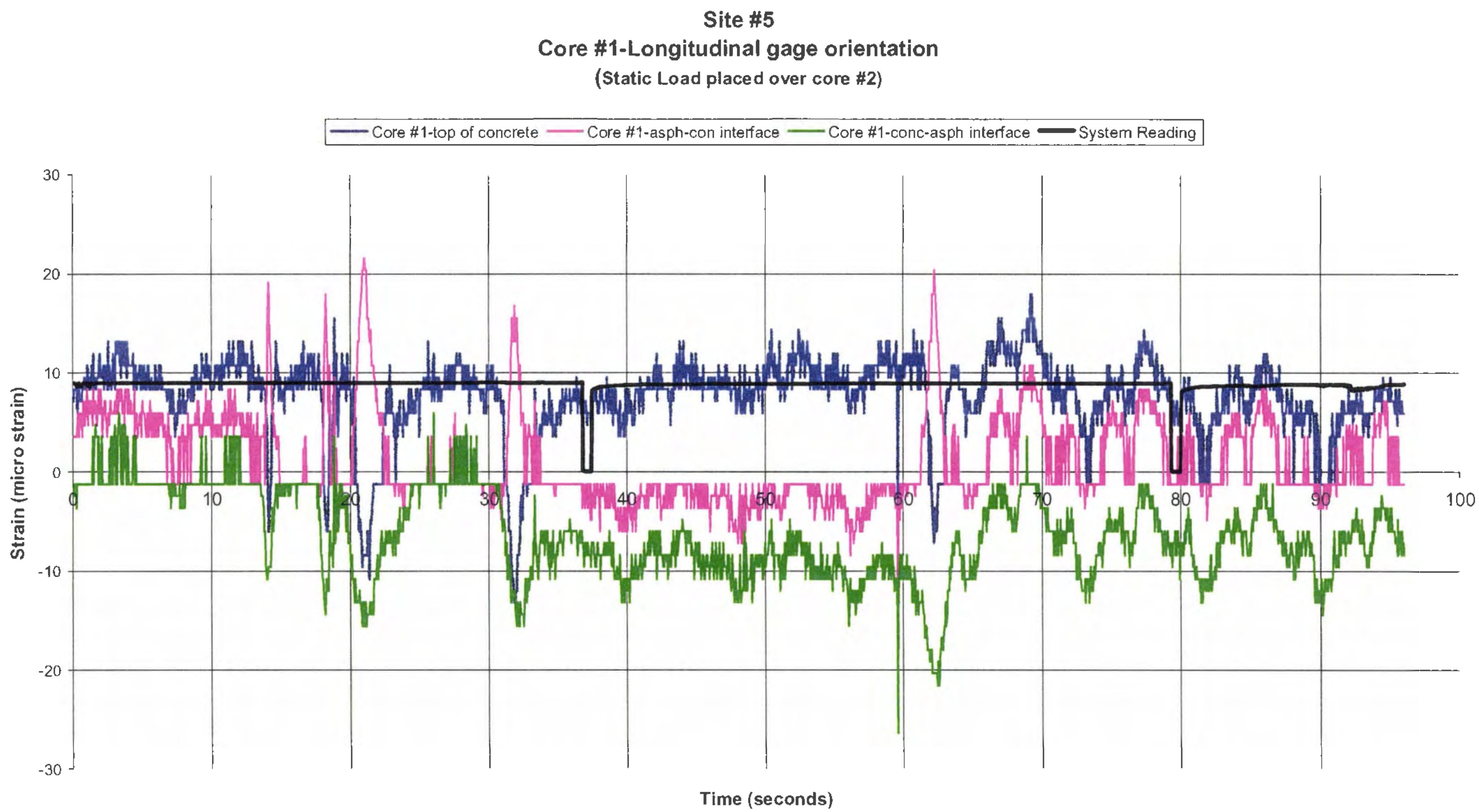
Site #5
Core #1-Longitudinal gage orientation
(Static Load placed over core #2)
Core #1-top of concrete
Core #1-asph-con interface
Core #1-conc-asph interface
System Reading
Strain (micro strain)
30
20
10
0
-10
-20
-30
0
10
20
30
40
50
60
70
80
90
100
Time (seconds)

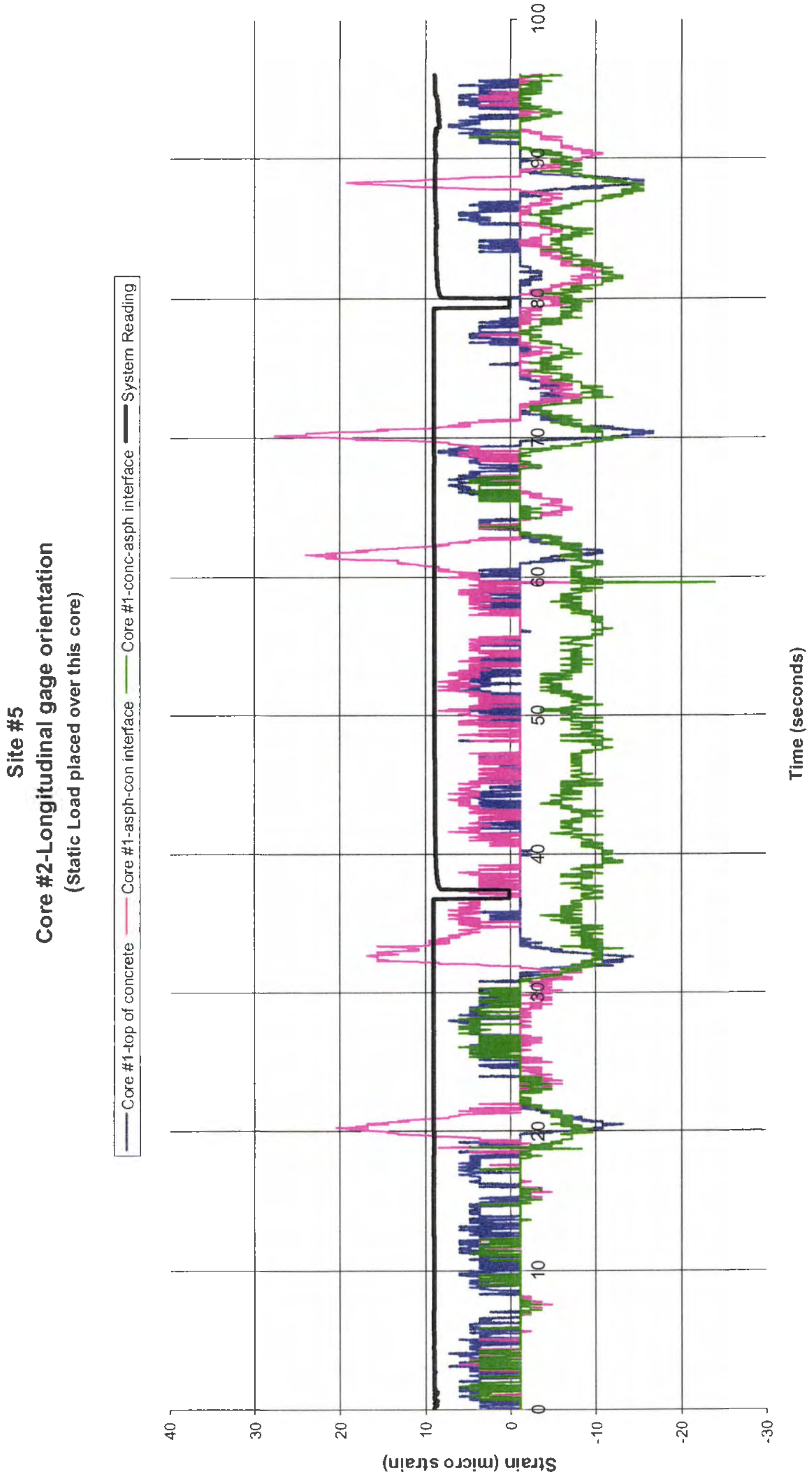
Site #5
Core #2-Longitudinal gage orientation
(Static Load placed over this core)
Core #1-top of concrete
Core #1-asph-con interface
Core #1-conc-asph interface
System Reading
Strain (micro strain)
Time (seconds)
40
30
20
10
0
-10
-20
-30
0
10
20
30
40
50
60
70
80
90
100

Site #5
Core #3-Longitudinal gage orientation
(Static Load placed over core #2)

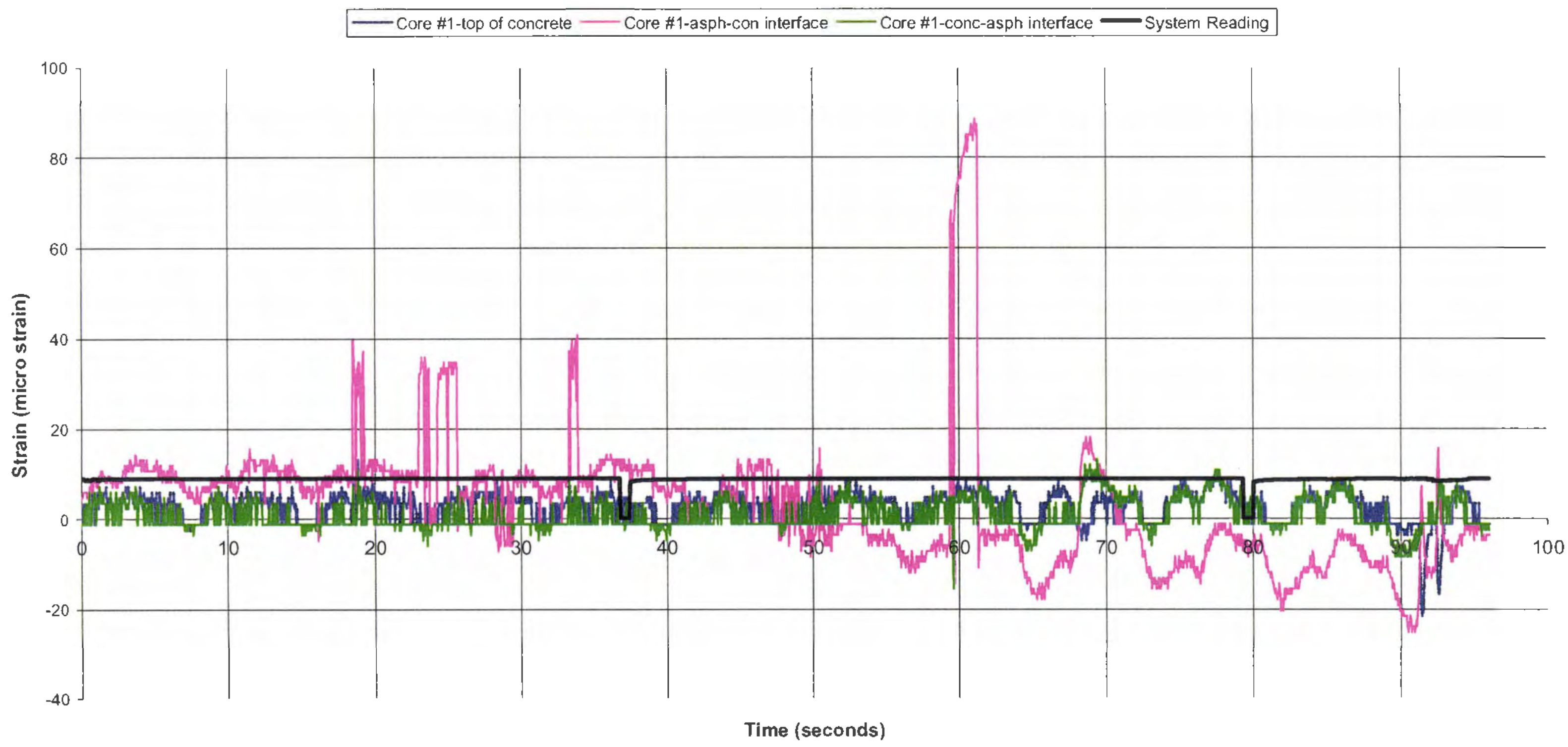

REFERENCES

1. Cable, J.K., M.L. Anthony, F.S. Fanous, and B.M. Phares, *Evaluation of Composite Pavement Unbonded Overlays: Phases I and II*, Center for Portland Cement Concrete Pavement Technology, Iowa State University, Ames, Iowa, 2003

2. *NCHRP Synthesis 338: Thin and Ultra-Thin Whitetopping*, Transportation Research Board, National Research Council, Washington D.C., 2002

3. Hutchinson, R.L., *NCHRP Synthesis of Highway Practice 99:Resurfacing with Portland Cement Concrete*, Transportation Research Board, National Research Council, Washington D.C., 1982

4. Tarr, S.M., M.J. Sheehan, and P.A. Okamoto, *Guidelines for the Thickness Design of Bonded Whitetopping in the State of Colorado*, Report No. CDOT-DTD-R-98-10, Colorado Department of Transportation, Denver, Colorado, Dec. 1998

5. Wu, C.L., S.M. Tarr, T.M. Refai, M.A. Nagi, and M.J. Sheehan, *Development of Ultra-Thin Whitetopping Design Procedure*, PCA Research and Development Serial No. 2124, Portland Cement Association, Skokie, Illinois, 1998

6. *Whitetopping – State of the Practice*, ACPA Publication EB210P, American Concrete Pavement Association, Skokie, Illinois, 1998

7. Cole, L.W., "Pavement Condition Surveys of Ultra-Thin Whitetopping Projects", *Proceedings of the 6th International Purdue Conference on Concrete Pavement Design and Materials for High Performance,* Vol. 2, Indianapolis, Indiana, 1997, pp. 175-187

8. Kumara, W., M. Tia, C.-:L. Wu, and B. Choubane, *Evaluation of Applicability of Ultrathin Whitetopping in Florida*, Transportation Research Board Annual Meeting, Washington D.C., January 2003

9. Nishizawa, T., Y. Murata, and K. Kokubun, *Mechanical Behavior of Ultrathin Whitetopping Structure Under Stationary and Moving Loads*, Transportation Research Board Annual Meeting, Washington D.C., January 2003

10. Vandenbossche, J.M., *Performance Analysis of Ultrathin Whitetopping Intersections on US-169: Elk River, Minnesota*, Transportation Research Board Annual Meeting, Washington D.C., January, 2003

11. Burnham, T., D. Rettner, *Whitetopping and Hot-Mix Asphalt Overlay Treatments for Flexible Pavement*, Transportation Research Board Annual Meeting, Washington D.C., January 2003

12. "Method of Test for Determining the Shearing Strength of Bonded Concrete", Test Method No. Iowa 406-C, Iowa Department of Transportation, Ames, May 2000

13. Fanous, F.S., Professor – Iowa State University, Personal Conversation, Unpublished data, 2004

14. Ceylan, H., Professor – Iowa State University, Personal Conversation, Unpublished data, October 2004

15. Ingram, D.N.J., *The Effect of the Dowel Bar Shape and Spacing in Portland Cement Concrete Pavements on the Load Transfer Efficiency of the Transverse Joint*, Iowa State University, Ames, Iowa, 2004

16. Hibbeler, R.C., *Structural Analysis*, Prentice Hall, Upper Saddle River, New Jersey, 1999

17. Hibbeler, R.C., *Mechanics of Materials*, Prentice Hall, Upper Saddle River, New Jersey, 1997

18. Huang, Y.H., *Pavement Analysis and Design*, Prentice Hall, Upper Saddle River, New Jersey, 1993

19. Kuo, C.-M., K.T. Hall, and M.I. Darter, *Three-Dimensional Finite element Model for Analysis of Concrete Pavement Support*, University of Illinois at Urbana-Champaign, Urbana, Ill., 1995

20. Voyiadjis, G.Z., P.I. Kattan, "Bending of Thick Plates on Elastic Foundation", *Advances in the Theory of Plates and Shells*, Studies in Applied Mechanics 24, Elsevier, Amsterdam, The Netherlands, 1990, pp. 87-121

21. Cable, J.K., Professor – Iowa State University, Personal Conversation, Unpublished data, October 2004

22. Coree, B., Professor – Iowa State University, Electronic Correspondence, Unpublished data, October 2004

23. Logan, D.L., *A First Course in the Finite Element Method*, Brooks/Cole, Pacific Grove, California, 2002

24. ANSYS User's Manual, ANSYS v.6.1, ANSYS Inc., Canonsburg, PA, 2004

ACKNOWLEDGEMENTS

The study presented herein was completed due to the combined efforts of Iowa State University Civil, Construction and Environmental Engineering (CCEE) department and the Iowa Department of Transportation (Iowa DOT).

The author would like to thank Dr. James K. Cable, retired faculty of Iowa State University CCEE, whose experience in the field of pavement engineering and commitment to the success of this project was very much appreciated.

The author would also like to recognize Douglas L. Wood, Structures Laboratory Manager, for his efforts in the instrumentation of the composite pavement on Iowa Highway 13, and also his assistance during the process of data interpretation.

Much credit goes to Dr. Fouad S. Fanous, professor at Iowa State University CCEE, for his valuable guidance and tireless efforts throughout the project and in the preparation of this report. His dedication to learning and excellence will always be appreciated.

Finally, the author wishes to thank his wife, Wing Hang Sharon Im, for her unceasing support throughout the course of the study, and without which the completion of the program of study would not have been possible.